NSF/RA-790035

PB 296455

SH - A COMPUTER PROGRAM FOR GENERATING FAR-FIELD TANGENTIAL TIME HISTORIES FOR POINT EARTHQUAKE SOURCES

BY

ROBERT B. HERRMANN AND CHIEN Y. WANG

SPONSORED BY THE NATIONAL SCIENCE FOUNDATION
APPLIED SCIENCE AND RESEARCH APPLICATIONS DIRECTORATE
DIVISION OF PROBLEM FOCUSED RESEARCH APPLICATION
GRANT ENV 78-20875

DEPARTMENT OF EARTH AND ATMOSPHERIC SCIENCES
SAINT LOUIS UNIVERSITY
221 NORTH GRAND BOULEVARD
SAINT LOUIS, MISSOURI 63103

JANUARY, 1979

50272-101

REPORT DOCUMENTATION PAGE	1. REPORT NO. NSF/RA-790035	2.	3. Recipient's Accession No. PB296455

4. Title and Subtitle
SH - A Computer Program for Generating Far-Field Tangential Time Histories For Point Earthquake Sources

5. Report Date
January 1979

6.

7. Author(s)
R.B. Herrmann, C.Y. Wang

8. Performing Organization Rept. No.

9. Performing Organization Name and Address
Saint Louis University
Department of Earth and Atmospheric Sciences
221 North Grand Boulevard
Saint Louis, Missouri 63103

10. Project/Task/Work Unit No.

11. Contract(C) or Grant(G) No.
(C)
(G) ENV7820875

12. Sponsoring Organization Name and Address
Applied Science and Research Applications (ASRA)
National Science Foundation
1800 G Street, N.W.
Washington, D.C. 20550

13. Type of Report & Period Covered

14.

15. Supplementary Notes

16. Abstract (Limit: 200 words)
A computer program is presented for the computation of far-field tangential time histories due to point earthquake sources. The program provides accurate results for frequencies of 0-10 Hz and for receiver distances from one source depth to 500 kilometers. Comparisons are made with an independent half-space solution to test the validity of the far-field assumption in representing time histories. A package of four computer programs is given: SHSPEC yields Fourier spectra on the surface of a multilayered medium at a specified distance from the point dislocation earthquake source; SHVEL combines the output of SHSPEC with a predetermined source pulse to generate velocity time histories; DSVLAC uses the output of SHVEL to generate displacement, velocity and acceleration time histories; and SDSVSA uses the output of DSVLAC to compute and tabulate the response spectra of each time history.

17. Document Analysis a. Descriptors

Earthquakes
Computer programs
Far field
Time studies

b. Identifiers/Open-Ended Terms

Tangential time histories
SHSPEC
SHVEL
Point earthquake sources
DSVLAC
SDSVSA
Response spectra

c. COSATI Field/Group
i.

18. Availability Statement	19. Security Class (This Report)	21. No. of Pages
NTIS		116
	20. Security Class (This Page)	22. Price A06-A01

(See ANSI-Z39.18)
See Instructions on Reverse
OPTIONAL FORM 272 (4-77)
(Formerly NTIS-35)
Department of Commerce

SH - A COMPUTER PROGRAM FOR GENERATING FAR-FIELD TANGENTIAL TIME HISTORIES FOR POINT EARTHQUAKE SOURCES

BY

ROBERT B. HERRMANN AND CHIEN Y. WANG

SPONSORED BY THE NATIONAL SCIENCE FOUNDATION
APPLIED SCIENCE AND RESEARCH APPLICATIONS DIRECTORATE
DIVISION OF PROBLEM FOCUSED RESEARCH APPLICATION
GRANT ENV 78-20875

DEPARTMENT OF EARTH AND ATMOSPHERIC SCIENCES
SAINT LOUIS UNIVERSITY
221 NORTH GRAND BOULEVARD
SAINT LOUIS, MISSOURI 63103

JANUARY, 1979

ABSTRACT

A computer program is presented for the computation of far-field tangential time histories due to point earthquake sources. The program provides accurate results for frequencies of 0-10 Hz and for receiver distances from one source depth to 500 kilometers. Comparisons are made with an independent half-space solution to test the validity of the far-field assumption in representing time histories.

A package of four computer programs is given: SHSPEC yields Fourier spectra on the surface of a multilayered medium at a specified distance from the point dislocation earthquake source; SHVEL combines the output of SHSPEC with a predetermined source pulse to generate velocity time histories; DSVLAC uses the output of SHVEL to generate displacement, velocity and acceleration time histories; and SDSVSA uses the output of DSVLAC to compute and tabulate the response spectra of each time history.

CONTENTS

PART I. INTRODUCTION

This report is an update of a publication by Herrmann (1977) for the U.S. Army Corps of Engineers. Since that time, there have been many advances in techniques for generating realistic earthquake ground motion time histories. At present, developments are being pursued with two approaches involving Laplace transform and Fourier transform techniques.

The Laplace transform, or Cagniard-de Hoop technique consists of generalized ray techniques, by which the seismic trace is constructed by a superposition of seismic arrivals which have taken separate paths between the earthquake source and receiver. An advantage is that the method is valid at high frequencies. Unfortunately, for large distances in a reasonable earth model, the number of rays contributing to the time history becomes very large so that considerable effort is involved in keeping track of the rays as well as computing them.

Helmberger and Malone (1975) applied the method to a study of local earthquakes. Heaton and Helmberger (1977, 1978) used the method to model the displacement time histories obtained from integrated accelerograms of the Borrego Mountain and Brawley earthquakes. To a certain extent, the earth model was a variable which could be modified under constraints to obtain a better fit to the data. However, good fits were obtained, demonstrating the effect of the transmission medium upon the ground displacements.

Displacements, rather than velocities or accelerations were modeled since lateral heterogeneities in the earth structure should affect the lower frequency displacements less.

The other approach involves expressing the solution in terms of a double integral transformation over wave number and frequency (Haskell, 1964; Hudson, 1969). This method does not consider the contribution of individual seismic arrivals, but rather yields the complete solution for an arbitrarily layered halfspace. A drawback is some difficulty encountered at high frequencies. On the other hand the complete solution is found.

The numerical solution is complicated by the presence of singularities in the wavenumber integrand. For an elastic medium, branch points and poles in the complex wavenumber plane are encountered. The solution may be obtained by a numerical approach to contour integration (Herrmann, 1977; Herrmann, 1979), or the by artifice of using slightly complex angular frequency to shift the complex singularities from the axis of integration (Bouchon and Aki, 1977). If an anelastic medium is considered, the singularities no longer lie on the real k-axis, so integration may procede simply. This is quite realistic since the earth is not perfectly elastic, so one assumes this from the start (Apsel, 1977).

The approach taken here is to expand Herrmann (1977, 1979) in detail because it is an independent method and because previous studies by Nuttli (1973, 1978) have indicated a very low rate of anelastic attenuation in the central United States. The method of Herrmann (1977) handles these conditions well.

PART II. THEORY

Haskell (1964) and Hudson (1969) obtained the solution for displacements generated by an elementary point force in the m'th layer of a structure consisting of plane parallel layers overlying a uniform halfspace. Each layer is homogeneous and isotropic with compressional wave velocity α_k, shear wave velocity β_k and density ρ_k (k = 1, N). The N'th layer corresponds to the halfspace. A cylindrical coordinate system (r, ϕ, z) is used with origin at the free surface above the source, with z-axis taken positive downward. The layer interfaces are the planes $z=z_k$ $(k=1, 2, \ldots, N-1)$ and the source is located on the plane $z=z_m + h_m$. For the purpose of derivation, the source is required to lie in a layer above the halfspace. The thickness of the m'th layer is $d_m=z_m-z_{m-1}$.

The expressions for the Fourier transformed displacements at the free surface z=0 are the following;

$$\bar{u}_z\ (r,\phi,0,\omega) = \sum_{n=0}^{\infty} \int_0^{\infty} dk\ \{g_z^{nc} \cos n\phi + g_z^{ns} \sin n\phi\}\ J_n(kr)/F_R\}$$

$$\bar{u}_r\ (r,\phi,0,\omega) =$$

$$\sum_{n=0}^{\infty} \int_0^{\infty} dk\ \{g_r^{nc} \cos n\phi + g_r^{ns} \sin n\phi)\ kJ_{n-1}\ (kr)/F_R$$

$$- (n/r)(g_r^{nc} \cos n\phi + g_r^{ns} \sin n\phi)\ J_n\ (kr)/F_R \qquad (1)$$

$$- (n/r)(g_\phi^{nc} \cos n\phi + g_\phi^{ns} \sin n\phi)\ J_n(kr)/F_L\}$$

$$\overline{u}_\phi(r,\phi,0,\omega) =$$

$$-\sum_{n=0}^{\infty} \int_0^\infty dk\ \{g_\phi^{ns} \cos n\phi - g_\phi^{nc} \sin n\phi)\ k\ J_{n-1}\ (kr)/F_L$$

$$-(n/r)\ (g_\phi^{ns} \cos n\phi - g_\phi^{nc} \sin n\phi)\ J_n\ (kr)/F_L$$

$$-(n/r)\ (g_r^{ns} \cos n\phi - g_r^{nc} \sin n\phi)\ J_n(kr)/F_R\}.$$

The displacements are defined such that the vertical displacement $u_z(r,\phi,0,t)$ is positive downward, that the radial displacement $u_r(r,\phi,0,t)$ is positive in a direction away from the source, and that the tangential displacement $u_\phi(r,\phi,0,t)$ is positive in a clockwise direction when looking in the positive z-direction.

Since this report is concerned with far-field tangential time histories, SH, explicit expressions for the P-SV functions g_z, g_r and F_R are not given here (c.f. Haskell, 1964). The expressions for the SH functions are as follow:

$$g_\phi^{nc} = (L_{21} - L_{11})S_1^{nc} + (L_{22} - L_{12})\ S_2^{nc}$$

$$g_\phi^{ns} = (L_{21} - L_{11})S_1^{ns} + (L_{22} - L_{12})\ S_2^{ns} \qquad (2)$$

and

$$F_L = J_{11} - J_{21}$$

where L_{ij} and J_{ij} are the elements of the L and J matrices which are defined as the matrix products.

$$\begin{aligned} J &= E_N^{-1} A_{N-1}(d_{N-1}) \ldots A_1(d_1) \\ L &= E_N^{-1} A_{N-1}(d_{N-1}) \ldots A_{m+1}(d_{m+1}) D_m(d_m - h_m). \end{aligned} \tag{3}$$

The layer matrices of Equation 3 are defined as

$$E_N^{-1} = \begin{bmatrix} \rho_N \nu_{\beta_N} & 0 \\ 0 & -1/\beta_N^2 \end{bmatrix}, \tag{4}$$

$$A(z) = \begin{bmatrix} C_\beta & S_\beta/\rho\beta^2\nu_\beta \\ \rho\beta^2\nu_\beta S_\beta & C_\beta \end{bmatrix} \tag{5}$$

and

$$D(z) = \begin{bmatrix} C_\beta/\rho & -S_\beta/\rho\nu_\beta \\ \beta^2\nu_\beta S_\beta & -\beta^2 C_\beta \end{bmatrix}, \tag{6}$$

where $C_\beta(z) = \cosh \nu_\beta z$, $S_\beta(z) = \sinh \nu_\beta z$, $k_\beta = \omega/\beta$,

and

$$\nu_\beta = \begin{cases} (k^2 - k_\beta^2)^{1/2} & k \geq k_\beta \\ i(k_\beta^2 - k^2)^{1/2} & k \leq k_\beta. \end{cases} \tag{7}$$

The elements of the matrices are to be evaluated using the layer parameters indicated by the matrix subscripts in Equation 3.

For a point shear dislocation model of an earthquake source, the source can be represented by two perpendicular dipoles. Let the orientation of the pressure and tension axes be given by the vectors $P = (p_1, p_2, p_3)$ and $T = (t_1, t_2, t_3)$, respectively. The source coefficients S_i^{nc} and S_i^{ns} are all zero except for the terms

$$
\begin{aligned}
S_1^{1c} &= -2\ (t_1\, t_3 - p_1\, p_3)/4\pi\beta_m^2 \\
S_1^{1s} &= -2\ (t_2\, t_3 - p_2\, p_3)/4\pi\beta_m^2 \qquad (8) \\
S_2^{2c} &= \quad k(t_2^{\,2} - t_1^{\,2} - p_2^{\,2} + p_1^{\,2})/4\pi\beta_m^2 \\
S_2^{2s} &= -2k(t_1\, t_2 - p_1\, p_2)/4\pi\beta_m^2 ,
\end{aligned}
$$

where k is the wavenumber and β_m is the shear velocity in the source layer. The expressions for E_N^{-1}, D and $S_i^{nc,s}$ differ from those given by Haskell (1964) in that they have been modified to eliminate some apparent singularities. The ratio $g^{nc,s}/F_L$ does not differ from that given by Haskell (1964) or Hudson (1969).

A simple examination of the excitation coefficients in Equation 8 shows that the SH contribution to the tangential displacements involves just a linear combination of two equivalent sources, a vertical dip-slip source which has only the n=1 term and a vertical strike-slip source which has only the n=2 term (a 45° dip-slip source is another source which involves just the n=2 term). This well known observation (Langston and Helmberger, 1975 and Harkrider, 1976) means that the tangential displacements from an arbitrary fault motion model can be represented by a linear combination of the solutions due to these two sources.

A right lateral vertical strike-slip motion on a fault striking north would be represented by P=(.707, .707,0) and T=(-.707,.707, 0). Reverse faulting on a fault dipping 45° to the east or west and striking north would be represented by P=(0,1,0) and T=(0,0,1). Vertical dip-slip faulting on a fault striking north with the east side downthrown would have P=(0, -.707, .707) and T=(0,.707,.707).

The transformed displacements in Equation 1 represent the displacements due to a delta function time history of motion on the fault. Usually this delta function response is convolved with s(t), the time history of the faulting process of the dislocation source, $s(t) = 0$ for $t<0$ and $s(t) = M_o$ for $t>>0$. The seismic moment M_o is defined by the relation $M_o = \mu\bar{u} A$, where μ is the rigidity modulus of the medium, $\bar{u}$ is the average dislocation and A is the fault area. M_o has units of dyne-cm in CGS units. The ground motion as a function of time is then obtained by taking the inverse Fourier transform of each transformed displacement in Equation 1. For example,

$$u_\phi(r,\phi,o,t) = (2\pi)^{-1} \int_{-\infty}^{\infty} s(\omega)\bar{u}_\phi(r,\phi,o,\omega)\exp(i\omega t)d\omega \tag{9}$$

where $s(\omega)$ is the Fourier transform of s(t).

Contour Integration

For a perfectly elastic medium, the evaluation of the wave number integrals of Equation 1 is complicated by complex singularities along the real k-axis. The integrals to be evaluated are of the form

$$F(r,\omega) = \int_0^\infty f(k,\omega)\ J_n(kr)dk, \tag{10}$$

where the function $f(k,\omega)$ has poles and branch points k_{α_N} and k_{β_N} along the real k-axis. The SH functions $g_\phi^{nc,s}$ and F_L do not have the k_{α_N} branch point because of the absence of the ν_{α_N} term in Equations 4, 5 and 6. Following Ewing, Jardetzky and Press (1957), branch cuts are taken along the negative imaginary k-axis $[-i\infty, 0]$ and along the real k-axis $[0, k_{\beta_N}]$.

Expressing the Bessel function as a sum of Hankel functions of the first and second kinds, performing contour integration in the first and fourth quadrants of the complex k-plane, $\xi = k + i\tau$, it is not difficult to show that Equation 10 becomes

$$\begin{aligned} F(r,\omega) = {} & \frac{1}{2}\int_0^{k_{\beta_N}} [f_+(k,\omega) - f_-(k,\omega)]\ H_n^{(2)}(kr)dk \\ & - \pi\ i \sum \text{Res}\ f(k,\omega)\ H_n^{(2)}(kr) \\ & +(1/\pi)\int_0^\infty [f_+(i\tau,\omega)\ \exp(-in\pi/2) \\ & +f_-(-i\tau,\omega)\exp(in\pi/2)]\ K_n(\tau r)d\tau, \end{aligned} \tag{11}$$

where $K_n(z)$ is the modified Bessel function. The + or - subscripts indicate that Im ν_{α_N}, $\nu_{\beta_N} > 0$ or that Im ν_{α_N}, $\nu_{\beta_N} < 0$ respectively, be used to evaluate the expression for $f(k,\omega)$. Equation 11 contains the contributions of a real axis branch line integral, the surface wave poles and the imaginary axis branch line integral. This expression can be used for P-SV terms as well as for SH terms since the two real axis branch line integrals can be combined into one in the case of P-SV functions if one is not interested in evaluating the individual contributions of each branch line integral.

PART III: NUMERICAL TECHNIQUES

Contour Integration

Since both the Hankel function and modified Bessel function are undefined for zero argument, there are some inherent limitations in evaluating Equation 10, even before the problems of numerical integration are introduced. Following Fuchs and Müller (1971) the real axis branch line integral is evaluated using the transformation $k = k_{\beta_N} \sin\gamma$, $\gamma = [0, \pi/2]$. The real-axis branch line integral is now of the form

$$k_{\beta_N} \int_0^{\pi/2} g(k_{\beta_N} \sin\gamma,) \, H_n^{(2)}(k_{\beta_N} \sin\gamma \; r) \cos\gamma \; d\gamma, \tag{12}$$

where

$$g(x,\omega) = \frac{1}{2}\,[f_+(x,\omega) - f_-(x,\omega)].$$

The reason for this transformation is that it permits the evaluation of the Sommerfeld integral, which is basic to the wave propagation problem. A trapezoidal rule can be used to evaluate Equation 12, but such a rule becomes inefficient at large distances and high frequencies due to the rapidly oscillating nature of the Hankel function and the $g(x,\omega)$ term. To address this problem, it is assumed that a $\Delta\gamma$ be chosen such that $g(x,\omega)$ varies slowly enough over the range $[\gamma, \gamma + \Delta\gamma]$ that it can be approximated by linear segments. The integral of Equation 12 is now

$$k_{\beta_N} \sum_{i=1}^{M} \int_{\gamma_i}^{\gamma_{i+1}} [(A_i + B_i(\gamma-\gamma_i)] \, H_n^{(2)}(k_{\beta_N} r \sin\gamma) \, d\gamma, \tag{13}$$

where

$$\gamma_i = (i-1)\Delta\gamma \text{ and } \Delta\gamma = (\pi/2M).$$

To evaluate Equation 13, a tabulated integral of the Hankel function from Abramowitz and Stegun (1964) is used together with recurrence relations of the Hankel functions. Define

$$h(x) = \int_0^x H_0^{(2)}(z)\, dz, \tag{14}$$

where the integral can be expressed in terms of Hankel functions and Struve functions (Abramowitz and Stegun, 1964). The following are indefinite integrals of the Hankel functions which are of use in this study:

$$\begin{aligned}
\int H_0^{(2)}(z)\, dz &= h(z) \\
\int zH_0^{(2)}(z)\, dz &= z\, H_1^{(2)}(z) \\
\int H_1^{(2)}(z)\, dz &= -\, H_0^{(2)}(z) \\
\int zH_1^{(2)}(z)\, dz &= -\, z\, H_0^{(2)}(z) + h(z) \\
\int H_2^{(2)}(z)\, dz &= -\, 2\, H_1^{(2)}(z) + h(z) \\
\int zH_2^{(2)}(z)\, dz &= -\, 2\, H_0^{(2)}(z) - z\, H_1^{(2)}(z)\ .
\end{aligned} \tag{15}$$

It can be shown that

$$\int_{\gamma_i}^{\gamma_i+\Delta\gamma} [A_i + B_i(\gamma-\gamma_i)]\, H_n^{(2)}(k_{\beta_N} r \sin\gamma)\, d\gamma$$

$$= \int_{k_{\beta_N} r \sin(\gamma_i)}^{k_{\beta_N} r \sin(\gamma_i+\Delta\gamma)} [C_i + D_i(t-t_i)]\, H_n^{(2)}(t)\, dt \quad .$$

$$= (C_i - D_i t_i)\ [h(t)_{i+1}) - h(t_i)]$$

$$+ D_i\ [t_{i+1}\ H_1^{(2)}\ (t_{i+1}) - t_i H_1^{(2)}(t_i)] \quad \text{for } n=o \qquad (16)$$

and

$$= -\ C_i\ [H_o^{(2)}\ (t_{i+1}) - H_o^{(2)}\ (t_i)]$$

$$+ D_i\ [h(t_{i+1}) - h(t_i) - (t_{i+1} - t_i)\ H_o^{(2)}\ (t_i)]$$

$$\text{for } n=1$$

where

$$t_i = k_{\beta_N} r \sin \gamma_i$$

$$t_{i+1} = k_{\beta_N}\ r \sin\ (\gamma_i + \Delta\gamma)$$

$$C_i = A_i / k_{\beta_N}\ r \cos\ \gamma_i$$

$$D_i = B_i / (k_{\beta_N}\ r \cos\ \gamma_i)^2.$$

In evaluating Equation 12, a test is made to determine if it is sufficient to calculate the integral using a trapezoidal rule rather than using Equation 16.

The residue contribution of a function $g(z)/h(z)$ having a simple pole at $z = z_o$ is very simply $g(z_o)/h'(z_o)$, where $h'(z)$ is the first derivative of $h(z)$ with respect to z. The simple poles of Equation 1 arise due to the zeroes of the functions F_R or F_L.

The third expression in Equation 11 is an integral of the form

$$\int_0^\infty G(\tau,\omega)K_n(\tau r)d\tau \qquad (17)$$

Since the function $K_n(z)$ decreases in an exponential manner and since it has a singularity at z=o, the use of a Gauss-Laguerre integration rule is suggested if $G(\tau,\omega)$ does not oscillate too rapidly. After a change in variable and some manipulation, application of the Gauss-Laguerre rule yields the following approximation to Equation 17:

$$(1/r)\sum_{j=1}^{m} W_j\, G(x_j/r,\omega)\exp(x_j)K_n(x_j), \qquad (18)$$

where x_j and W_j are the abscissas and weights of an m'th order integration rule. Error is introduced due to the oscillatory nature of the function $G(\tau,\omega)$. However, this can be mitigated by using a very high order rule, so that the abscissas are spaced closely enough to sample the oscillations of $G(\tau,\omega)$. Because the weights decrease rapidly for large x_j, one can truncate the number of terms in the summation without significantly affecting the result. Following the suggestion of Davis and Rabinowitz (1975), the first 24 abscissas and weights of an m=68 rule are used.

The numerical contour integration techniques were tested by applying them to two integrands for which known analytic solutions exist. These are

$$\int_0^\infty \exp(-\nu_\beta z)\ J_0(kr)\ k\ dk$$

$$= (z/R^2)\ (1/R + ik_\beta)\ \exp(-ik_\beta R) \tag{19}$$

and

$$\int_0^\infty \exp(-\nu_\beta z)\ (k/\nu_\beta)\ J_1(kr)\ k\ dk$$

$$= (r/R^2)\ (1/R + ik_\beta)\ \exp(-ik_\beta R) \tag{20}$$

where $R^2 = r^2 + z^2$. Equations 19 and 20 are obtained by taking the partial derivatives $-\partial/\partial z$ and $-\partial/\partial r$, respectively, of the Sommerfeld integral. A detailed study of Equations 1-8 shows that the functions of Equations 19 and 20 are directly proportional to the far-field SH wave solution in an infinite medium excited by vertical dip-slip and vertical strike-slip sources, respectively. To a first order, SH wave displacements in a layered medium will involve similar terms. Thus these integrals provide a realistic test of the numerical integration techniques. The branch point at $k = k_\beta$ introduces a singularity in the real axis integration for Equation 20, but the change in variable $k = k_\beta \sin \gamma$ removes the singularity. In a layered halfspace, surface wave poles can coincide with the branch point. Even though the change in variable may alleviate this problem, it is avoided numerically by taking the range of γ as $[0,\pi/2-\varepsilon]$. An $\varepsilon = 0.0001$ gives good results for Equations 19 and 20 even at $r = 500$ km and frequencies up to 10 hz.

The integrals of Equations 19 and 20 were evaluated numerically using the techniques outlined in Equations 13 and 18. A value of β = 3.55 km/sec was used. The results of the tests are simply outlined. First, the numerical solution is valid at distances, r, as small as one-half source depth z, for all frequencies. At smaller distances, numerical evaluation of Equation 17 using the Gauss-Laguerre rule of Equation 18 breaks down due to inadequate sampling of the oscillating function $G(x_j/r,\omega)$ at low frequencies; a higher order rule would have to be used. At large distances and high frequencies the numerical integration of Equation 12 can fail due to the rapidly oscillating nature of the Hankel functions. Good results were obtained for Equation 20 at distances up to 500 km and frequencies up to 10 Hz using M=100, 200 and 300 for the frequency intervals (0,1), (1,5), and (5,10) Hz, respectively. On the other hand, the same choices of M only yielded good results for Equation 19 to distances of 100 km at frequencies of 10 Hz. This is due to the more rapid oscillation of the integrand of the real axis integral for Equation 19 than for Equation 20. Equation 19 really fails since one is trying to duplicate a z/R^2 dependence numerically for $R \gg z$. Experience with more complicated earth models indicates that the size of the error in evaluating the real axis branch line integral for a vertical dip-slip source is acceptable, since the contribution of the branch line integrals are quite small compared to the larger contributions of the surface wave poles, It can be shown that the function $g(x,\omega)$ in Equation 12 can be written as

$$g(k,\omega) = i \text{ Im } f_+(k,\omega) \quad , \tag{21}$$

since $f_+(k,\omega)$ is the complex conjugate of $f_-(k,\omega)$ for the SH problem and also for similar terms of the P-SV problem. Since $g(k,\omega)$ is an oscillatory function, it is informative to plot Im $f_+(k,\omega)$ as a function of frequency and wavenumber for various sources and earth models to obtain an appreciation of the nature of the integrand in Equation 12. In the following figures G1I is kIm $f_+(k,\omega)$ for the vertical dip-slip source and G2I is Im $f_+(k,\omega)$ for the vertical strike-slip source excitation of SH waves.

Figures 1, 2 and 3 show normalized G1I and G2I for focal depths of 1, 10 and 20 km, respectively, in a homogeneous halfspace model given in Table 1. The horizontal axis varies from $k=0$ to $k=k_{\beta_N}$. The functions are plotted at frequencies of 0.1, 0.5, 1.0, 5.0 and 10.0 Hz. The singularity at $k=k_{\beta_N}$ is due to the branch point for the halfspace problem.

Figures 4-6 present G1I and G2I for various depths in the single layer over a halfspace model of Table 1, while Figures 7-9 present the integrands for the four layer over a halfspace model of Table 1.

The integrands of Figures 1-3 are just those of Equations 19 and 20. It is seen that an increase in frequency or in focal

Table 1

Earth Models

	d(km)	α(km/sec)	β(km/sec)	ρ(gm/cm^3)
Halfspace				
	--	6.00	3.55	2.8
Simple Crustal Model (SCM)				
	40	6.15	3.55	2.8
	--	8.09	4.67	3.3
Central U. S. Model (CUS)				
	1	5.00	2.89	2.5
	9	6.10	3.52	2.7
	10	6.40	3.70	2.9
	20	6.70	3.87	3.0
	--	8.15	4.70	3.4

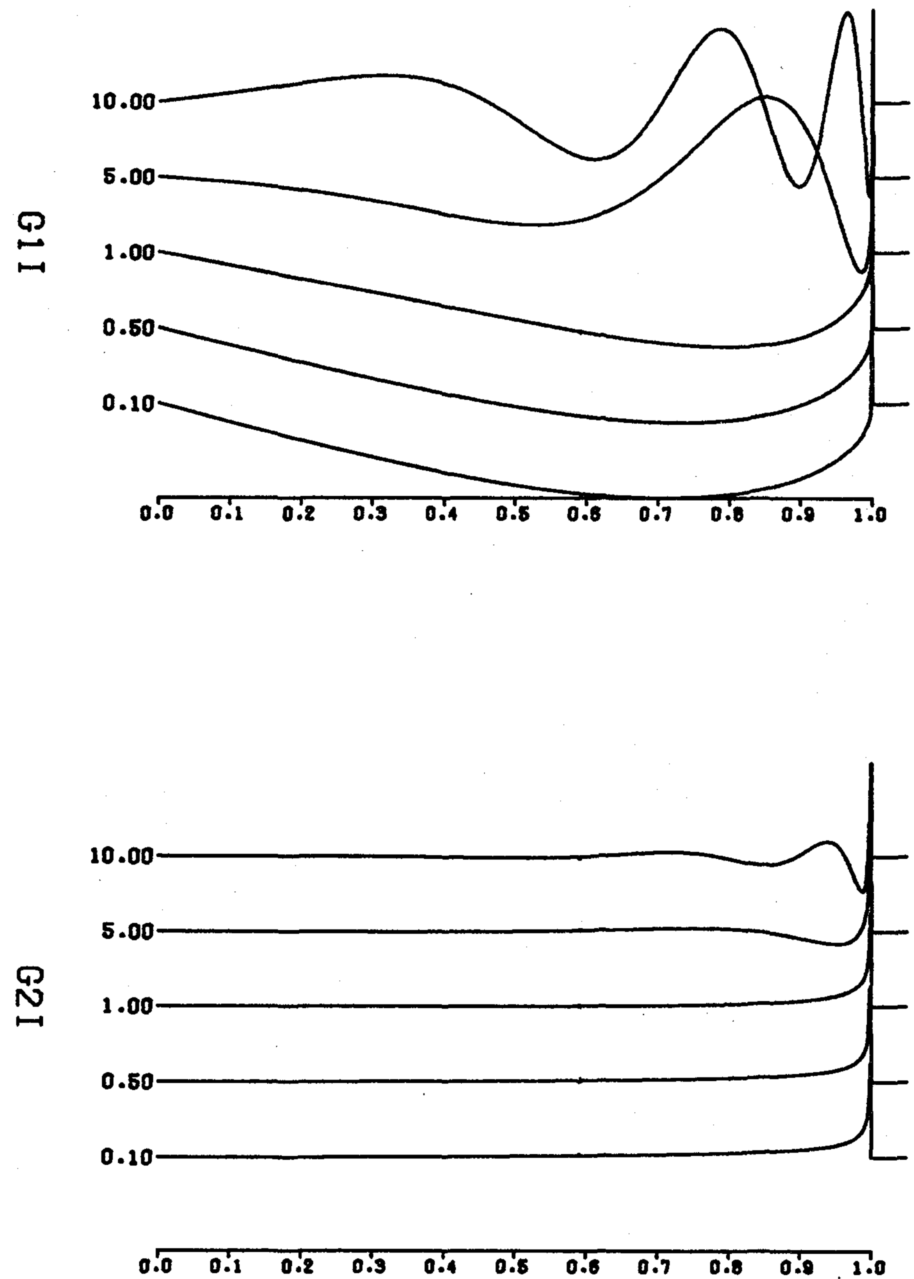

Fig. 1. G1I and G2I as a function of dimensionless wavenumber (k/k_{β_N}) for frequencies of 0.1, 0.5, 1.0, 5.0 and 10.0 Hz. The source is at a depth of 1 km in a simple halfspace.

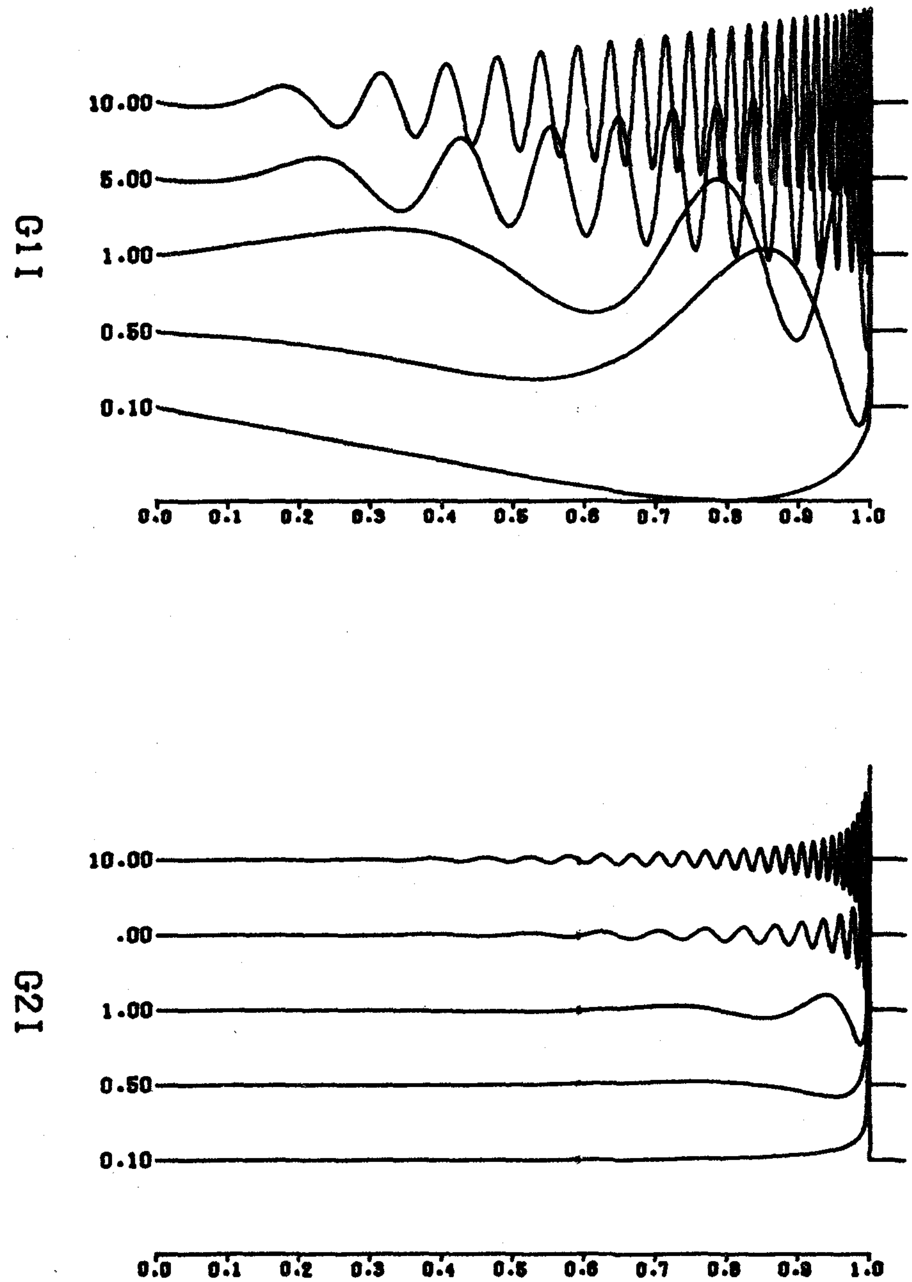

Fig. 2. G1I and G2I for a source at a depth of 10 km in a simple halfspace.

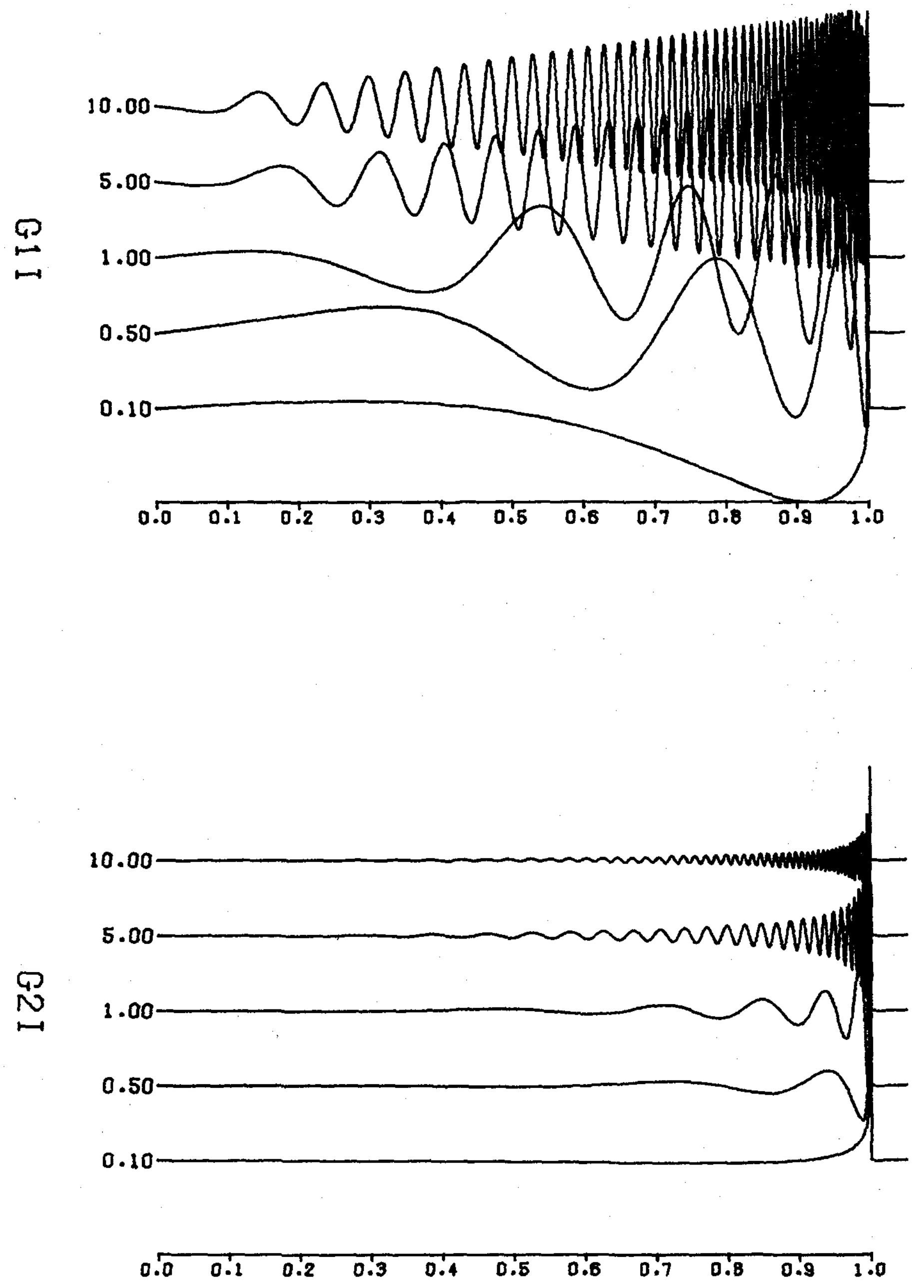

Fig. 3. G1I and G2I for a source at a depth of 20 km in a simple halfspace.

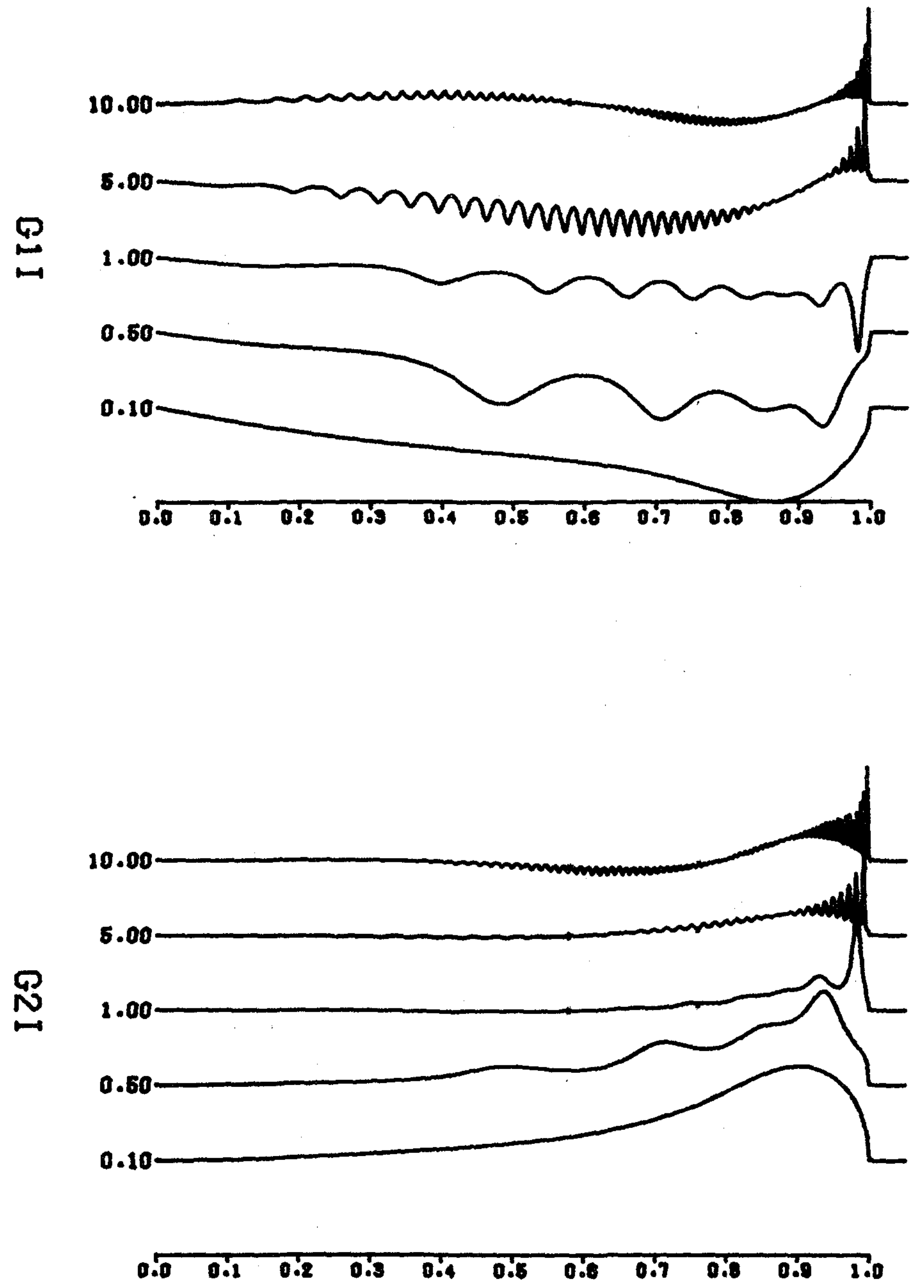

Fig. 4. G1I and G2I for a source at a depth of 1 km in the simple crustal model.

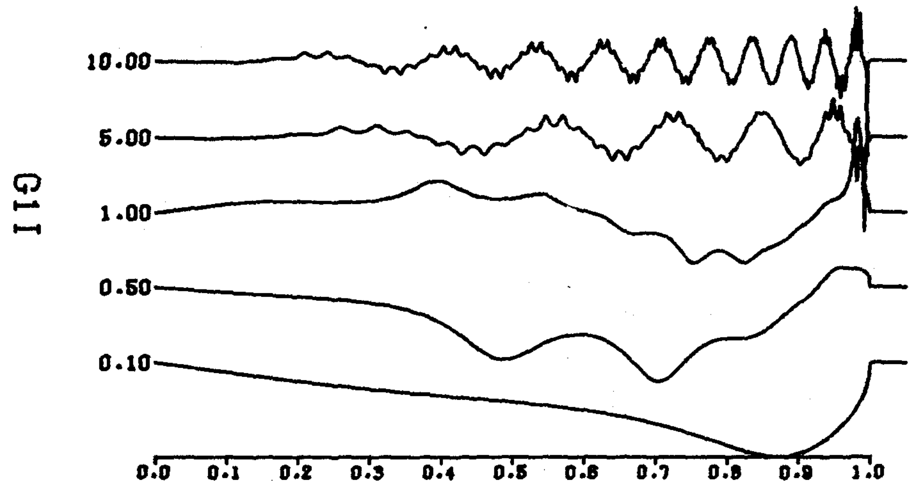

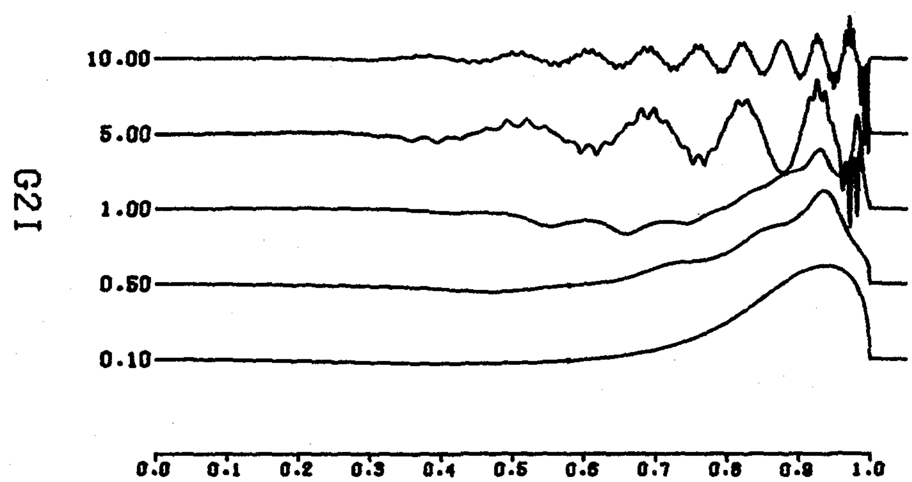

Fig. 5. G1I and G2I for a source at a depth of 10 km in the simple crustal model.

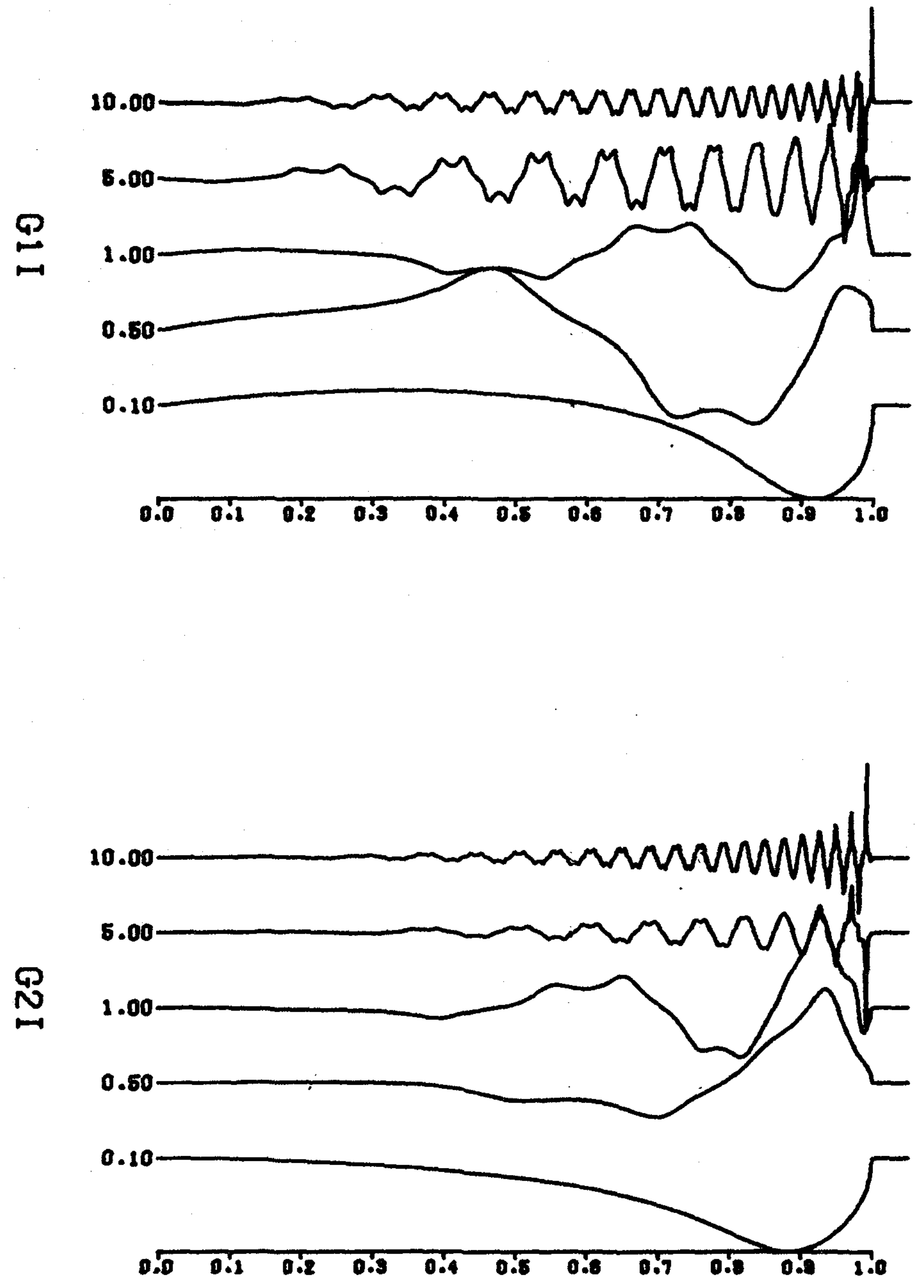

Fig. 6. G1I and G2I for a source at a depth of 20 km in the simple crustal model.

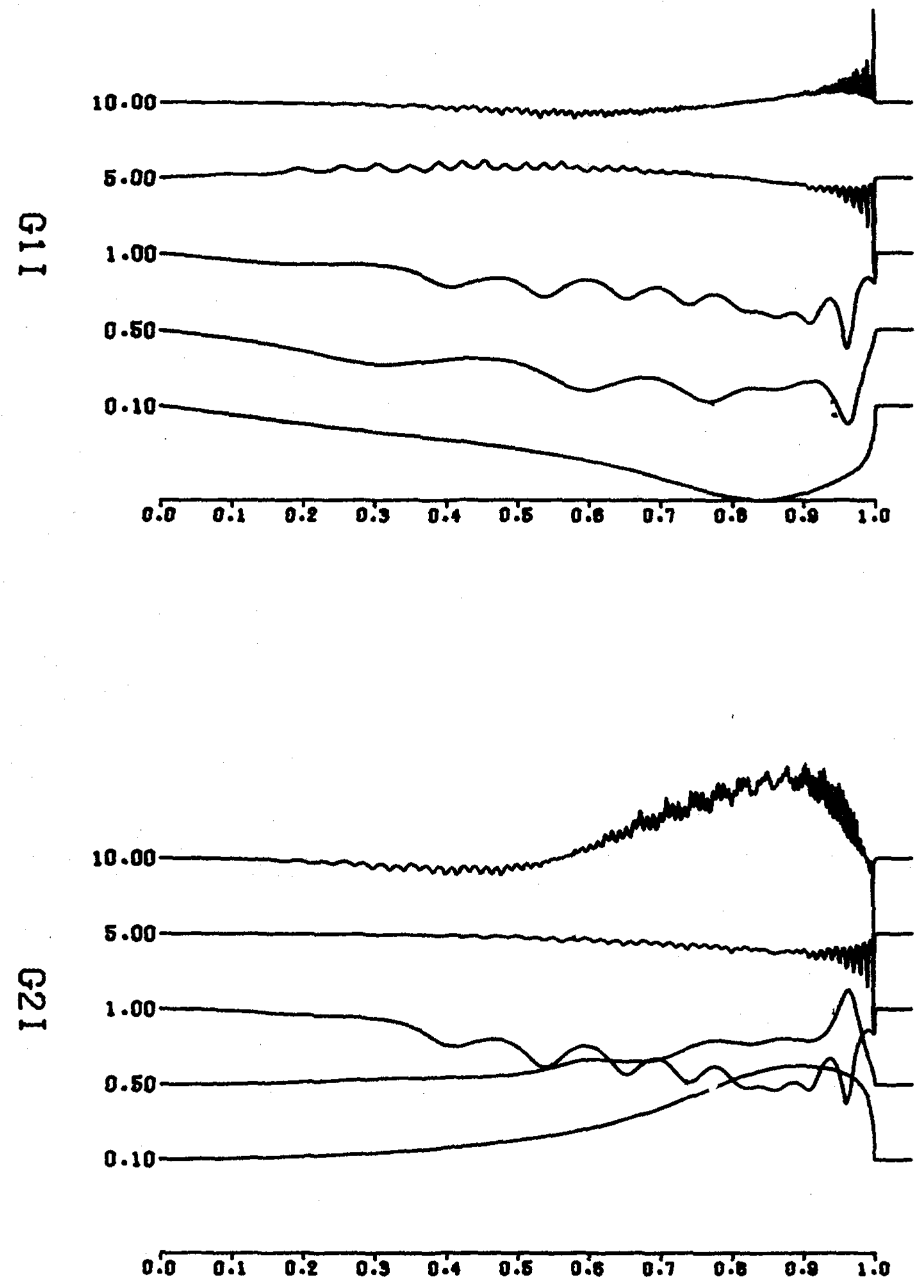

Fig. 7. G1I and G2I for a source at a depth of 1 km in the central U.S. model.

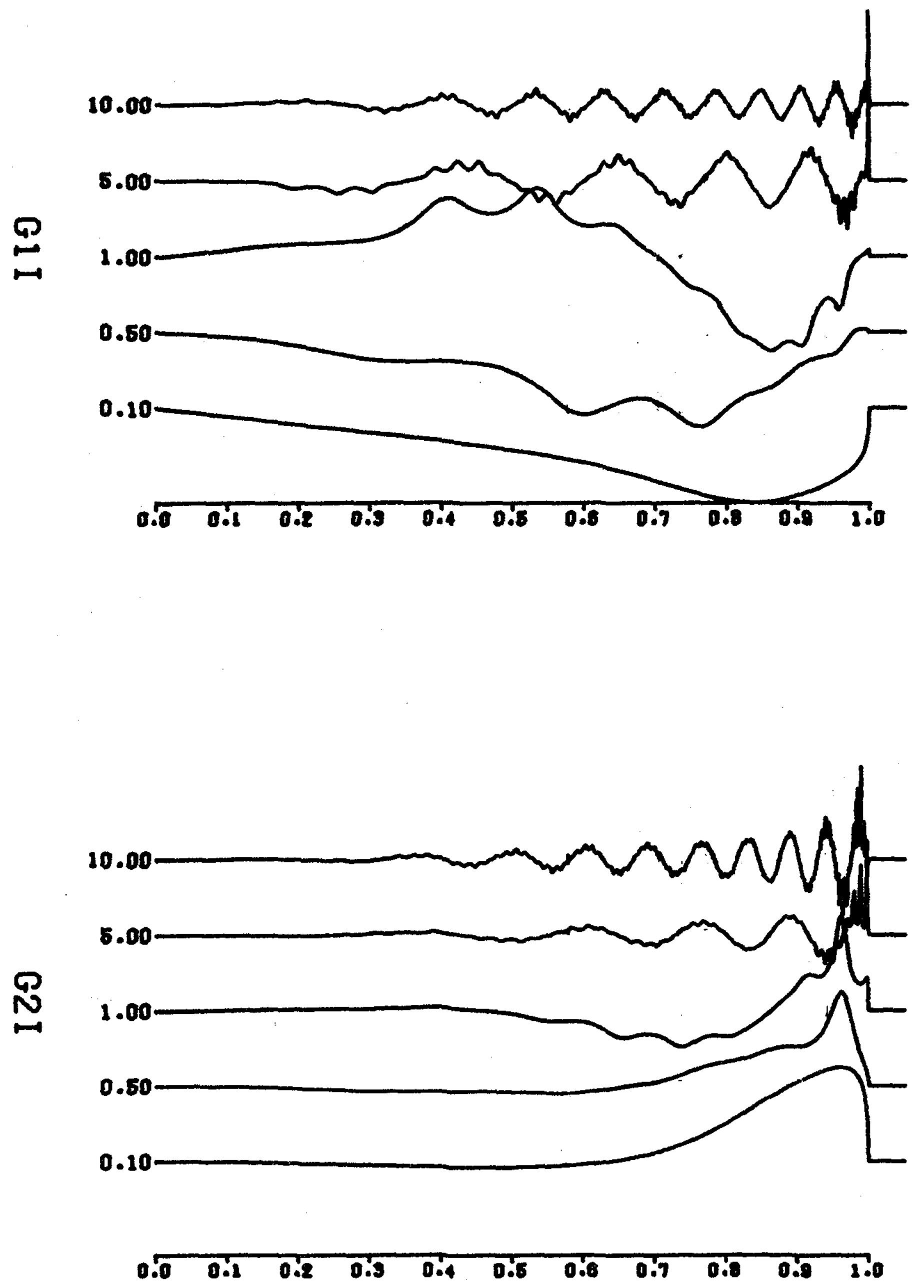

Fig. 8. G1I and G2I for a source at a depth of 10 km in the central U. S. model.

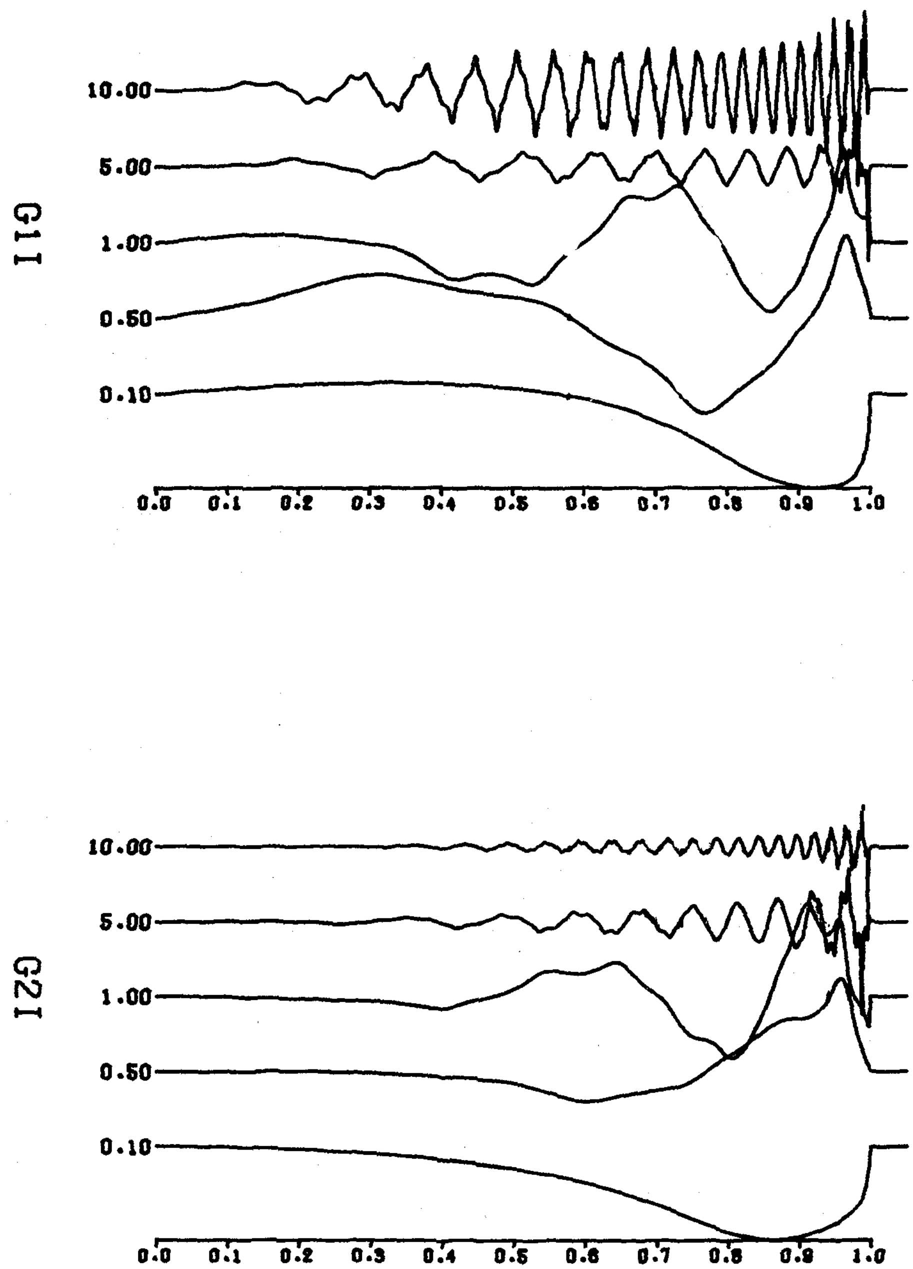

Fig. 9. G1I and G2I for a source at a depth of 20 km in the central U. S. model.

depth causes the function $g(k,\omega)$ to oscillate more rapidly. The effect of a more complicated structure is to introduce character to $g(k,\omega)$, but the simple observations still hold. The integration techniques used in the program SHSPEC have proven to work well to distances of 500 km and frequencies of up to 4 Hz (we have not yet run higher frequencies routinely).

The numerical techniques just described in this section are used by the computer program SHSPEC.

Velocity Time Histories

The spectra computed by the program SHSPEC are combined with a source time function in the program SHVEL to yield a velocity time history. A velocity time history is computed rather than a displacement time history because a discrete Fourier transform is used to convert spectra to time histories. Near the earthquake source, a final static offset is expected in the ground displacements. This offset cannot be handled by a discrete Fourier transform because of the inherent periodicity of the time series. To obtain the velocity time history of the ground motion, one need only convolve the impulse response of the medium with the velocity time history of the rupture process. The following two pulses are possible representations of this source function.

$$\tau\, s_1(t) = \begin{cases} 0 & t \le 0 \\ t/\tau & 0 \le t \le \tau \\ 2 - t/\tau & \tau \le t \le 2\tau \\ 0 & t \ge 2\tau \end{cases} \tag{22}$$

and

$$2\tau\, s_2(t) = \begin{cases} 0 & t \le 0 \\ \frac{1}{2}\,(t/\tau)^2 & 0 \le t \le \tau \\ -\frac{1}{2}\,(t/\tau)^2 + 2(t/\tau)-1 & \tau \le t \le 3\tau \\ \frac{1}{2}\,(t/\tau)^2 - 4(t/\tau)+8 & 3\tau \le \tau \le 4\tau \\ 0 & t \ge 4\tau \end{cases} \tag{23}$$

These pulses have been normalized such that the area under each pulse equals unity. The Fourier amplitude spectrum of $s_1(t)$ is such that its shape can be enveloped by an f^o and f^{-2} asymptote, which intersect at a corner frequency $f_c = (1/(\pi\tau)$ Hz. The Fourier amplitude spectrum of the other pulse can be enveloped by f^o and f^{-3} asymptotes which intersect at a corner frequency of $f_c = 1/(4.36\tau)$.

The corner frequencies are mentioned since the estimation of the corner frequency and seismic moment of an earthquake is current practice in the specification of an earthquake by seismologists today. Most observations of the ground motion spectra of earthquakes indicate that the high frequency spectra varies as f^{-2}. Thus the source pulse $s_1(t)$ might be favored. However, this choice is not very appealing on theoretical or numerical grounds since the whole-space solutions of Equation 19 and 20 would indicate delta function discontinuities in the acceleration time history at large distances, whereas the $s_2(t)$ large distance accelerations have only step discontinuities. Boore and Joyner (1978) provided a partial explanation. While $s_2(t)$ might be a good representation of a source time function to use for a small portion of the fault surface or for a faulting process involving coherent rupture, if one were to superimpose many $s_2(t)$ sources on the fault surface which "turn on" during an incoherent rupture process, the observed far-field spectrum will be enriched in high frequencies due to this incoherence, In the case of incoherent rupture one might be able to have both finite far-field accelerations as well as a high frequency spectral asymptote varying as f^{-2}.

Since the input to SHSPEC specified layer velocities in units of km/sec, distances in units of km and densities in units of gm/cm^3, source velocity pulses with unit area, such as $s_1(t)$ and $s_2(t)$, will correspond to sources with a seismic moment of 1.0E+20 dyne-cm.

Two time histories are presented, G1 and G2. G1 is the solution for the vertical dip-slip source and G2 is the solution for the vertical strike-slip source. Combining Equations 1, 2 and 8, the general equation for far-field displacements (those involving only g_ϕ kJ_{n-1}) are

$$U_\phi(t) = G_1[-2(t_2t_3-p_2p_3)\cos\phi +2(t_1t_3-p_1p_3)\sin\phi] \qquad (24)$$
$$+ G_2[-2(t_1t_2-p_1p_2)\cos2\phi-(t_2{}^2-t_1{}^2-p_2{}^2+p_1{}^2)\sin2\phi]$$

Displacement and Acceleration Time Histories

The program DSVLAC uses the velocity time history output of SHVEL to compute the ground displacement and acceleration time histories. The numerical realization of these time histories is not as obvious as it seems, especially for the ground accelerations. The output of SHVEL consists of ground velocity time histories at discrete points in time. Some assumption has to be made concerning the velocity variation at times in between, prior to integration or differentiation of the time series. Several approaches were considered, including the use of cubic spline interpolation. After much thought, the variation of ground velocity was assumed to be linear between the discretely sampled values. Thus, ground displacements can be computed using a simple two-point trapezoidal integration rule.

The acceleration time history then consists of a sequence of step segments. While this method of presenting the acceleration time history may seem odd, there are certain advantages. The cubic spline interpolation method was discounted because the smoothing process introduced ripples, which were purely an artifact of the smoothing process, into the acceleration time histories. The use of linear segments for the velocity time history permits an estimate of the acceleration that is not obscured by a smoothing process and also points out the discrete nature of the ground motion synthesis.

Response Spectra

The program SDSVSA uses the output of the program DSVLAC to compute the response spectra of the seismic traces. The input to SDSVSA from DSVLAC consists of the velocity time history at a given distance for the particular source as well as the computed maximum displacement, velocity and acceleration of the time history. The development of SDSVSA follows that of Nigam and Jennings (1969), with the modification that the velocity varies linearly between two time samples for the reasons used in discussing DSVLAC,

The equation of motion of a single degree of freedom oscillator with natural frequency ω and fraction of critical damping ζ subjected to a base acceleration a(t) is

$$\ddot{x} + 2\zeta\omega\dot{x} + \omega^2 x = -a(t). \tag{25}$$

To find the motion x(t) in the time interval $t_i \leq t \leq t_{i+1}$, the change of variable $\tau = t - t_i$ is introduced so that the equation of motion becomes

$$\frac{d^2x(\tau)}{d\tau^2} + 2\zeta\omega \frac{dx(\tau)}{d\tau} + \omega^2 x(\tau) = -a(\tau). \tag{26}$$

Integrating with respect to τ, one obtains

$$\dot{x}(\tau) - \dot{x}(o) + 2\zeta\omega x(\tau) - 2\zeta\omega x(o) + \omega^2 \int_o^\tau x(\tau')\, d\tau' = -\{v(\tau)-v(o)\} \tag{27}$$

When $v(\tau)$ is given by linear segments, then

$$v(\tau) = v(0) + \frac{\Delta v(0)}{\Delta\tau} \cdot \tau \quad . \tag{28}$$

Equation 27 now becomes

$$\dot{x}(\tau) + 2\zeta\omega x(\tau) + \omega^2 \int_0^\tau x(\tau')d\tau' = \dot{x}(o) + 2\zeta\omega x(o) - \frac{\Delta v(o)}{\Delta\tau} \cdot \tau \tag{29}$$

This equation can be solved by using Laplace transform techniques. After some algebraic manipulation, the motion of the oscillator at time t_{i+1} can be found iteratively by the relation

$$\begin{vmatrix} x_{i+1} \\ \dot{x}_{i+1} \end{vmatrix} = \begin{vmatrix} a_{11} & a_{12} \\ a_{21} & a_{22} \end{vmatrix} \begin{vmatrix} x_i \\ \dot{x}_i \end{vmatrix} + \begin{vmatrix} b_1 \\ b_2 \end{vmatrix} \begin{vmatrix} v_{i+1} - v_i \end{vmatrix} \tag{30}$$

where

$a_{11} = C + \omega\zeta\ S$

$a_{12} = S$

$a_{21} = -\ \omega^2 S$

$a_{22} = C - \omega\zeta\ S$

$b_1 = (-1 + C + \omega\zeta\ S)/\ \omega^2\Delta t$

$b_2 = -S/\Delta t$

$C = \exp(-\ \zeta\omega\Delta t)\ \cos\ (\omega_d\Delta t)$

$S = \exp(-\zeta\omega\Delta t)\ \sin\ (\omega_d\Delta t)/\omega_d$

and

$$\omega_d = \omega\ (1 - \zeta^2)^{1/2}$$

These results could also be obtained from Nigam and Jennings (1969) by setting their $a_i = a_{i+1}$.

The response spectra are defined as

$$SD = MAX\ [\ x_i(\omega,\zeta)\ ]$$

$$SV = MAX\ [\ x_i(\omega,\xi)\ ] \tag{31}$$

and

$$SA = MAX\ [\ \ddot{z}\ (\omega,\zeta)\ ]\ ,$$

where

$$\ddot{z} = -\ (2\zeta\omega x_i + \omega^2 x_i\ )\ .$$

The pseudo velocity spectra is defined as

$$PSV = \omega\ SD\ .$$

PART IV. NUMERICAL EXAMPLES

Truncation

A term by term inspection of Equation 1 shows that the tangential displacement can be thought to be made up of a far-field SH term, a near-field SH term, and a near-field P-SV term. Since it is much easier and faster to compute the SH functions than the P-SV terms, it is of interest to see the distance range at which a truncated version would provide acceptable results. To do this, a computer program developed by Johnson (1974) was used to compute the tangential displacements at the surface of an elastic halfspace for a north-south striking right lateral strike-slip source and for a north-south striking vertical dip-slip source, with west side downthrown, at a receiver azimuth of 0^{o}. A seismic moment of 3.53 E +21 dyne-cm was used together with the source function $s_2(t)$ with $\tau = 0.5$ sec at a depth of 10 km in a halfspace with $\alpha = 6.15$ km/sec, $\beta = 3.55$ km/sec and $\rho = 2.8$ gm/cm^3.

Figures 10, 11 and 12 show the computed displacement, velocity and acceleration time histories, respectively, at distances of 10,25, 50 and 75 km for the vertical dip-slip source. Figures 13, 14 and 15 are the corresponding displacement, velocity and acceleration time histories, respectively, for the vertical strike-slip source. The units for displacement, velocity and acceleration are cm, cm/sec and cm/sec^2, respectively. At each distance, the trace on the left

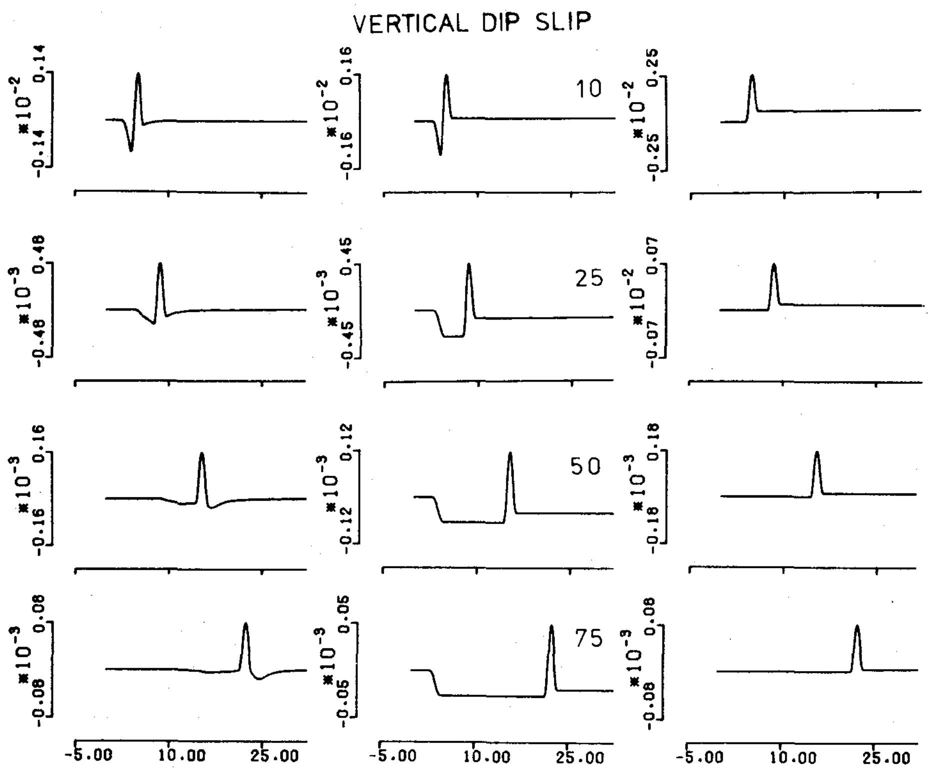

Fig. 10. Study of truncation effect for tangential displacement *time histories for a vertical dip-slip source at a depth of* 10 km in a halfspace. Left column is complete solution, center column includes near and far field SH contribution, and the right column corresponds to the far field SH contribution at various distances.

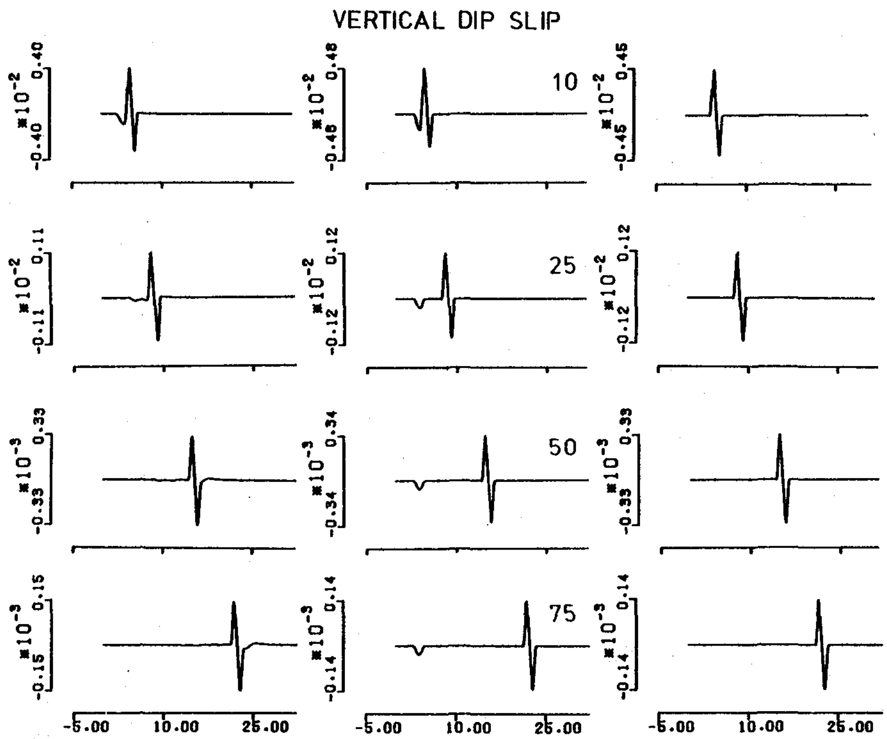

Fig. 11 Same as Fig. 10. but for corresponding velocity time histories.

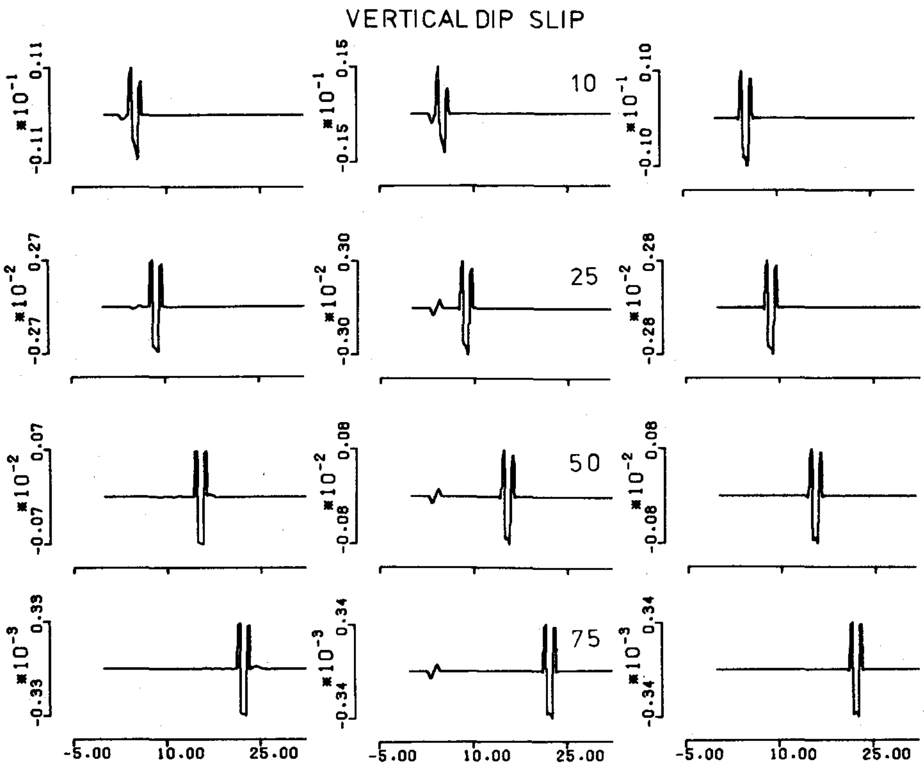

Fig. 12. Same as Fig. 10, but for corresponding acceleration time histories.

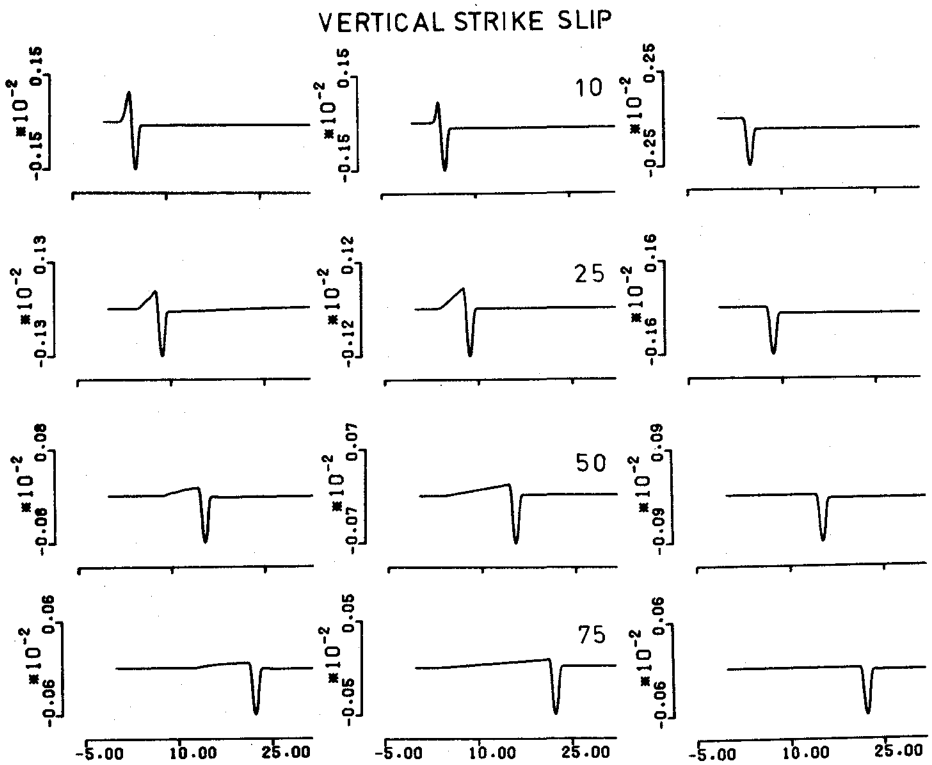

Fig. 13. Same as Fig. 10, but for displacement time histories for the vertical strike-slip source.

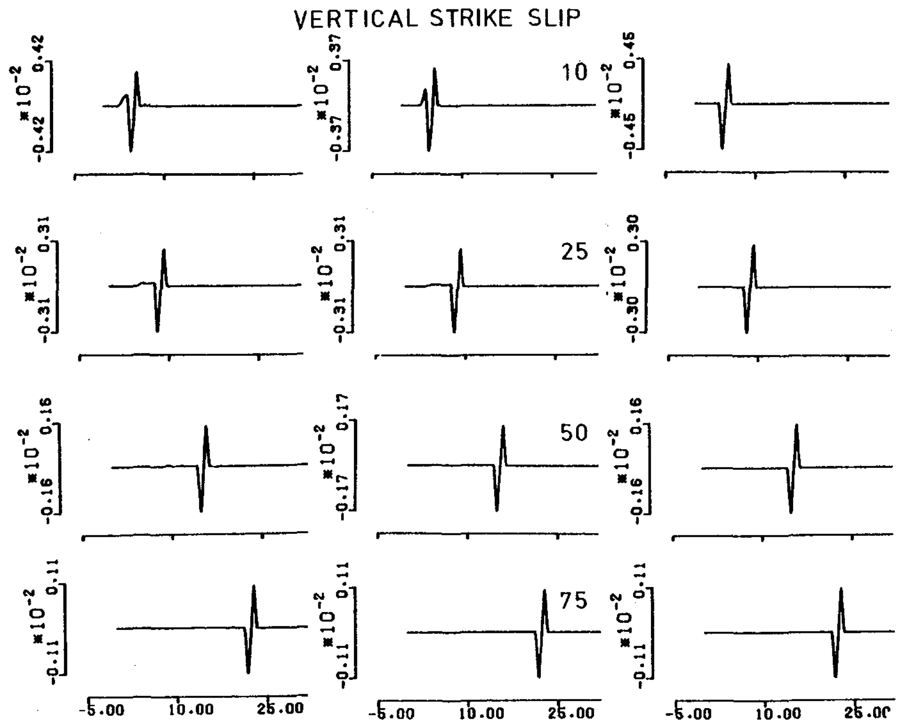

Fig. 14. Truncation study for velocity time histories of a vertical strike-slip source.

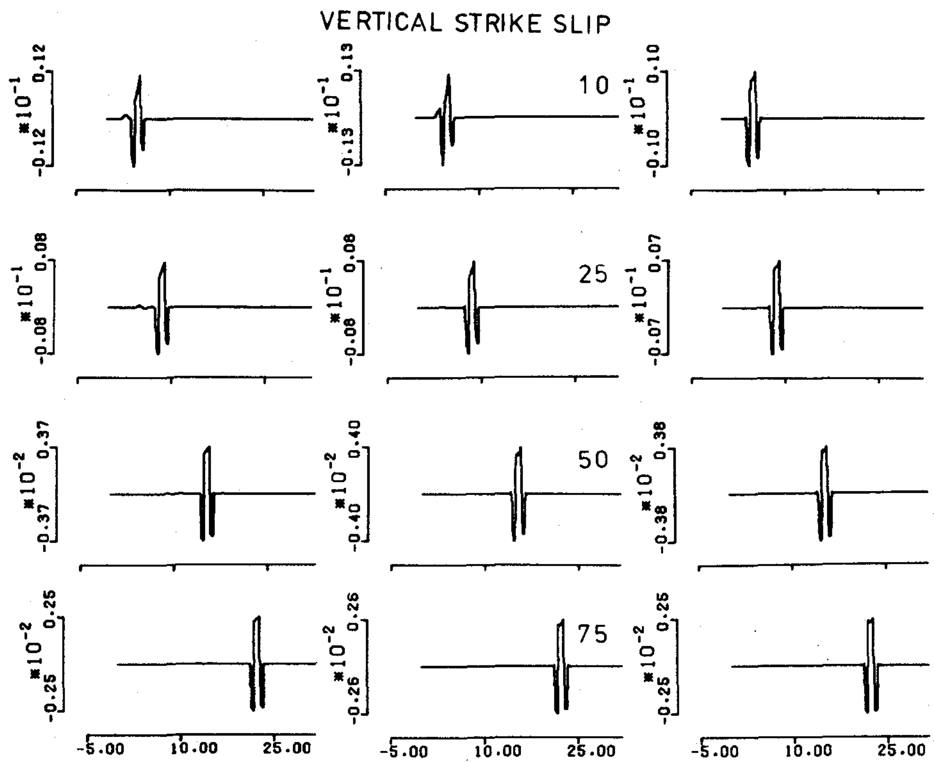

Fig. 15. Same as Fig. 13, but for acceleration time histories of a vertical strike-slip source.

corresponds to the complete solution, the center trace corresponds to the solution when the g_r/F_R term is dropped, while the trace on the right corresponds to the far-field SH solution obtained by using only the term $g_\phi k J_{n-1}(kr)/F_L$ in Equation 1.

Remarkably, the complete solution (left trace) and the far-field solution (right trace) are very similar at distances greater than 25 km. At nearer distances, the near-field P and SV wave contributions change the character of the signal, especially for the ground displacements. The center trace shows the presence of non-causal, non-propagating arrivals, especially for the vertical dip-slip source. Herrmann (1978) interpreted this as an effect of improper truncation, in that the non-causal arrival must be cancelled by a similar "arrival" in the P-SV term. The difference between the true and far-field solution is clearly frequency dependent, with the difference becoming smaller at higher frequencies, as can be seen by comparing the displacement, velocity and acceleration time histories, or by a study of the wave number dependence of the terms in Equation 1.

Similar figures were computed using $\tau = 1.0$ which indicated significant differences between true and far-field displacements at distances less than 50 km, whereas the velocity and acceleration time histories were reasonally close at distances as small as 25 km. Because of the lack of a similar complete solution for a layered medium problem, it is assumed that the observations made here concerning the adequacy of the far-field solution will still hold.

From this point onward only the time histories associated with far-field SH contributions will be computed.

Contribution of Singularities

To understand the relative importance of each term in Equation 11, a series displacement of time histories were prepared. These are shown in Figures 16 and 17 for a source at a depth of 10 km in the Central U.S. model of Table 1 with a seismic moment of 3.53 E +22 dyne-cm, a source time function $s_2(t)$ with $\tau = 0.5$ sec and a low pass filter set at 1.0 Hz. The traces on the left and right of Figure 16 correspond to solutions at a distance of 25 km due to vertical dip-slip and vertical strike-slip sources, respectively. Solution (a) is just the contribution of the poles, (b) is the effect of adding the real axis branch line integral to the pole contribution, and (c) is the complete solution consisting of the pole contributions and real and imaginary axis branch line integrals. The pole contributions yield a non-causal arrival for both sources (the later arrivals are in fact early negative time arrivals due to the inherent periodicity of the discrete Fourier transform). The addition of the real axis branch line integral improves causality and raises signal amplitudes to their final levels. The branch line integral along the negative imaginary k-axis, affects the signal amplitude slightly while making the signal causal.

Figure 17 is similar to Figure 16 except that the comparison

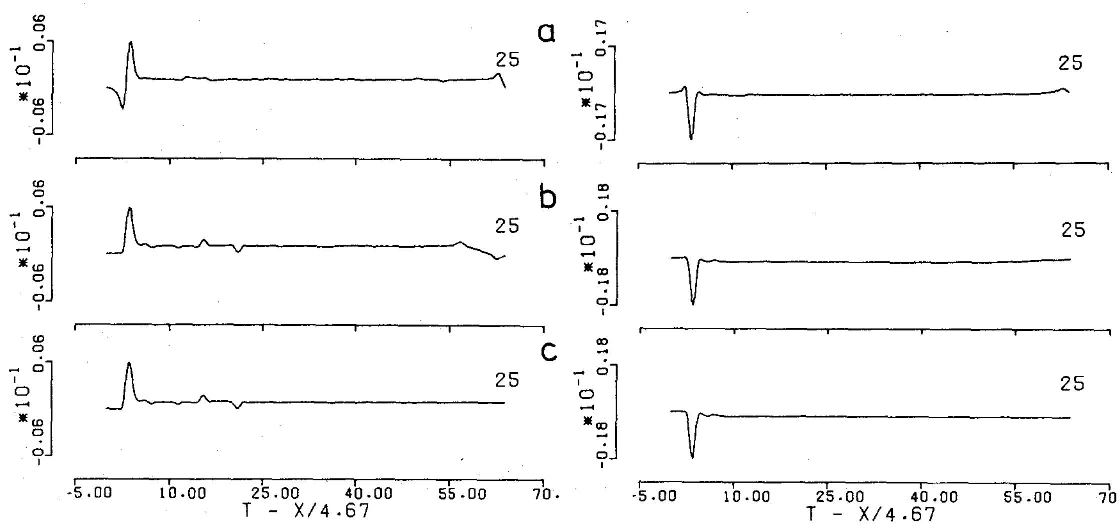

Fig. 16. Study of contribution of various components of contour integration on the far field SH contribution to displacement time histories for a vertical dip-slip source, left column, and a vertical strike-slip source, right column, at a distance of r = 25 km. (a) pole contribution alone; (b) pole contribution plus real axis branch line integral; and (c) pole contribution together with real axis and negative imaginary axis branch line integrals.

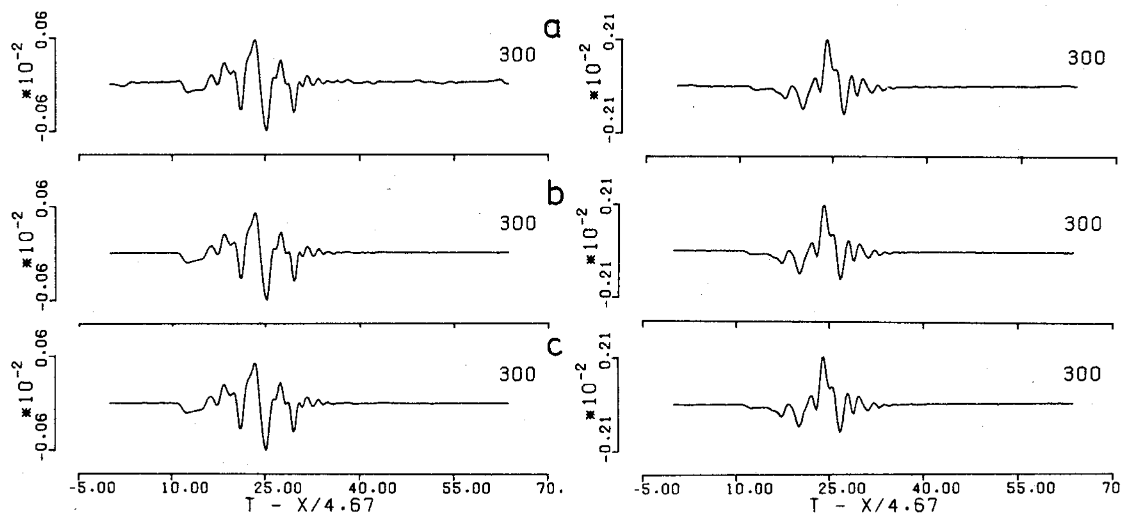

Fig. 17. Same comparison as for Fig. 16, but at a distance of r = 300 km.

is made at a distance of 300 km. Surprisingly, this figure shows that at large distances the pole contributions describe the signal quite well, even the S_n phases. The addition of the real axis branch line integral just improves causality, while the imaginary axis branch line integral has little effect because of the 1/r factor in Equation 18. Using other values of τ the waveform distortion obtained at short distances using just the poles, or poles and real axis branch line integrals, is found to get worse as higher frequencies are excluded.

An insight has been obtained on saving computer time. At short distances, the complete solution with poles and branch line integrals is required for proper description of low frequency response. At large distances, especially if one is not bothered by low amplitude non-causal arrivals, the pole contributions are all that are required for a realistic estimate of the solution. By not having to perform the imaginary axis branch line integral at distances greater than 100 km, computer time savings can be significant. Swanger and Boore (1978) presented some examples showing how the individual surface wave modes add to form the solution. Their study also shows how well the pole contributions alone can fit real strong motion data.

Model Studies

To obtain an idea of the process of wave propagation, far-field time histories were computed for two of the earth models given in Table 1. A point dislocation source with a seismic moment of 3.53 E +22 dyne-cm and a source time function $s_2(t)$ with $\tau = 0.5$ sec is placed at a depth of 10 km. The signals have been windowed to exclude all frequencies greater than 1.0 Hz. The resulting ground velocity time histories at various distances are given in Figure 18 for the single layer over a halfspace crustal model and in Figure 19 for the four layer over a halfspace crustal model. In these figures, the traces in column "a" correspond to a receiver at the given distance due north of a north-south striking vertical dip-slip source with the west side downthrown while those in column "b" correspond to ground motions due north of a north-south striking right lateral vertical strike-slip source. In Figure 18, it is seen that the first arrival is followed by two similar pulses of lower amplitude for the dip-slip source. These arrivals are the first Moho reflections due to downward and upward rays leaving the source. As distance increases, these reflections undergo a phase change when supercritical reflection occurs. The subcritical, non-phase changed, reflections are of low amplitude relative to the supercritical reflections. The surface wave can be said to emerge at a distance greater than 75 km as the number of supercritical reflections in the signal increases. A similar effect can be seen with the vertical strike-slip source,

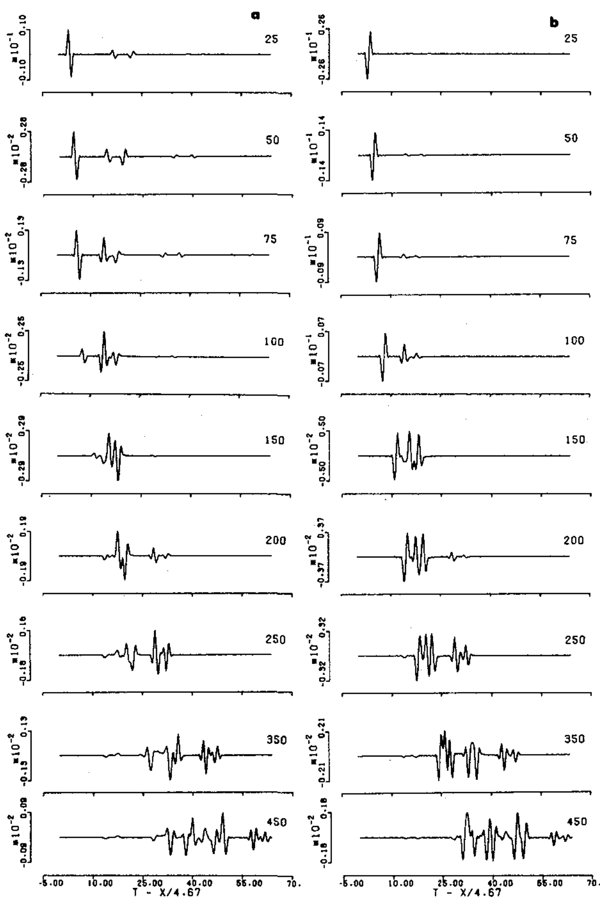

Fig. 18. Suite of far field tangential velocity time histories for the simple crustal model of Table 1 for a vertical dip-slip source (a) and for a vertical strike-slip source (b) as a function of distance in kilometers.

column "b", except that the near vertical reflections at short distances are not very large. This is because the vertical dip-slip source has a maximum in its SH radiation pattern at vertical take-off angles, while the vertical strike-slip source has a mode for vertical take-off angles (Helmberger, 1974).

For a complicated structure, Figure 19, interpretation of the various arrivals in terms of particular ray paths is not very obvious. The vertical dip-slip source, column "a", shows some very distinct reflected phases which can be followed out to 75 km. At larger distances, the number of significant arrivals within a short time interval becomes so large that they are not seen as distinct arrivals, but rather as a composite surface wave. Refracted S_n arrivals can be seen emerging from the surface wave group at larger distances. An interesting point is the significant variation in the signal character over distances of only fifty kilometers, whereas gross properties such as maximum velocity only vary slightly.

Figures 20 and 21 show the pseudo velocity response spectra at distances of 25 and 300 km, respectively for a vertical strike slip source at a depth of 5 km in the central U. S. model of Table 1. A seismic moment of 5.0 E +19 dyne-cm, a source pulse $s_2(t)$ with $\tau = 0.5$ sec, and a low pass filter set at 4.0 Hz were used. The insert in each figure shows the computed acceleration time histories. Tabulated values of the output of SDSVSA corresponding to the plots, Figures 20 and 21, are given in Figures 22 and 23.

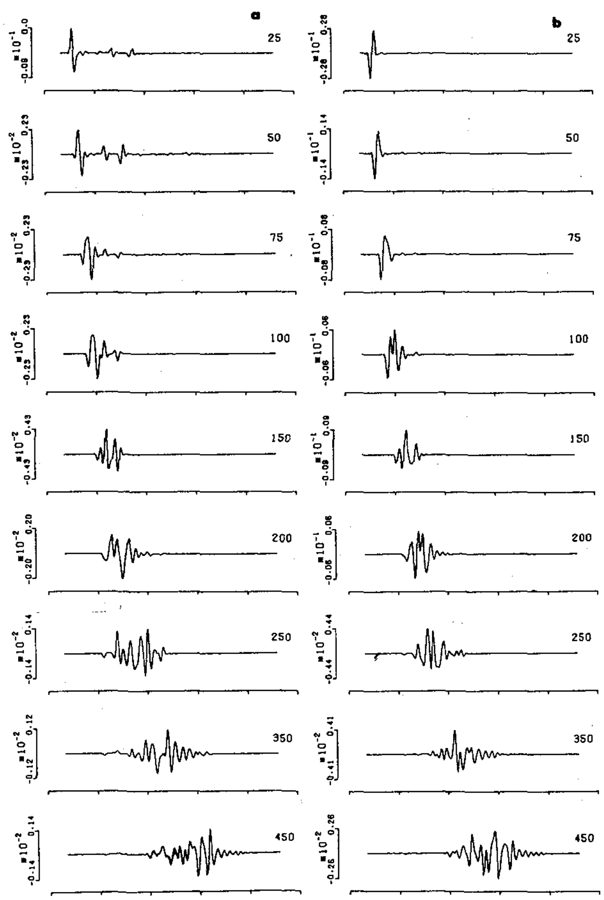

Fig. 19. Suite of far field tangential velocity time histories for the central U. S. model of Table 1 for a vertical dip-slip source (a) and for a vertical strike-slip source (b) as a function of distance in kilometers.

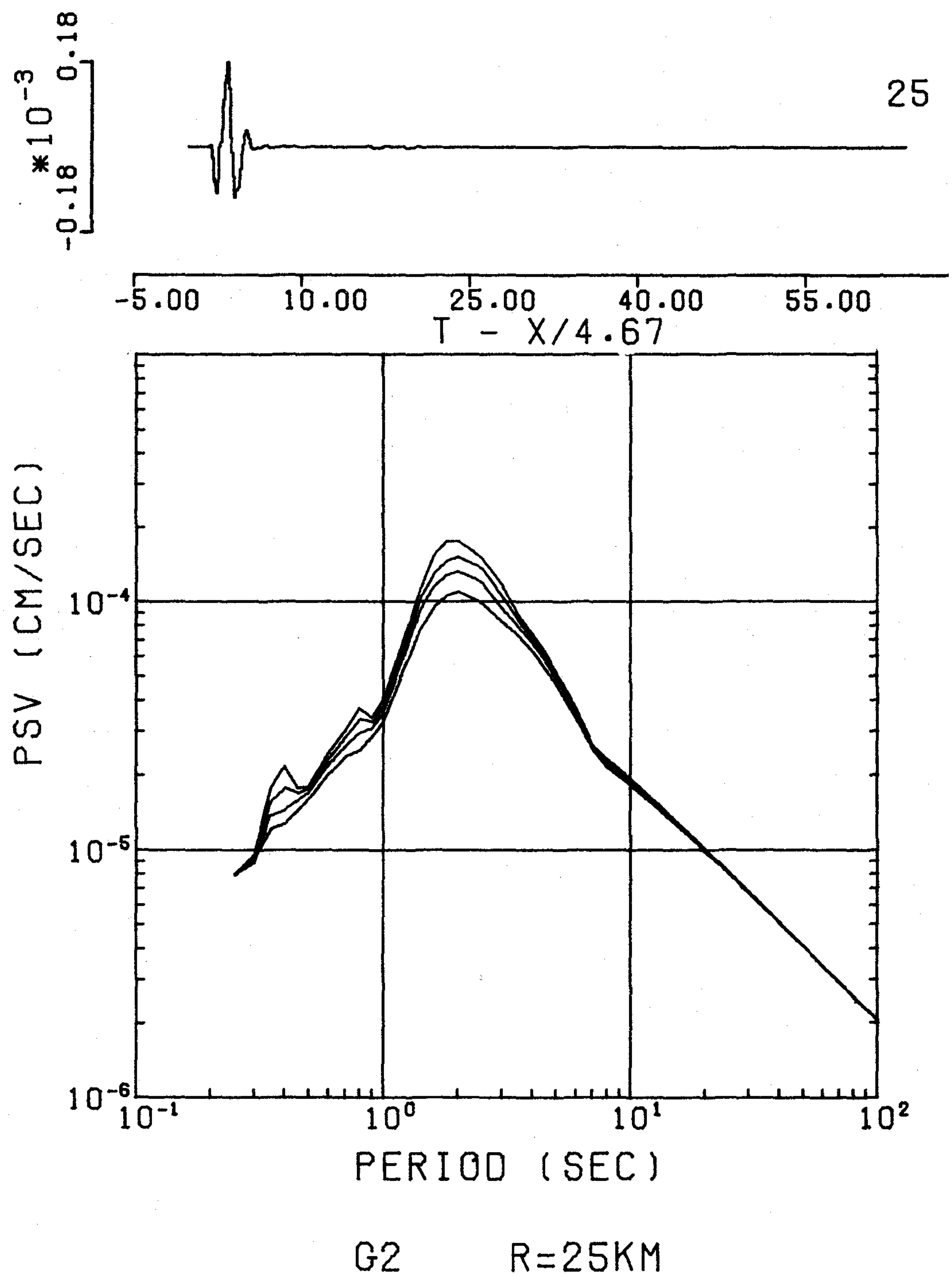

Fig. 20. Pseudo velocity response spectra of a vertical strike-slip source at a distance of 25 km for 0, 2, 5, and 10 percent critical damping. The inset is the acceleration time history.

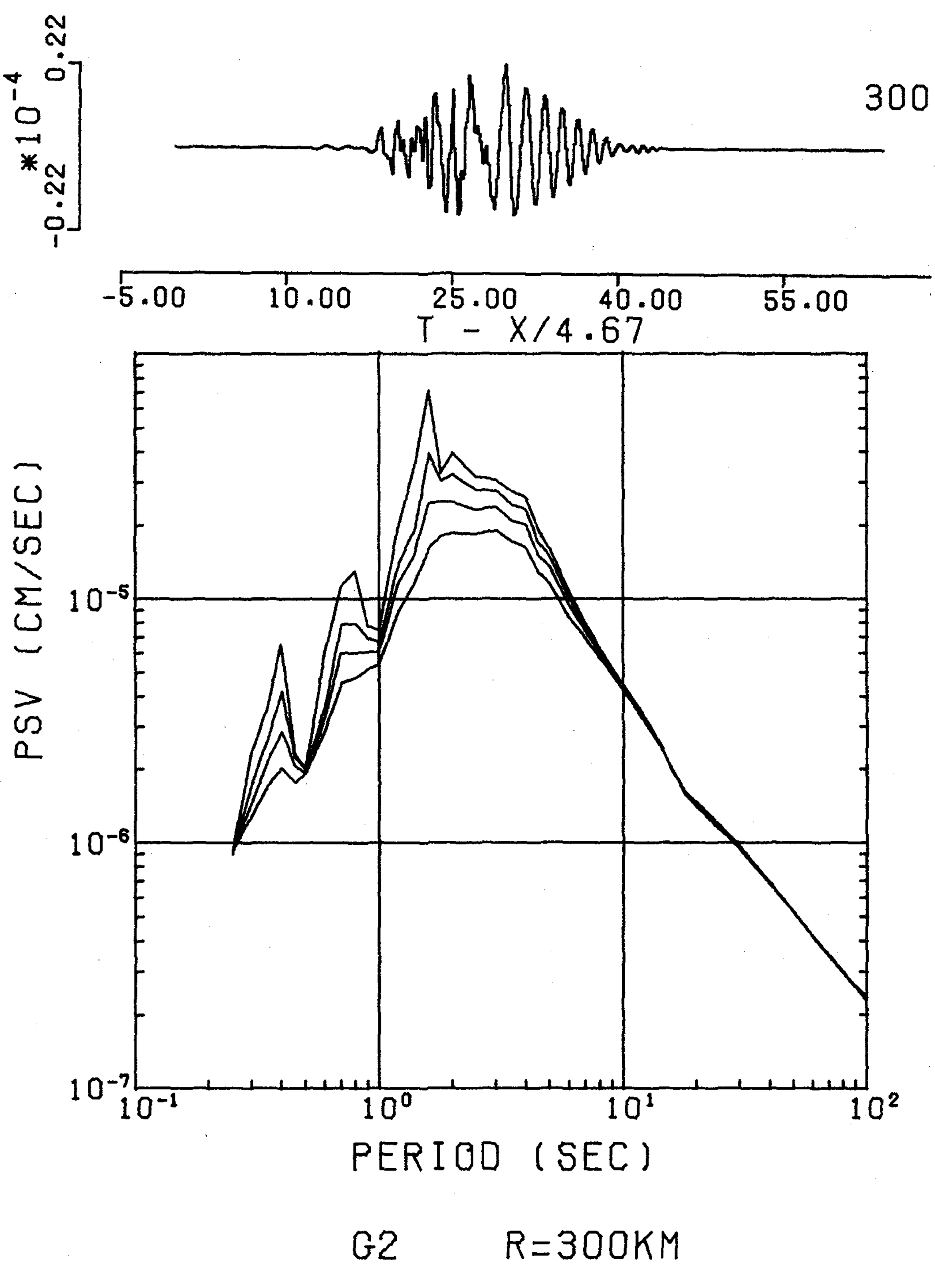

Fig. 21. Pseudo velocity response spectra of a vertical strike-slip source at a distance of 300 km for 0, 2, 5 and 10 percent critical damping. The inset is the acceleration time history.

G2 (R= 25.00 KM DEPTH= 5.00 KM)

AMAX= 0.18E-03 VMAX= 0.53E-04 DMAX= 0.33E-04

		DAMP=0.				DAMP=0.02				DAMP=0.05				DAMP=0.10			
PERIOD	FS	SD	SV	SA	PSV	SD	SV	SA	PSV	SD	SV	SA	PSV	SD	SV	SA	PSV
0.25	.16-7	.32-6	.30-5	.20-3	.80-5	.32-6	.29-5	.20-3	.80-5	.32-6	.28-5	.20-3	.80-5	.31-6	.25-5	.20-3	.79-5
0.30	.41-5	.45-6	.51-5	.20-3	.95-5	.43-6	.39-5	.19-3	.89-5	.42-6	.32-5	.19-3	.89-5	.44-6	.29-5	.19-3	.93-5
0.35	.79-5	.97-6	.10-4	.31-3	.17-4	.87-6	.83-5	.28-3	.16-4	.77-6	.63-5	.25-3	.14-4	.67-6	.50-5	.22-3	.12-4
0.40	.17-4	.14-5	.18-4	.34-3	.22-4	.11-5	.13-4	.28-3	.18-4	.92-6	.10-4	.23-3	.14-4	.81-6	.80-5	.20-3	.13-4
0.45	.28-5	.13-5	.87-5	.25-3	.18-4	.12-5	.83-5	.24-3	.17-4	.11-5	.77-5	.22-3	.16-4	.10-5	.75-5	.20-3	.14-4
0.50	.15-7	.14-5	.64-5	.23-3	.18-4	.14-5	.63-5	.22-3	.18-4	.14-5	.67-5	.21-3	.17-4	.13-5	.72-5	.20-3	.16-4
0.60	.63-5	.23-5	.13-4	.26-3	.24-4	.22-5	.12-4	.24-3	.23-4	.21-5	.12-4	.23-3	.22-4	.19-5	.11-4	.21-3	.20-4
0.70	.21-4	.34-5	.26-4	.27-3	.30-4	.31-5	.24-4	.25-3	.28-4	.29-5	.21-4	.23-3	.26-4	.26-5	.17-4	.22-3	.24-4
0.80	.24-4	.47-5	.28-4	.29-3	.37-4	.43-5	.25-4	.26-3	.33-4	.37-5	.23-4	.23-3	.29-4	.32-5	.20-4	.20-3	.25-4
0.90	.13-4	.49-5	.23-4	.24-3	.34-4	.47-5	.22-4	.23-3	.33-4	.44-5	.20-4	.22-3	.31-4	.41-5	.19-4	.20-3	.28-4
1.00	.10-7	.64-5	.27-4	.25-3	.40-4	.61-5	.25-4	.24-3	.38-4	.57-5	.23-4	.23-3	.36-4	.53-5	.22-4	.21-3	.33-4
1.20	.36-4	.13-4	.54-4	.35-3	.68-4	.12-4	.50-4	.33-3	.64-4	.11-4	.46-4	.31-3	.58-4	.99-5	.41-4	.27-3	.52-4
1.40	.98-4	.24-4	.99-4	.49-3	.11-3	.23-4	.89-4	.45-3	.10-3	.20-4	.75-4	.40-3	.90-4	.17-4	.63-4	.34-3	.76-4
1.60	.15-3	.39-4	.15-3	.60-3	.15-3	.33-4	.13-3	.51-3	.13-3	.29-4	.10-3	.45-3	.11-3	.24-4	.84-4	.37-3	.94-4
1.80	.18-3	.51-4	.18-3	.62-3	.18-3	.42-4	.15-3	.51-3	.15-3	.37-4	.13-3	.45-3	.13-3	.30-4	.96-4	.37-3	.11-3
2.00	.18-3	.56-4	.18-3	.56-3	.18-3	.48-4	.15-3	.48-3	.15-3	.42-4	.13-3	.42-3	.13-3	.35-4	.10-3	.35-3	.11-3
2.50	.15-3	.60-4	.15-3	.38-3	.15-3	.54-4	.14-3	.34-3	.14-3	.48-4	.13-3	.30-3	.12-3	.39-4	.11-3	.25-3	.98-4
3.00	.12-3	.56-4	.13-3	.25-3	.12-3	.50-4	.12-3	.22-3	.11-3	.45-4	.11-3	.20-3	.94-4	.39-4	.98-4	.18-3	.82-4
3.50	.88-4	.49-4	.10-3	.16-3	.89-4	.47-4	.98-4	.15-3	.84-4	.44-4	.95-4	.14-3	.79-4	.40-4	.89-4	.13-3	.72-4
4.00	.70-4	.47-4	.95-4	.12-3	.74-4	.45-4	.93-4	.11-3	.71-4	.43-4	.91-4	.11-3	.68-4	.40-4	.87-4	.10-3	.63-4
4.50	.56-4	.45-4	.90-4	.87-4	.62-4	.43-4	.89-4	.85-4	.61-4	.41-4	.87-4	.81-4	.58-4	.38-4	.84-4	.78-4	.54-4
5.00	.46-4	.42-4	.86-4	.66-4	.52-4	.40-4	.85-4	.64-4	.51-4	.39-4	.83-4	.62-4	.49-4	.37-4	.81-4	.61-4	.46-4
6.00	.32-4	.35-4	.79-4	.39-4	.37-4	.35-4	.78-4	.38-4	.36-4	.34-4	.77-4	.38-4	.35-4	.32-4	.76-4	.38-4	.34-4
7.00	.23-4	.30-4	.73-4	.24-4	.27-4	.29-4	.73-4	.24-4	.26-4	.29-4	.73-4	.24-4	.26-4	.28-4	.72-4	.25-4	.25-4
8.00	.18-4	.30-4	.69-4	.18-4	.23-4	.29-4	.69-4	.18-4	.23-4	.28-4	.69-4	.18-4	.22-4	.27-4	.68-4	.19-4	.21-4
9.00	.14-4	.30-4	.66-4	.15-4	.21-4	.30-4	.66-4	.15-4	.21-4	.29-4	.66-4	.15-4	.20-4	.28-4	.66-4	.16-4	.20-4
10.00	.11-4	.31-4	.64-4	.12-4	.19-4	.30-4	.64-4	.12-4	.19-4	.30-4	.64-4	.12-4	.19-4	.29-4	.64-4	.14-4	.18-4
12.00	.78-5	.31-4	.61-4	.86-5	.16-4	.31-4	.61-4	.85-5	.16-4	.30-4	.61-4	.90-5	.16-4	.30-4	.61-4	.10-4	.16-4
14.00	.55-5	.32-4	.59-4	.64-5	.14-4	.31-4	.59-4	.64-5	.14-4	.31-4	.59-4	.69-5	.14-4	.30-4	.59-4	.81-5	.14-4
16.00	.42-5	.32-4	.57-4	.49-5	.13-4	.32-4	.57-4	.50-5	.12-4	.31-4	.58-4	.54-5	.12-4	.31-4	.58-4	.66-5	.12-4
18.00	.33-5	.32-4	.56-4	.39-5	.11-4	.32-4	.56-4	.40-5	.11-4	.32-4	.57-4	.44-5	.11-4	.31-4	.57-4	.56-5	.11-4
20.00	.27-5	.32-4	.56-4	.32-5	.10-4	.32-4	.56-4	.33-5	.10-4	.32-4	.56-4	.37-5	.10-4	.31-4	.56-4	.48-5	.98-5
25.00	.18-5	.32-4	.55-4	.20-5	.81-5	.32-4	.55-4	.22-5	.81-5	.32-4	.55-4	.26-5	.80-5	.32-4	.55-4	.34-5	.79-5
30.00	.13-5	.33-4	.54-4	.14-5	.68-5	.32-4	.54-4	.15-5	.68-5	.32-4	.54-4	.19-5	.67-5	.32-4	.55-4	.27-5	.67-5
35.00	.99-6	.33-4	.54-4	.11-5	.59-5	.32-4	.54-4	.12-5	.58-5	.32-4	.54-4	.15-5	.58-5	.32-4	.54-4	.22-5	.57-5
40.00	.79-6	.33-4	.53-4	.81-6	.51-5	.33-4	.53-4	.91-6	.51-5	.32-4	.54-4	.12-5	.51-5	.32-4	.54-4	.18-5	.50-5
45.00	.65-6	.33-4	.53-4	.64-6	.46-5	.33-4	.53-4	.73-6	.45-5	.32-4	.53-4	.10-5	.45-5	.32-4	.54-4	.16-5	.45-5
50.00	.54-6	.33-4	.53-4	.52-6	.41-5	.33-4	.53-4	.61-6	.41-5	.32-4	.53-4	.88-6	.41-5	.32-4	.54-4	.14-5	.41-5
60.00	.41-6	.33-4	.53-4	.36-6	.34-5	.33-4	.53-4	.45-6	.34-5	.33-4	.53-4	.68-6	.34-5	.32-4	.53-4	.11-5	.34-5
70.00	.34-6	.33-4	.53-4	.26-6	.29-5	.33-4	.53-4	.35-6	.29-5	.33-4	.53-4	.55-6	.29-5	.32-4	.53-4	.92-6	.29-5
80.00	.29-6	.33-4	.53-4	.20-6	.26-5	.33-4	.53-4	.28-6	.26-5	.33-4	.53-4	.46-6	.26-5	.32-4	.53-4	.79-6	.26-5
90.00	.26-6	.33-4	.53-4	.16-6	.23-5	.33-4	.53-4	.23-6	.23-5	.33-4	.53-4	.40-6	.23-5	.33-4	.53-4	.69-6	.23-5
100.00	.23-6	.33-4	.53-4	.13-6	.21-5	.33-4	.53-4	.20-6	.21-5	.33-4	.53-4	.35-6	.21-5	.33-4	.53-4	.61-6	.20-5

Fig. 22. Tabulated output of SDSVSA corresponding to Fig. 20 plot.

G2 (R= 300.00 KM DEPTH= 5.00 KM)

AMAX= 0.22E-04 VMAX= 0.80E-05 DMAX= 0.38E-05

PERIOD	FS	DAMP=0. SD	SV	SA	PSV	DAMP=0.02 SD	SV	SA	PSV	DAMP=0.05 SD	SV	SA	PSV	DAMP=0.10 SD	SV	SA	PSV
0.25	.72-8	.36-7	.54-6	.23-4	.90-6	.36-7	.50-6	.23-4	.92-6	.37-7	.54-6	.23-4	.93-6	.37-7	.57-6	.23-4	.93-6
0.30	.16-5	.11-6	.18-5	.49-4	.24-5	.83-7	.11-5	.37-4	.17-5	.70-7	.98-6	.31-4	.15-5	.62-7	.85-6	.27-4	.13-5
0.35	.71-6	.20-6	.28-5	.66-4	.37-5	.15-6	.18-5	.49-4	.27-5	.12-6	.14-5	.39-4	.22-5	.96-7	.11-5	.32-4	.17-5
0.40	.52-5	.42-6	.58-5	.10-3	.66-5	.27-6	.33-5	.66-4	.42-5	.18-6	.22-5	.45-4	.29-5	.13-6	.14-5	.32-4	.20-5
0.45	.34-6	.17-6	.18-5	.33-4	.23-5	.16-6	.18-5	.31-4	.22-5	.15-6	.16-5	.29-4	.21-5	.13-6	.14-5	.25-4	.18-5
0.50	.92-8	.16-6	.13-5	.25-4	.20-5	.16-6	.14-5	.25-4	.20-5	.15-6	.14-5	.24-4	.19-5	.15-6	.13-5	.24-4	.19-5
0.60	.43-5	.57-6	.50-5	.62-4	.60-5	.35-6	.30-5	.39-4	.37-5	.31-6	.25-5	.34-4	.33-5	.28-6	.20-5	.31-4	.29-5
0.70	.78-5	.13-5	.11-4	.10-3	.11-4	.88-6	.73-5	.71-4	.79-5	.67-6	.48-5	.55-4	.60-5	.50-6	.35-5	.42-4	.45-5
0.80	.10-4	.17-5	.12-4	.10-3	.13-4	.10-5	.66-5	.62-4	.79-5	.77-6	.52-5	.48-4	.60-5	.60-6	.37-5	.38-4	.47-5
0.90	.30-5	.11-5	.66-5	.54-4	.78-5	.99-6	.57-5	.48-4	.69-5	.87-6	.48-5	.43-4	.61-5	.74-6	.41-5	.37-4	.52-5
1.00	.67-8	.12-5	.66-5	.47-4	.74-5	.11-5	.58-5	.42-4	.67-5	.96-6	.50-5	.39-4	.60-5	.86-6	.42-5	.34-4	.54-5
1.20	.61-5	.38-5	.19-4	.10-3	.20-4	.27-5	.12-4	.74-4	.14-4	.22-5	.98-5	.61-4	.12-4	.17-5	.73-5	.48-4	.90-5
1.40	.34-4	.77-5	.34-4	.16-3	.35-4	.43-5	.20-4	.87-4	.19-4	.34-5	.13-4	.70-4	.15-4	.26-5	.98-5	.54-4	.12-4
1.60	.71-4	.18-4	.71-4	.28-3	.71-4	.10-4	.40-4	.16-3	.40-4	.63-5	.23-4	.97-4	.25-4	.41-5	.14-4	.63-4	.16-4
1.80	.31-4	.93-5	.34-4	.11-3	.33-4	.87-5	.31-4	.11-3	.30-4	.72-5	.26-4	.87-4	.25-4	.52-5	.18-4	.64-4	.18-4
2.00	.35-4	.13-4	.41-4	.12-3	.40-4	.10-4	.33-4	.10-3	.32-4	.80-5	.27-4	.79-4	.25-4	.59-5	.19-4	.59-4	.19-4
2.50	.27-4	.13-4	.34-4	.79-4	.32-4	.11-4	.31-4	.70-4	.28-4	.92-5	.26-4	.59-4	.23-4	.73-5	.20-4	.48-4	.18-4
3.00	.27-4	.15-4	.35-4	.64-4	.31-4	.13-4	.31-4	.58-4	.28-4	.11-4	.27-4	.51-4	.24-4	.91-5	.21-4	.41-4	.19-4
3.50	.24-4	.15-4	.33-4	.49-4	.28-4	.14-4	.30-4	.44-4	.24-4	.12-4	.27-4	.38-4	.21-4	.96-5	.22-4	.32-4	.17-4
4.00	.22-4	.16-4	.26-4	.41-4	.26-4	.15-4	.24-4	.37-4	.23-4	.13-4	.21-4	.32-4	.20-4	.10-4	.18-4	.26-4	.16-4
4.50	.18-4	.14-4	.25-4	.27-4	.19-4	.12-4	.24-4	.24-4	.17-4	.11-4	.21-4	.21-4	.15-4	.92-5	.18-4	.18-4	.13-4
5.00	.13-4	.13-4	.20-4	.20-4	.16-4	.12-4	.19-4	.19-4	.15-4	.11-4	.18-4	.17-4	.14-4	.93-5	.16-4	.15-4	.12-4
6.00	.80-5	.10-4	.14-4	.11-4	.11-4	.98-5	.13-4	.11-4	.10-4	.90-5	.13-4	.10-4	.95-5	.80-5	.12-4	.92-5	.84-5
7.00	.49-5	.89-5	.11-4	.72-5	.80-5	.86-5	.11-4	.70-5	.78-5	.82-5	.10-4	.68-5	.74-5	.77-5	.99-5	.67-5	.69-5
8.00	.33-5	.81-5	.10-4	.50-5	.63-5	.79-5	.10-4	.49-5	.62-5	.77-5	.99-5	.49-5	.61-5	.73-5	.93-5	.50-5	.58-5
9.00	.25-5	.74-5	.10-4	.36-5	.52-5	.74-5	.10-4	.36-5	.51-5	.72-5	.98-5	.36-5	.50-5	.70-5	.94-5	.38-5	.49-5
10.00	.20-5	.70-5	.99-5	.28-5	.44-5	.70-5	.98-5	.28-5	.44-5	.69-5	.96-5	.28-5	.43-5	.67-5	.93-5	.31-5	.42-5
12.00	.17-5	.65-5	.97-5	.18-5	.34-5	.65-5	.96-5	.18-5	.34-5	.63-5	.95-5	.18-5	.33-5	.62-5	.92-5	.21-5	.32-5
14.00	.13-5	.57-5	.95-5	.12-5	.26-5	.57-5	.94-5	.12-5	.26-5	.57-5	.93-5	.12-5	.26-5	.56-5	.91-5	.15-5	.25-5
16.00	.97-6	.50-5	.92-5	.76-6	.19-5	.50-5	.92-5	.78-6	.20-5	.50-5	.91-5	.87-6	.20-5	.51-5	.90-5	.11-5	.20-5
18.00	.72-6	.46-5	.90-5	.56-6	.16-5	.46-5	.90-5	.57-6	.16-5	.45-5	.89-5	.64-6	.16-5	.46-5	.88-5	.85-6	.16-5
20.00	.55-6	.47-5	.88-5	.46-6	.15-5	.46-5	.88-5	.47-6	.15-5	.45-5	.88-5	.52-6	.14-5	.44-5	.87-5	.70-6	.14-5
25.00	.34-6	.47-5	.85-5	.30-6	.12-5	.46-5	.85-5	.31-6	.12-5	.46-5	.85-5	.35-6	.12-5	.45-5	.84-5	.47-6	.11-5
30.00	.18-6	.46-5	.83-5	.20-6	.97-6	.46-5	.83-5	.21-6	.96-6	.45-5	.83-5	.26-6	.95-6	.45-5	.83-5	.36-6	.94-6
35.00	.93-7	.45-5	.82-5	.15-6	.81-6	.45-5	.82-5	.16-6	.80-6	.45-5	.82-5	.20-6	.80-6	.44-5	.82-5	.30-6	.79-6
40.00	.70-7	.44-5	.81-5	.11-6	.69-6	.44-5	.81-5	.12-6	.69-6	.44-5	.81-5	.16-6	.68-6	.43-5	.81-5	.25-6	.68-6
45.00	.63-7	.43-5	.81-5	.83-7	.60-6	.43-5	.81-5	.95-7	.59-6	.43-5	.81-5	.13-6	.59-6	.42-5	.81-5	.22-6	.59-6
50.00	.53-7	.42-5	.81-5	.66-7	.52-6	.42-5	.81-5	.77-7	.52-6	.42-5	.81-5	.11-6	.52-6	.42-5	.81-5	.20-6	.52-6
60.00	.29-7	.40-5	.81-5	.44-7	.42-6	.40-5	.81-5	.55-7	.42-6	.40-5	.81-5	.88-7	.42-6	.40-5	.81-5	.17-6	.42-6
70.00	.12-7	.39-5	.80-5	.31-7	.35-6	.39-5	.80-5	.41-7	.35-6	.39-5	.80-5	.74-7	.35-6	.39-5	.80-5	.15-6	.35-6
80.00	.17-7	.38-5	.80-5	.23-7	.30-6	.38-5	.80-5	.33-7	.30-6	.38-5	.80-5	.65-7	.30-6	.38-5	.80-5	.13-6	.30-6
90.00	.25-7	.37-5	.80-5	.18-7	.26-6	.37-5	.80-5	.28-7	.26-6	.37-5	.80-5	.57-7	.26-6	.38-5	.80-5	.11-6	.26-6
100.00	.30-7	.37-5	.80-5	.14-7	.23-6	.37-5	.80-5	.25-7	.23-6	.37-5	.80-5	.52-7	.23-6	.37-5	.80-5	.10-6	.23-6

Fig. 23. Tabulated output of SDSVSA corresponding to Fig. 21 plot.

It is interesting to note how much character is introduced into the response spectrum at the larger distance, which is due just to wave propagation effects.

As a practical application of the theory presented, the variation of maximum velocity with distance, focal depth, and source duration was studied. The signals were generated using a frequency window of 0 - 1 Hz, as before. To enable comparison with a simpler model, the single layer over a halfspace crustal model was used, and the results were compared to those for a uniform halfspace with properties of just the layer. Figure 24 shows the effect of focal depth. The source pulse had $\tau = 1$ sec and a seismic moment of 3.53 E + 21 dyne-cm. The computed single layer over a halfspace solutions are given by the symbols, while the halfspace solutions are given by the solid curves. Figure 25 shows the variation with source pulse duration, seismic moment fixed. Several points are immediately apparent. First, out to distances of about 75 km the halfspace solution is quite good. At distances greater than 75 km the halfspace solution breaks down, especially for the vertical dip-slip source, for which the apparent geometrical spreading changes from r^{-2} to r^{-1}. This is the result of the contribution of supercritically reflected arrivals, or equivalently, the process of surface wave formation. Note the difference in apparent geometrical spreading between the vertical dip-slip and vertical strike-slip sources. Finally the variation of maximum velocity with source pulse

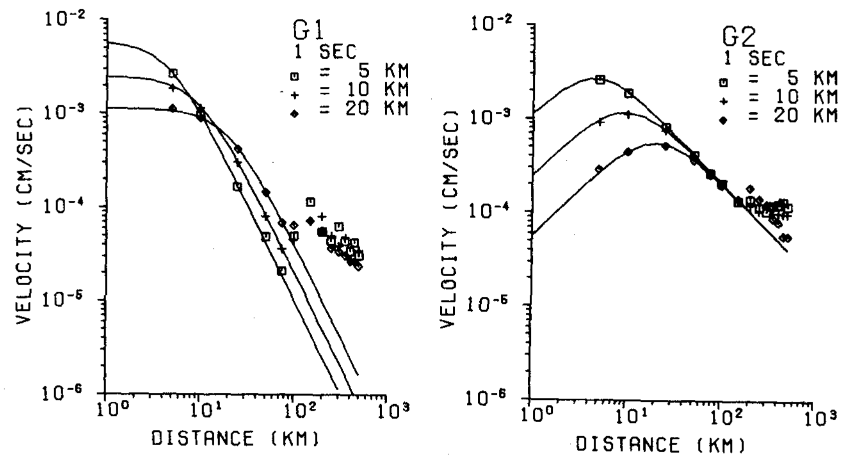

Fig. 24. Effect of variation in focal depth upon the maximum ground velocity for a vertical dip-slip source, G1, and for a vertical strike-slip source, G2, for fixed source pulse duration. The solid curves correspond to a halfspace solution, while the symbols correspond to the corresponding simple crustal model solution.

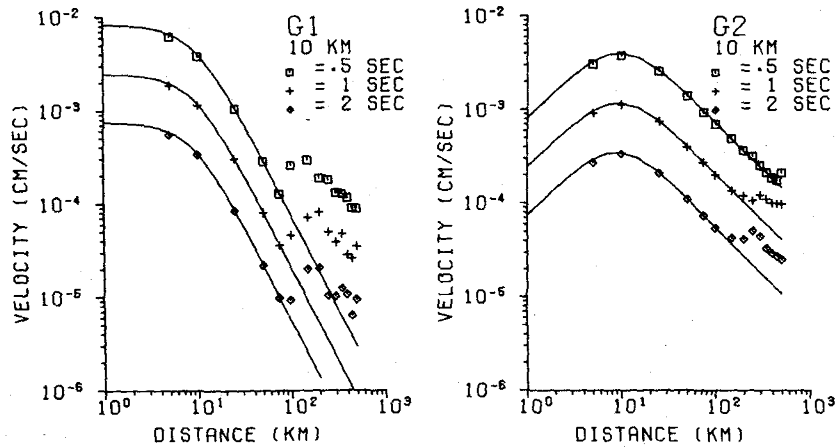

Fig. 25. Effect of variation in source pulse duration upon the maximum ground velocity for a vertical dip-slip source, G1, and for a vertical strike-slip source, G2, fixed focal depth. The halfspace solutions, solid curves, are compared to the simple crustal model solutions, symbols.

duration can be used with source spectrum scaling laws to see how this parameter varies with the size of the earthquakes, e.g. if seismic moment is proportional to the cube of source pulse duration, "constant stress drop" scaling, an increase in seismic moment by a factor of 8 would yield an increase in maximum velocity by a factor of about 2. This may be of value in scaling strong motion. Since only the far-field SH term was used, the scaling at short distances is only approximate.

PART V. CONCLUSIONS

The theory for the far-field ground motion due to dislocation earthquakes has been presented together with a description of the numerical techniques used for this realization. Some examples were presented to provide an insight to the numerical methods as well as to present some examples of how wave shapes are affected by propagation through a layered earth.

The computer programs documented in this report should be useful for more detailed studies of wave generation due to complex earthquake rupture processes as well as for inferring more realistic ground motion scaling rules than are currently being used.

REFERENCES

Abramowitz, M. and I. A. Stegun (1964). Handbook of Mathematical Functions, Nat. Bur. Stand. Appl. Math. Ser. No. 55, U. S. Govt. Printing Office, Washington, D. C.

Apsel, R. J. (1977). Computation of complete seismograms in a multi-layered viscoelastic halfspace (abstract) EOS, Trans. Amer. Geophys. Union 58, 1192.

Boore, David M. and William B. Joyner (1978). The influence of rupture incoherence on seismic directivity, Bull. Seism. Soc. Am. 68, 283-300.

Bouchon, M. and K. Aki (1977). Discrete wave-number representation of seismic-source wave fields, Bull. Seism. Soc. Am. 67, 259-277.

Davis, P. J. and P. Rabinowitz (1975). Methods of Numerical Integration, Academic Press, New York.

Ewing, W. M., W. S. Jardetzky, and F. Press (1957). Elastic Waves in Layered Media, McGraw-Hill, New York.

Fuchs, K. and G. Müller (1971). Computation of synthetic seismograms with the reflectivity method and comparison with observations, Geophys. J. 23, 417-433.

Harkrider, D. G. (1976). Potentials and displacements for two theoretical sources, Geophys. J. 47, 97-133.

Haskell, N. A. (1964). Radiation pattern of surface waves from point sources in a multi-layered medium, Bull. Seism. Soc. Am. 54, 377-393.

Heaton, T. H. and D. V. Helmberger (1977). A study of the strong ground motion of the Borrego Mountain, California, earthquake, Bull. Seism. Soc. Am. 67, 315-330.

Heaton, T. H. and D. V. Helmberger (1978). Predictability of strong ground motion in the Imperial Valley: Modeling the M4.9 November 4,1976 Brawley earthquake, Bull. Seism. Soc. Am. 68, 31-48.

Helmberger, D. V. (1974). Generalized ray theory for shear dislocations, Bull. Seism. Soc. Am. 64, 45-64.

Helmberger, D. V. and S. D. Malone (1975). Modeling local earthquakes as shear dislocations in a layered halfspace, J. Geophys. Res. 80, 4881-4888.

Herrmann, R. B. (1977). Earthquake generated SH waves in the near field and near-regional field. Final Report under Contract DACW39-39-76-C-0058, Waterways Experiment Station, Vicksburg.

Herrmann, R. B. (1978). A note on causality problems in the numerical solution of elastic wave propagation in cylindrical coordinate systems, Bull. Seism. Soc. Am., 68, 117-123.

Herrmann, R. B. (1979). SH wave generation by dislocation sources - a numerical study, Bull. Seism. Soc. Am. 69, 000-000.

Hudson, J. A. (1969). A quantitative evaluation of seismic signals at teleseismic distances - II. Body waves and surface waves from an extended source, Geophys. J. 18, 353-370.

Johnson, L. R. (1974). Green's function for Lamb's problem, Geophys. J. 37, 99-131.

Langston, C. A. and D. V. Helmberger (1975). A procedure for modeling shallow dislocation sources, Geophys. J. 42, 117-130.

Nigam, N. C. and P. C. Jennings (1969). Calculation of response spectra from strong-motion earthquake records, Bull. Seism. Soc. Am. 59, 909-922.

Nuttli, O. W. (1973). Seismic wave attenuation and magnitude relations for eastern North America, J. Geophys. Res. 78, 876-885.

Nuttli, O. W. (1978). A time-domain study of the attenuation of 10 Hz waves in the New Madrid Seismic Zone, Bull. Seism. Soc. Am. 68, 343-355.

Stroud, A. H. and D. M. Secrest (1966). Gaussian Quadrature Formulas, Prentice-Hall, Englewood Cliffs.

Swanger, H. J. and D. G. Boore (1978). Simulation of strong-motion displacements using surface-wave modal superposition, Bull. Seism. Soc. Am. 68, 907-922.

APPENDIX A: COMPUTER PROGRAM SHSPEC

Function

This program computes the far-field complex Fourier spectra for point vertical strike-slip and vertical dip-slip earthquake sources at a fixed depth in a layered medium. The program is written in FORTRAN IV for the Honeywell 6023 digital computer at Saint Louis University. The programming has been kept simple to facilitate conversion to other computers. As it stands, the program provides good results for the distance range of about 5 km to 500 km for frequencies up to 10 Hz. Special normalization has been introduced to take into account the fact that the Honeywell 6023 floating point number is limited to the range 10^{-38} to 10^{+38}.

Input

Input is from card through File 60. A description of input variables is given in Table A1.

Output

Output is through File 61 and also through standard printer output using the PRINT statement. A description of printer output is given in Table A2.

File Codes

The following file codes are used for I/O functions:

11	Mass storage file used for temporary storage by subroutines EXCIT and WVINT
12	Mass storage file used to store G1 and G2 solutions in frequency domain for specified distances. Contents of this file are used as

input by the program SHVEL.

60	Card Reader
61	Printer output using WRITE(61,n) statement.
--	Printer output using PRINT n, statement.

Sample Input

Sample input data for generating the traces of Figure 19 are given in Table A3.

Program Listing

A description of the various subroutines of the program is given in Table A4, while a listing of the program is given in Table A5.

Table A1

Input Variables

Card	Variable Name	Columns	Format	Description
1	DEPTH	1-10	F10.5	Focal depth in km
	FL	11-20	F10.5	Low frequency cutoff in Hz
	FU	21-30	F10.5	High frequency cutoff in Hz
	DT	31-40	F10.5	Sample interval in seconds. Time series in N*DT seconds long.
	N	41-45	I5	Number of points in time series. Must be power of two and .LE.1024. Large N requires much computer time
	VRED	46-55	F10.5	Used to compute reduced travel time t-R/VRED for shifted time axis. If VRED.EQ.0, no reduced time used.
2	D	1-10	F10.5	Layer thickness in km. Read Card 2's until end of model indicated by D.LE.0
	A	11-20	F10.5	Layer P wave velocity in km/sec
	B	21-30	F10.5	Layer S wave velocity in km/sec
	RHO	31-40	F10.5	Layer density in gm/cm^3
3	R	1-10	F10.5	Epicentral distance in km. Keep reading Card 3's until one found with R.LT.0, then end program and close files.
	XOUT	11-20	F10.5	Control variable XOUT=0--complete solution XOUT=1--solution using poles and real axis branch line integral XOUT=2--solution using poles only
	TO	21-30	F10.5	.EQ.0 use VRED to plot time series as a function of reduced travel time .NE.0 TO is the time shift for plot

Table A2

Output Variables

Name	Descritpion
Output File 61:	
FL	Low frequency cutoff
FU	High frequency cutoff
DF	Frequency interval (DF=1/(N*DT))
N1	Index to indicate array position of FL
N2	Index to indicate array position of FU
DEPTH	Focal depth in km
FREQ	Frequencies at which theoretical response is calculated
R	Epicentral distance in km
IOUT	Type of output. IOUT=3-XOUT, XOUT defined in Tabel A1
TO	Computed time shift from input TO of VRED input
Output File for PRINT statement	
D	Layer thickness in km
A	Layer P wave velocity in km/sec
B	Layer S wave velocity in km/sec
RHO	Layer density in gm/cm^3

Table A3

Sample Input

0 1	1 0	2 0	3 0	4 0	4 5	5 0	6 0	7 0
10.	0.0	1.0	0.25	256				
1.0	5.0	2.89	2.50					
9.0	6.1	3.52	2.70					
10.	6.4	3.70	2.90					
20.	6.7	3.87	3.00					
0.0	8.15	4.70	3.40					
25.	0.0							
50.	0.0							
75.	0.0							
100.	0.0							
150.	0.0							
200.	0.0							
250.	0.0							
350.	0.0							
450.	0.0							
-1.0								

Table A4

Subroutine Description

Subroutine Name	Function
RSHOF	Computes the functions of Equation 2 for given values of real wavenumber k and frequency
EXCIT	Computes ratios of the type g_1/F_L and g_1/F_L' for various values of k for each frequency and stores the results on File 11 for later calls by WVINT
WVINT	Performs numerical integration
HANK	Evaluates Hankel functions $H_{1,2}^{(2)}(kr)$
IHANK	Evaluates $\int_0^z H_0^{(2)}(z)\, dz$
AXIMAG	Performs numerical integration along negative imaginary k-axis
SHCFIK	Computes ratio of the type g_1/F_L for imaginary values of wavenumber
BESMOD	Computes modified Bessel function values
SRCMOD	Reads in earth model parameters
SRCLYR	Using the given focal depth, this searches for source layer
SHCOEF	Computes matrix products of Equation 3

Table A5


```
C     PROGRAM SHSPEC
      COMPLEX DUM1,DUM2
      COMMON / MODEL / D(15),A(15),B(15),RHO(15),MMAX
      COMMON/SOURCE/DEPTH,LMAX,DPH
      COMMON / INT / IOUT
      DIMENSION DATA(2048),DATA1(2048)
C     THIS PROGRAM EVALUATES THE SH WAVE GENERATION BY A
C     SOURCE IN A LAYERED MEDIUM.  FOR REFERENCES SEE
C        J.A.HUDSON  (1969) GEOPHYS.J. VOL 18 PP 353-370.
C        N.A.HASKELL (1964) B.S.S.A.   VOL 54 PP 377-393.
C
C
C     DATA SHOULD BE ENTERED IN THE FOLLOWING ORDER
C
C     CARD 1 DEPTH,FL,FU,DT,N
C     CARD 2 D,A,B,RHO
C     ,....., EARTH MODEL READ IN
C     ,....., MORE CARD 2 - D.LE.0 FOR HALFSPACE
C     CARD 3 R,IOUT,T0
C     ......, MORE CARD 3 - USE R.LT.0 TO END CARD 3 SEQUENCE
C
C     TO SAVE COMPUTER STORAGE, INTERMEDIATE RESULTS ARE
C     WRITTEN ON FILE 11. FILE 12 CONTAINS COMPLEX SPECTRA
C     AT DISTANCE R.
C
C     READ IN FOCAL DEPTH, LOWER AND UPPER FREQUENCY BOUNDS,
C     DT AND N
      READ(60,1) DEPTH,FL,FU,DT,N,VRED
    1 FORMAT(4F10.5,I5,F10.5)
      IF(DEPTH.LT.0.0) GO TO 9998
      WRITE(12,1) DEPTH,FL,FU,DT,N,VRED
      CALL SRCMOD
      CALL SRCLYR
      DF = 1./(N*DT)
      N1 = FL/DF
      N2 = FU/DF
      N1 = N1 + 1
      N2 = N2 + 1
      NYQ = (N/2) + 1
      NYQ2 = 2 * NYQ
      WRITE(61,9) FL,FU,DF,N1,N2,DEPTH
    9 FORMAT(1H0,4HFL =,F10.5,5X,4HFU =,F10.5,5X,4HDF =,F10.
     15,5X,4HN1 =,I4,5X,4HN2 =,I4,5X,7HDEPTH =,F10.2)
      WRITE(61,2)
    2 FORMAT(1H0,39HFREQUENCIES FOR WHICH RESPONSE COMPUTED)
```

```
      DO 100 I = N1,N2
      FREQ = (I-1) * DF
      WRITE(61,3) FREQ
    3 FORMAT(1H ,F10.6)
      CALL EXCIT(FREQ)
  100 CONTINUE
  500 READ(60,1) R,XOUT,TO
C     R = EPICENTRAL DISTANCE
C     XOUT = 0.0 POLES + REAL AXIS BRANCH LINE + IMAGINARY
C     AXIS BRANCH LINE INTEGRALS
C     XOUT = 1.0 POLES + REAL AXIS BRANCH LINE
C     XOUT = 2.0 POLES
C     TO .EQ. 0 USE REDUCED TRAVEL TIME,OTHERWISE USE TO
      IF(XOUT.LT.0.0.OR.XOUT.GT.2.0) XOUT = 0.0
      IOUT = 3. - XOUT
      REWIND 11
C     REDUCED TRAVEL TIME TIME SHIFT
      TO = 0.0
      IF(VRED.GT.0.0) TO = R/VRED
      WRITE(12,601)R,IOUT,TO
  601 FORMAT(E11.4,I5,E11.4)
      IF(R.LT.0.0) GO TO 9998
      WRITE(61,580) DEPTH,R,IOUT,TO
  580 FORMAT(1X,6HDEPTH=,F6.2,3X,2HR=,F6.2,3X,5HIOUT=,I4,3X,
     13HTO=,E11.4)
C     EVALUATION OF WAVENUMBER INTEGRALS
      NN = 2 * N
      DO 250 I = 1,NN
      DATA1(I) = 0.0
  250 DATA(I) = 0.0
      DO 300 I = N1,N2
      FREQ = (I-1) * DF
      FAC = 6.2831853 * FREQ * TO
      XR = COS(FAC)
      XI = SIN(FAC)
      CALL WVINT(R,FREQ,AR1,AI1,AR2,AI2)
      DUM1 = CMPLX(XR,XI) * CMPLX(AR1,AI1)
      DUM2 = CMPLX(XR,XI) * CMPLX(AR2,AI2)
      AR1 = REAL(DUM1)
      AI1 = AIMAG(DUM1)
      AR2 = REAL(DUM2)
      AI2 = AIMAG(DUM2)
      J = 2 *I -1
      K = 2 * I
      DATA(J) = AR1
```

```
      DATA(K) = AI1
      DATA1(J) = AR2
      DATA1(K) = AI2
  300 CONTINUE
      WRITE(12,600)(DATA(I),I=1,NYQ2)
      WRITE(12,600)(DATA1(I),I=1,NYQ2)
  600 FORMAT(8E11.4)
      GO TO 500
 9998 CONTINUE
      REWIND 12
      STOP
      END

      SUBROUTINE EXCIT(FREQ)
      DIMENSION P1(300),P2(300),WVN(300),WVC(300)
      COMPLEX G1(300),G2(300)
      COMPLEX X1,X1P,X1M,X2,X2P,X2M,FL,FLP,FLM
      COMPLEX EYEPI
      COMMON / MODEL / D(15),A(15),B(15),RHO(15),MMAX
      COMMON/ SPACE / G1,G2,P1,P2,WVN,WVC
      EYEPI = (0.0,-3.1415927)
C     LATER ON ADD BMAX AND BMIN INTO MODEL
      CMAX = B(MMAX)
      CMIN = B(1)
      OMEGA = 6.2831853*FREQ
      WVMN = OMEGA/CMAX
      WVMX = OMEGA/CMIN
      IF(FREQ.EQ.0.0) GO TO 4000
C      APPROXIMATE NUMERICAL INTEGRATION
C     TEST FOR A FINER GRID FOR HIGHER FREQUENCIES
C     THIS SHOULD BE VALID FOR DISTANCES UP TO ABOUT 500 KM
C     AT FREQUENCIES LESS THAN 10HZ.
      NGAM = 100
      IF(FREQ.GE.1.0.AND.FREQ.LT.5.0) NGAM = 200
      IF(FREQ.GE.5.0) NGAM = 300
      DGAM = 1.57079633/NGAM
      NROOT= NGAM - 1
      DO 3998 I=1,NGAM
      GAM  = I * DGAM
      IF(I.EQ.NGAM) GAM=0.9999*1.57079633
      WVNO = WVMN * SIN(GAM)
      WVNC = WVMN * COS(GAM)
      CALL RSHOF(X1,X2,FL,OMEGA,WVNO,EXE1,EXL1)
      WVN(I) = WVNO
      WVC(I) = WVNC
```

```
      ELJ  = EXL1 - EXE1
      FACX = 0.0
      IF(ELJ.GT.-70.) FACX = EXP(ELJ)
      X1 = X1/FL
      X2 = X2/FL
      T1 = FACX*WVNO*WVNC
      P1(I) = AIMAG(X1)*T1
      P2(I) = AIMAG(X2)*T1
 3998 CONTINUE
      WRITE(11,6) OMEGA,NGAM,DGAM
      WRITE(11,2) ((WVN(J),WVC(J),P1(J),P2(J)),J=1,NGAM)
    6 FORMAT(E13.6,I5,E13.6)
 4000 CONTINUE
      NROOT = 0
C     NMX IS CHOSEN FOR A 40 KM CRUSTAL MODEL, FOR SHALLOWER
C     THICKNESSES A PROPORTIONATELY SMALL NMX CAN BE USED.
      NMX = 100 + (FREQ*100.)
      DK = (WVMX-WVMN)/NMX
      IF(DK.LT.1.0E-8) GO TO 5001
C     SEARCH FOR ROOTS OF PERIOD EQUATION
      C1 = WVMN + 0.01*DK
      CALL RSHOF(X1,X2,FL,OMEGA,C1,EXE1,EXL1)
      DEL1 = REAL(FL)
      NMX1 = NMX + 1
      DO 5000 I=2,NMX1
      C2 = WVMN + (I-1) * DK
      CALL RSHOF(X1,X2,FL,OMEGA,C2,EXE1,EXL1)
      DEL2 = REAL(FL)
      IF(SIGN(1.0,DEL1)*SIGN(1.0,DEL2).GE.0.0) GO TO 4999
      NROOT = NROOT + 1
      C4 = C2
      DEL4 = DEL2
      DO 4990 II=1,5
      C3 = 0.5*(C1+C4)
      CALL RSHOF(X1,X2,FL,OMEGA,C3,EXE1,EXL1)
      DEL3 = REAL(FL)
      IF(SIGN(1.0,DEL1)*SIGN(1.0,DEL3).GE.0.0) GO TO 4991
      DEL4 = DEL3
      C4 = C3
      GO TO 4992
 4991 DEL1 = DEL3
      C1 = C3
 4992 CONTINUE
 4990 CONTINUE
      C3 = 0.5*(C1+C4)
```

```
      CALL RSHOF(X1P,X2P,FLP,OMEGA,C3+0.1*DK,EJP,ELP)
      CALL RSHOF(X1M,X2M,FLM,OMEGA,C3-0.1*DK,EJM,ELM)
      DFJ = EJP-EJM
      DFL = ELP-ELM
      ELJ = ELM-EJM
      X1P=X1P*EXP(DFL)
      X2P=X2P*EXP(DFL)
      FLP=FLP*EXP(DFJ)
      FACX = 0.0
      IF(ELJ.GT.-70.) FACX = EXP(ELJ)
C     DFDK = (REAL(FLP)-REAL(FLM))/(2.*0.1*DK)
      DFDK =  5.*(REAL(FLP)-REAL(FLM))/DK
      G1(NROOT) = 0.5 * REAL(X1P + X1M) * EYEPI / DFDK
      G1(NROOT) = G1(NROOT)*FACX
      G2(NROOT) = 0.5 * REAL(X2P + X2M) * EYEPI / DFDK
      G2(NROOT) = G2(NROOT)*FACX
      WVN(NROOT) = C3
 4999 C1 = C2
      DEL1 = DEL2
 5000 CONTINUE
 5001 CONTINUE
      WRITE(11,5) OMEGA,NROOT
      IF(NROOT.EQ.0) GO TO 5002
      WRITE(11,2) ((WVN(J),G1(J),G2(J)),J=1,NROOT)
    2 FORMAT(10E13.6)
    5 FORMAT(E13.6,I5)
 5002 CONTINUE
      RETURN
      END

      SUBROUTINE WVINT(R,FREQ,AR1,AI1,AR2,AI2)
      DIMENSION P1(300),P2(300),WVN(300),WVC(300)
      COMPLEX G1(300),G2(300)
      COMPLEX H0,H1,H01,H11,HI,SUM,SUM0,SUM1,SUM2
      COMMON / SPACE / G1,G2,P1,P2,WVN,WVC
      COMMON / MODEL / D(15),AA(15),BB(15),RHO(15),MMAX
      COMMON / SOURCE/ DEPTH,LMAX,DPH
      COMMON /  INT  / IOUT
      FCT = 1./(12.5663706*BB(LMAX)*BB(LMAX))
      PIL = 3.141592653
      AR1 = 0.0
      AI1 = 0.0
      AI2 = 0.0
      AR2 = 0.0
      OMEGA = 6.2831853*FREQ
```

```
      SUM1 = CMPLX(0.,0.)
      SUM2 = CMPLX(0.,0.)
      IF(FREQ.EQ.0.0) GO TO 4000
C      APPROXIMATE NUMERICAL INTEGRATION
C     ALONG BRANCH LINE FROM K = 0 TO K = K-BETA(MAX)
      READ(11,6) OMEGA,NK,DGAM
      READ(11,2) ((WVN(J),WVC(J),P1(J),P2(J)),J=1,NK)
    6 FORMAT(E13.6,I5,E13.6)
      IF(IOUT.EQ.1) GO TO 4000
      WVNO = WVN(1)
      T01  = WVNO*R
      CALL HANK(T01,1.0,H01,H11)
      SUM1 = 0.5*P1(1)*H01*DGAM
      SUM2 = 0.5*P2(1)*H11*DGAM
      CALL IHANK(T01,H01,H11,SUM0)
      DO 200 I=2,NK
      I1   = I-1
      WVNO = WVN(I)
      T0   = WVNO*R
      CALL  HANK(T0,1.0,H0,H1)
      CALL IHANK(T0,H0,H1,SUM)
      ITST = 1
      IF((T0-T01).LT.PIL) ITST=2
      GO TO (150,160),ITST
  150 CONTINUE
      HI   = SUM-SUM0
      SLP  = WVC(I1)*R
      SLP2 = SLP*SLP
      A    = P1(I1)
      B    = (P1(I)-P1(I1))/DGAM
      SUM1 = SUM1+A*HI/SLP
      SUM0 = T0*H1-T01*(HI+H11)
      SUM1 = SUM1+B*SUM0/SLP2
      A    = P2(I1)
      B    = (P2(I)-P2(I1))/DGAM
      SUM2 = SUM2+A*(H01-H0)/SLP
      SUM0 = HI+(T01-T0)*H0
      SUM2 = SUM2+B*SUM0/SLP2
      GO TO 170
  160 CONTINUE
      SUM1 = SUM1+0.5*(P1(I)*H0+P1(I1)*H01)*DGAM
      SUM2 = SUM2+0.5*(P2(I)*H1+P2(I1)*H11)*DGAM
  170 CONTINUE
      H01  = H0
      H11  = H1
```

```
      T01  = T0
      SUM0 = SUM
  200 CONTINUE
      SUM1 = SUM1*CMPLX(0.0,-1.0)
      SUM2 = SUM2*CMPLX(0.0,-1.0)
 4000 CONTINUE
C      POLE CONTRINUTIONS
      READ(11,5) OMEGA1,NK
    5 FORMAT(E13.6,I5)
      IF(NK.EQ.0) GO TO 399
      READ(11,2) ((WVN(J),G1(J),G2(J)),J=1,NK)
    2 FORMAT(10E13.6)
      DO 300 I = 1,NK
      WVNO = WVN(I)
      CALL HANK(WVNO,R,H0,H1)
      SUM1 = SUM1-H0*G1(I)*WVNO
      SUM2 = SUM2-H1*G2(I)*WVNO
  300 CONTINUE
  399 CONTINUE
      AR1 = REAL(SUM1)*FCT
      AR2 = REAL(SUM2)*FCT
      AI1 = AIMAG(SUM1)*FCT
      AI2 = AIMAG(SUM2)*FCT
C     NUMERICAL INTEGRATION ALONG IMAGINARY AXIS BRANCH LINE
      IF(IOUT.NE.3) GO TO 403
      CALL AXIMAG(CONT1,CONT2,OMEGA,R)
      AR1 = AR1 - CONT1*FCT
      AR2 = AR2 - CONT2*FCT
  403 CONTINUE
      RETURN
      END

      SUBROUTINE HANK(WVNO,R,H0,H1)
      COMPLEX H0,H1
      REAL J0,J1,J1Z
      Z = WVNO*R
  100 IF(Z.GT.3.0) GO TO 200
      X = (Z/3.)*(Z/3.)
      J0 = 1.-X*(2.2499997-X*(1.2656208-X*(.3163866-X*(
     1.0444479-X*(.0039444-X*(.0002100))))))
      J1Z = 0.5-X*(.56249985-X*(.21093573-X*(.03954289-X*(
     1.00443319-X*(.00031761-X*(.00001109))))))
      J1 = Z * J1Z
      Y0 = (2./3.1415927)*ALOG(0.5*Z)*J0 + 0.36746691 +X*(
     1.60559366-X*(.74350384-X*(.25300117-X*(.04261214-X*(
```

```
     2.00427916-X*(.00024846))))))
      Y1Z = (2./3.1415927)*Z*ALOG(0.5*Z)*J1 - 0.6366198+X*(
     1.2212091+X*(2.1682709+X*(-1.3164827+X*(.3123951+X*(
     2-.0400976+X*(.0027873))))))
      H0 = CMPLX(J0,-Y0)
      H1 = CMPLX(J1,-Y1Z/Z)
      RETURN
  200 CONTINUE
      X = 3./Z
      FAC = 1./SQRT(Z)
      F0 = .79788456+X*(-.00000077 + X*(-.00552740 + X*(
     1-.00009512+X*(.00137237+X*(-.00072805+X*(.00014476))))
     2))
      T0 = Z - .78539816+X*(-.04166397+X*(-.00003954+X*(
     1.00262573+X*(-.00054125+X*(-.00029333+X*(.00013558))))
     2))
      F1 = .79788456+X*(.00000156+X*(.01659667+X*(.00017105+
     1X*(-.00249511+X*(.00113653+X*(-.00020033))))))
      T1 = Z-2.35619449+X*(.12499612+X*(.00005650+X*(
     1 -.00637879+X*(.00074348+X*(.00079824+X*(-.00029166)))
     2)))
      J0 = FAC * F0 * COS(T0)
      Y0 = FAC * F0 * SIN(T0)
      J1 = FAC * F1 * COS(T1)
      Y1 = FAC * F1 * SIN(T1)
      H0 = CMPLX(J0,-Y0)
      H1 = CMPLX(J1,-Y1)
      RETURN
      END

      SUBROUTINE IHANK(X,H0,H1,SUM)
      COMPLEX H0,H1,SUM
      REAL IJ0,IY0
      IF(X.GT.5.0) GO TO 1000
      IF(X.GT.2.0) GO TO 101
      IJ0=1.49457E-5+X*(.9994805+X*(.0027178+X*(-.0884971+
     *     X*(.0042605+X*(.0017411)))))
      GO TO 200
  101 IF(X.GT.4.0) GO TO 102
      IJ0=0.1680514+X*(.6216918+X*(.3516254+X*(-.2553154+
     *     X*(.0458084+X*(-.0025809)))))
      GO TO 200
  102 IJ0=-4.093215+X*(5.493378+X*(-1.870851+
     *     X*(.2501106+X*(-.0114415))))
  200 IF(X.GT.0.5) GO TO 201
```

```
      IY0=X*(-2,983395+X*(10,69899+X*(-30,65599+
     *      X*(48,83985+X*(-30,89077)))))
      GO TO 999
  201 IF(X.GT.1,0) GO TO 202
      IY0=-0.0851148+X*(-1,649919+X*(1.878571+
     *      X*(-1,218732+X*(,5532593+X*(-,1151309)))))
      GO TO 999
  202 IF(X.GT.3,0) GO TO 203
      IY0=-,2089732+X*(-1.081949+X*(,7960879+X*(-,1464996+
     *      X*(,0037485+X*(.0005744)))))
  203 IY0=.9766188+X*(-2.799556+X*(1.780798*X*(-,4238574+
     *      X*(.0416846+X*(-,0013983)))))
  999 CONTINUE
      SUM=CMPLX(IJ0,-IY0)
      RETURN
 1000 Z=1,/X
      S0=-3,08168E-7+Z*(,6366825+Z*(-,0004799+
     *    Z*(-,6797933+Z*(,889303))))
      S1=,6366201+Z*(-6,88024E-5+Z*(,639624+
     *    Z*(-,0508577+Z*(-1,689329+Z*(2,711393)))))
      S0=S0-AIMAG(H0)
      S1=S1-AIMAG(H1)
      SUM=X*(H0+1,57079633*(S0*H1-S1*H0))
      RETURN
      END

      SUBROUTINE AXIMAG(SM1,SM2,OMEGA,R)
C     THIS PERFORMS BRANCH LINE INTEGRATION ALONG THE IMAGIN
C     THE INTEGRATION IS PERFORMED BY LAGUERRE S RULE AND IS
C     R.GT. 0.5 H , WHERE H IS THE SOURCE DEPTH
C     TO IMPROVE THE EVALUATION NOTE THAT BMOD0 AND BMOD1 AR
C     OMEGA, HENCE THIS FUNCTION CAN BE COMBINED WITH THE WE
C     AN EARLY INTIALIZATION.
      COMPLEX G1,G2
      DIMENSION X(24),W(24)
      DATA (X(I),I=1,24)/0,02110687,0,11122305,0,27339875,
     10.50775546,0.81442137,1,1935599,1,6453733,2,1701028,
     22.7680303,3.4394792,4.1848148,5,0044459,5,8988261,
     36.8684550,7,9138802,9.0356983,10.234558,11.511161,
     412.866265,14.300688,15,815308,17,411070,19.088986,
     520.850141/, (W(I),I=1,24)/.05303710,0.11284582,
     60.15082452,0.16279133,0.15185641,0,12593625,.09419893,
     70.64078814E-01,0.39845646E-01,0,22724136E-01,
     80.11912235E-01,0.57483106E-02,0,25559349E-02,
     9.10478123E-02,.39617000E-03,.13816206E-03,
```

```
     A.44439761E-04,.13180466E-04,.36033694E-05,
     B.90760433E-06,.21049269E-06,.44918756E-07,
     C.88129729E-08,.15882974E-08/
      TWOPI = 0.63661977
      SM1 = 0.0
      SM2 = 0.0
      DO 100 II = 1,24
      I = 25 - II
C     THE FIRST 24 TERMS OF AN N=68 GAUSS-LAGUERRE INTEGRAL
C     APPROXIMATION ARE USED.  THE ERROR IN DROPPING THE
C     HIGHER TERMS SHOULD BE LESS THAN 1.0E-09
      TAU = X(I)/R
      Z = X(I)
      CALL SHCFIK(G1,G2,OMEGA,TAU)
      CALL BESMOD(BMOD0,BMOD1,Z)
      SM1 = SM1 + AIMAG(G1) * BMOD0 * W(I)
      SM2 = SM2 + REAL(G2) * BMOD1 * W(I)
  100 CONTINUE
      SM1 = - TWOPI * SM1 / (R*R)
      SM2 =   TWOPI * SM2 / (R*R)
      RETURN
      END

      SUBROUTINE SHCFIK(G1,G2,OMEGA,TAU)
C     THIS ROUTINE EVALUATES THE G1 AND G2 COEFFICIENTS FOR
C     A PURELY IMAGINARY WAVENUMBER
      COMMON / MODEL / D(15),A(15),B(15),RHO(15),MMAX
      COMMON/SOURCE/DEPTH,LMAX,DPH
      COMPLEX G1,G2
      COMPLEX EJ11,EJ21,EL11,EL12,EL21,EL22,FL,E1,E2
      A11 = 1.0
      A12 = 0.0
      A21 = 0.0
      A22 = 1.0
      ED11 = 1.0
      ED12 = 0.0
      ED21 = 0.0
      ED22 = 1.0
      E22 = -1./(B(MMAX)*B(MMAX))
      XKB = OMEGA/B(MMAX)
      E11I= SQRT(TAU*TAU+XKB*XKB)*RHO(MMAX)
      E11R = 0.0
C     TO AVOID NUMERICAL PROBLEMS, MATRIX MULTIPLICATION
C     GOES FROM BOTTOM LAYER UPWARD
      MMM1 = MMAX - 1
```

```
      DO 1340 K = 1,MMM1
      M = MMAX - K
      XKB = OMEGA/B(M)
      RB = SQRT(TAU*TAU + XKB*XKB)
      Q = D(M) * RB
      H = RHO(M) * B(M) * B(M)
      IF(RB.EQ.0.0) GO TO 1401
      COSQ = COS(Q)
      SINQ = SIN(Q)
      Y = SINQ/(H*RB)
      Z = - H * RB * SINQ
      GO TO 1402
 1401 Y = D(M)/H
      Z = 0.0
      COSQ = 1.0
 1402 CONTINUE
      EA11 = A11 * COSQ + A12 * Z
      EA12 = A11 * Y + A12 * COSQ
      EA21 = A21 * COSQ + A22 * Z
      EA22 = A21 * Y + A22 * COSQ
      A11 = EA11
      A12 = EA12
      A21 = EA21
      A22 = EA22
      L1 = LMAX + 1
      IF(L1.NE.M) GO TO 1340
      ED11 = A11
      ED12 = A12
      ED21 = A21
      ED22 = A22
 1340 CONTINUE
      H = RHO(LMAX) * B(LMAX) * B(LMAX)
      XKB = OMEGA / B(LMAX)
      RB = SQRT(TAU*TAU + XKB*XKB)
      Q = DPH * RB
      IF(RB.EQ.0.0) GO TO 1501
      COSQ = COS(Q)
      SINQ =  SIN(Q)
      Y = SINQ/(H*RB)
      Z =-H * RB * SINQ
      GO TO 1502
 1501 CONTINUE
      Y = DPH/H
      Z = 0.0
      COSQ = 1.0
```

```
 1502 CONTINUE
      D11 = (ED11 * COSQ + ED12 * Z)/RHO(LMAX)
      D12 =-(ED11 * Y + ED12 * COSQ)*B(LMAX)*B(LMAX)
      D21 = (ED21 * COSQ + ED22 * Z)/RHO(LMAX)
      D22 =-(ED21 * Y + ED22 * COSQ)*B(LMAX)*B(LMAX)
      E1 = CMPLX(E11R,E11I)
      E2 = CMPLX(E22,0.0)
      EJ11 = E1 * A11
      EJ21 = E2 * A21
      EL11 = E1 * D11
      EL12 = E1 * D12
      EL21 = E2 * D21
      EL22 = E2 * D22
      FL = EJ11 - EJ21
      G1 = (EL21 - EL11) / FL
      G2 = (EL22 - EL12) * CMPLX(0.0,TAU) / FL
      RETURN
      END

      SUBROUTINE BESMOD(BMOD0,BMOD1,Z)
C     THIS SUBROUTINE EVALUATES THE FUNCTIONS
C        BMOD0 = Z * EXP(Z) * K0(Z)
C        BMOD1 = Z * EXP(Z) * K1(Z)
C     WHERE K0 AND K1 ARE THE MODIFIED BESSEL FUNCTIONS
      DIMENSION T(11),U(11),V(11)
      DATA (T(I),I=1,11)/0.0,0.05,0.1,0.2,0.3,0.4,0.5,0.6,
     11.,1.5,2./, (U(I),I=1,11)/0.0,0.163695,0.268232,
     20.428151,0.555788,.665073,.762055,.8500425,1.144463,
     31.437315,1.683136/,(V(I),I=1,11)/1.0,1.046523,
     41.089018,1.166677,1.237547,1.303469,1.3655048,
     51.424352,1.63615349,1.86474881,2.1349418/
      IF(Z.GT.0.0) GO TO 100
      BMOD0 = 0.0
      BMOD1 = 1.0
      RETURN
  100 IF(Z.GE.2.0) GO TO 200
C     IN THIS RANGE OF FUNCTIONAL, LINEAR INTERROLATION IS
C     ALL RIGHT
      DO 150 I = 1,10
      IJ = I
      IF(Z.GT.T(I).AND.Z.LE.T(I+1))   GO TO 151
  150 CONTINUE
  151 CONTINUE
      BMOD0=U(IJ)+(Z-T(IJ))*(U(IJ+1)-U(IJ))/(T(IJ+1)-T(IJ))
      BMOD1=V(IJ)+(Z-T(IJ))*(V(IJ+1)-V(IJ))/(T(IJ+1)-T(IJ))
```

```
      RETURN
  200 CONTINUE
      X = 2./Z
      BMOD0 = SQRT(Z)*(1.25331414+X*(-.07832358+X*(.02189568
     1+X*(-.01062446+X*(.00587872+X*(-.00251540+X*(.00053208
     2)))))))
      BMOD1 = SQRT(Z)*(1.25331414+X*(.23498619+X*(-.03655620
     1+X*(.01504268+X*(-.00780353+X*(.00325614+X*(-.00068245
     2)))))))
      RETURN
      END

      SUBROUTINE SRCMOD
C     READ IN EARTH MODEL
      COMMON / MODEL / D(15),A(15),B(15),RHO(15),MMAX
      DO 20 I = 1,15
      READ(60,1) D(I),A(I),B(I),RHO(I)
    1 FORMAT(4F10.3)
      MMAX = I
      IF(D(I).LE.0.0) GO TO 21
   20 CONTINUE
   21 CONTINUE
      MMX1 = MMAX - 1
      PRINT 2
    2 FORMAT(1H0,7X,1HD, 9X,1HA,9X,1HB,9X,3HRHO/)
      DO 400 I = 1,MMX1
    3 FORMAT(1H ,4F10.2)
  400 PRINT 3,D(I),A(I),B(I),RHO(I)
      PRINT 5,A(MMAX),B(MMAX),RHO(MMAX)
    5 FORMAT(1H ,10X,3F10.2/1H0)
      RETURN
      END

      SUBROUTINE SRCLYR
      COMMON / MODEL / D(15),A(15),B(15),RHO(15),MMAX
      COMMON/SOURCE/DEPTH,LMAX,DPH
C     LMAX = SOURCE LAYER
C     DEPTH = SOURCE DEPTH
C      DPH = HEIGHT OF SOURCE ABOVE LMAX + 1 INTERFACE
C     LMAX = 0 IS THE FREE SURFACE
      DEP = 0.0
      MMX1 = MMAX - 1
      DO 100 M = 1,MMX1
      DEP = DEP + D(M)
      DPH = DEP - DEPTH
```

```
      LMAX = M
      IF(DPH.GE.0.0) GO TO 101
  100 CONTINUE
  101 CONTINUE
      RETURN
      END

      SUBROUTINE RSHOF(GG1,GG2,FL,OMEGA,WVNO,EXE,EXL)
      COMPLEX EJ11,EJ21,EL11,EL12,EL21,EL22,E1,E2,FL,GG1,GG2
      CALL SHCOEF(A11,A12,A21,A22,D11,D12,D21,D22,E11R,E11I,
     1E22,OMEGA,WVNO,EXE,EXL)
      E1 = CMPLX(E11R,E11I)
      E2 = CMPLX(E22,0.0)
      EJ11 = E1 * A11
      EJ21 = E2 * A21
      EL11 = E1 * D11
      EL12 = E1 * D12
      EL21 = E2 * D21
      EL22 = E2 * D22
      GG1 = (EL21 - EL11)
      GG2 = (EL22 - EL12) * WVNO
      FL = EJ11 - EJ21
      RETURN
      END

      SUBROUTINE SHCOEF(A11,A12,A21,A22,D11,D12,D21,D22,E11R
     1,E11I,E22,OMEGA,WVNO,EXE,EXL)
      COMMON / MODEL / D(15),A(15),B(15),RHO(15),MMAX
      COMMON /SOURCE/ DEPTH,LMAX,DPH
C      SINCE THIS IS WRITTEN FOR A MACHINE WHOSE LARGEST
C     NUMBER IS 1.0E+39, SPECIAL NORMALIZATION IS USED TO
C     AVOID EXPONENT OVERFLOW OR UNDERFLOW
      A11 = 1.0E-20
      A21 = 0.0
      A12 = 0.0
      A22 = 1.0E-20
      ED11 = 1.0E-20
      ED12 = 0.0
      ED21 = 0.0
      ED22 = 1.0E-20
      EXE = 0.0
      EXL = 0.0
      WVNO2 = WVNO*WVNO
      E22 = -1./(B(MMAX)*B(MMAX))
      XKB = OMEGA/B(MMAX)
```

```
      RB = SQRT(ABS(WVNO2-XKB*XKB))
      E11R = 0.0
      E11I = 0.0
      FAC = RHO(MMAX)*RB
      IF(WVNO.GT.XKB) E11R=FAC
      IF(WVNO.LT.XKB) E11I = FAC
C     TO AVOID NUMERICAL PROBLEMS, MATRIX MULTIPLICATION
C     GOES FROM BOTTOM LAYER UPWARD
      MMM1 = MMAX - 1
      DO 1340 K = 1,MMM1
      M = MMAX - K
      XKB = OMEGA/B(M)
      RB = SQRT(ABS(WVNO2 - XKB*XKB))
      Q = D(M) * RB
      H = RHO(M)*B(M)*B(M)
      IF(WVNO-XKB)1231,1221,1209
 1231 SINQ = SIN(Q)
      Y = SINQ/(H*RB)
      Z = -H*RB*SINQ
      COSQ = COS(Q)
      GO TO 1242
 1221 COSQ = 1.0
      Y = D(M)/H
      Z = 0.0
      GO TO 1242
 1209 IF(Q.GT.5.0) GO TO 1208
      EXQP = EXP(Q)
      EXQM = 1./EXQP
      SINQ = (EXQP-EXQM)/2.
      Y = SINQ/(H*RB)
      Z = SINQ*H*RB
      COSQ = (EXQP+EXQM)/2.
      GO TO 1242
 1208 EXE = EXE + Q
      Z = 0.5*H*RB
      Y = 0.5/(H*RB)
      COSQ = 0.5
 1242 CONTINUE
      EA11 = A11*COSQ + A12*Z
      EA12 = A11*Y + A12*COSQ
      EA21 = A21*COSQ + A22*Z
      EA22 = A21*Y + A22*COSQ
      A11 = EA11
      A12 = EA12
      A21 = EA21
```

```
      A22 = EA22
      L1 = LMAX+1
      IF(L1.NE.M) GO TO 1340
      EXL = EXE
      ED11 = A11
      ED12 = A12
      ED21 = A21
      ED22 = A22
 1340 CONTINUE
      H = RHO(LMAX)*B(LMAX)*B(LMAX)
      XKB = OMEGA/B(LMAX)
      RB = SQRT(ABS(WVNO2-XKB*XKB))
      Q = DPH * RB
      IF(WVNO-XKB)1131,1121,1111
 1131 SINQ = SIN(Q)
      Y = SINQ/(H*RB)
      Z = -H*RB*SINQ
      COSQ = COS(Q)
      GO TO 1142
 1121 COSQ = 1.0
      Y = DPH/H
      Z = 0.0
      GO TO 1142
 1111 IF(Q.GT.5.0) GO TO 1108
      EXQP = EXP(Q)
      EXQM = 1./EXQP
      SINQ = (EXQP-EXQM)/2.
      Y = SINQ/(H*RB)
      Z = SINQ*H*RB
      COSQ = (EXQP+EXQM)/2.
      GO TO 1142
 1108 EXL = EXL + Q
      Z = H*RB*0.5
      Y = 0.5/(H*RB)
      COSQ = 0.5
 1142 CONTINUE
      D11 = (ED11*COSQ + ED12*Z)/RHO(LMAX)
      D12 = -(ED11*Y + ED12*COSQ)*B(LMAX)*B(LMAX)
      D21 = (ED21*COSQ + ED22*Z)/RHO(LMAX)
      D22 = -(ED21*Y + ED22*COSQ)*(B(LMAX)*B(LMAX))
      RETURN
      END
```

APPENDIX B: COMPUTER PROGRAM SHVEL

Function

This program performs the inverse Fourier transform of Equation 9, using the source velocity pulse $s_2(t)$ of Equation 23. The source pulse, its Fourier amplitude spectrum and the filtered source pulse are plotted as output. The output of SHSPEC is read in on File 12, the pulse parameters are read from card on File 60, printer output is on File 61, CALCOMP off-line plots are on File 10, and the velocity time histories are on File 20 for use by the program DSVLAC.

The card input is very simple and is given below rather in a table:

Card	Variable Name	Columns	Format	Description
1	TL	1-10	F10.5	The pulse parameter τ of Equation 23.
	XMOM	11-20	E10.3	A scaling factor used to adjust source spectrum level. G1 and G2 are output from SHSPEC for a seismic moment of 1.0E+20 dyne-cm since the area under $s_2(t)$ is unity. XMOM permits the use of another moment as well as the adjustment for focal mechanism. XMOM is the desired seismic moment times the terms in the square brackets of Equation 24. XMOM.LT.1 is interpreted as XMOM=1.0E+20

(More Card 1's are read until one with TL.LE.0 is found, which causes program termination and closing of files). To generate Figure 19, TL=0.5 and XMOM=7.06E+22 were used (seismic moment of 3.53E+22 dyne-cm and a focal mechanism factor of 2.0).

The printer output of SHVEL is mostly diagnostic. File 61 gives the values of TL, DT, and XMOM (DT is read from File 12). Under the system standard printer output (PRINT statement), YMAX and YMIN are the maximum and minimum amplitudes of each time plot; R, IOUT and TSHIFT are the parameters R, IOUT and TO written on File 12 by the program SHSPEC.

A description of the subroutines is given in Table B1. The program listing is given in Table B2.

Table B1

Subroutine Description

Subroutine Name	Function
PULSE	Defines the source pulse of Equation 23. Other normalized source pulses can be used by rewriting this subroutine.
FOUR	Performs numerical approximation to the Fourier integral by using a fast Fourier transform.
SEISPLT	Sets up a CALCOMP plot of ground motion time histories. Other plotters can be used by rewriting this subroutine.
SPPLT	Sets up log-log CALCOMP plot of Fourier amplitude spectra.
ALOGAXES	Sets up log-log axes for SPPLT.

Table B2


```
C       PROGRAM SHVEL
        DIMENSION DATA(2048),X(1026),Y(1026),DATAS(1026)
        DIMENSION DATA1(2048)
        DIMENSION IBUF(1000)
C       INPUT DATA
C
C       CARD 1 TL, XMOM
C       TL IS SOURCE PULSE PARAMETER, XMOM IS SEISMIC MOMENT
C       IN DYNE-CM. IF XMOM=0 PROGRAM DEFAULTS TO 1.0E+20 D-CM
C       ..... MORE CARD 1 - USE TL.LT.0 TO END CARD 1 SEQUENCE
        CALL PLOTS(IBUF,1000,10)
  9998  CONTINUE
        REWIND 12
        READ(12,1)  DEPTH,FL,FU,DT,N,VRED
        NYQ = N/2 + 1
        NYQ2 = 2*NYQ
        DF = 1./(N*DT)
        N1 = FL/DF
        N2 = FU/DF
        READ(60,111) TL,XMOM
     1  FORMAT(4F10.5,I5,F10.5)
    11  FORMAT(F10.5,2I5,2F10.5)
   111  FORMAT(F10.5,E10.3)
        NS = 2
        WRITE(20,11)TL,NS,N,DT,DEPTH
        IF(TL.LE.0.0) GO TO 9999
        WRITE(61,4) TL,DT,XMOM
     4  FORMAT(1H0,4HTL =,F10.5,5X,4HDT =,F10.5,5X,4HMOM=,
       1E10.3)
        XMOM = XMOM / 1.0E20
        IF(XMOM.LT.1.0E-20) XMOM = 1.0
        CALL PULSE(X,Y,N,DT,TL)
        CALL SEISPLT(X,Y,N,0.0,0,6HINPUT )
C       PLOT SOURCE PULSE AND SPECTRA
        DO 200 I = 1,N
        J = 2 * I - 1
        K = 2 * I
        DATA(J) = Y(I)
   200  DATA(K) = 0.0
        CALL FOUR(DATA,N,-1,DT,DF)
        DO 205 I = 1,NYQ
        J = 2 * I - 1
        K = 2 * I
        IF(I.GE.N1.AND.I.LE.N2) GO TO 205
        DATA(J) =0.0
```

```
      DATA(K) = 0.0
  205 CONTINUE
      CALL SPPLT(DATA,X,Y,NYQ,DF,6H SPEC )
      DO 206 I = 1,NYQ2
  206 DATAS(I) = XMOM * DATA(I)
      CALL FOUR(DATA,N,+1,DT,DF)
      DO 210 I = 1,N
      J = 2 * I - 1
      X(I) = (I-1) * DT
      Y(I) = DATA(J)
  210 CONTINUE
C     PLOT FILTERED SOURCE PULSE
      CALL SEISPLT(X,Y,N,0.0,0,6H FILT )
 9997 CONTINUE
      READ(12,601)R,IOUT,T0
  601 FORMAT(E11.4,I5,E11.4)
      WRITE(20,601) R,IOUT,T0
      IF(R.LT.0.0) GO TO 9998
      PRINT 5,R,IOUT,T0
    5 FORMAT(1H0,4H R =,F8.2,8H  IOUT =,I3,5X,10H  TSHIFT =,
     1F8.2)
      READ(12,600) (DATA(I),I=1,NYQ2)
      READ(12,600)(DATA1(I),I=1,NYQ2)
  600 FORMAT(8E11.4)
      DO 700 I = 1,NYQ
      J = 2*I - 1
      K = 2 * I
      AR1 = DATA(J)
      AI1 = DATA(K)
      AR2 = DATA1(J)
      AI2 = DATA1(K)
      DATA(J) = DATAS(J)*AR1 - DATAS(K)*AI1
      DATA(K) = DATAS(K)*AR1 + DATAS(J)*AI1
      DATA1(J) = DATAS(J)*AR2 - DATAS(K)*AI2
      DATA1(K) = DATAS(K)*AR2 + DATAS(J)*AI2
      IF(I.EQ.1) GO TO 700
      II = N + 2 - I
      JJ = 2 * II - 1
      KK = 2 * II
      DATA(JJ) = DATA(J)
      DATA(KK) = - DATA(K)
      DATA1(JJ) = DATA1(J)
      DATA1(KK) = - DATA1(K)
  700 CONTINUE
  303 CONTINUE
```

```
      CALL FOUR(DATA,N,+1,DT,DF)
      CALL FOUR(DATA1,N,+1,DT,DF)
      DO 400 I = 1,N
      J = 2 * I - 1
      X(I) = DATA(J)
      Y(I) = DATA1(J)
  400 CONTINUE
      WRITE(20,600)(X(I),I=1,N)
      WRITE(20,600)(Y(I),I=1,N)
      GO TO 9997
 9999 CONTINUE
      CALL PLOT(12.0,0.0,999)
      STOP
      END

      SUBROUTINE PULSE(T,F,N,DT,TL)
      DIMENSION T(1),F(1)
      T1 = 0.0
      T2 = T1 + TL
      T3 = T2 + TL
      T4 = T3 + TL
      T5 = T4 + TL
      DO 100 I = 1,N
      T(I) = (I-1) * DT
      Y = T(I)
      Z = Y - T1
      F(I) = 0.0
      IF(Y.GT.T1) GO TO 101
      GO TO 100
  101 IF(Y.GT.T2) GO TO 102
      F(I) = (Z/TL)*(Z/TL)*0.5
      GO TO 100
  102 IF(Y.GT.T3) GO TO 103
      F(I) = - (Z/TL)*(Z/TL)*0.5 + 2.0*(Z/TL) - 1.0
      GO TO 100
  103 IF(Y.GT.T4) GO TO 104
      F(I) = - (Z/TL)*(Z/TL)*0.5 + 2.0*(Z/TL) - 1.
      GO TO 100
  104 IF(Y.GT.T5) GO TO 105
      F(I) = (Z/TL)*(Z/TL) * 0.5 -4.0 * (Z/TL) + 8.0
      GO TO 100
  105 F(I) = 0.0
  100 CONTINUE
C     AREA OF PULSE NORMALIZED TO UNITY
      DO 200 I = 1,N
```

```
  200 F(I) = F(I) /(2.*TL)
      RETURN
      END
      SUBROUTINE FOUR(DATA,NN,ISIGN,DT,DF)
C     THE COOLEY-TOOKEY FAST FOURIER TRANSFORM IN USASI
C     BASIC FORTRAN TRANSFORM(J)=SUM(DATA(I)*W**(I-1)(J-1)),
C     WHERE I AND J RUN FROM 1 TO NN AND W=EXP(ISIGN*2*PI*
C     SQRT(-1)/NN). DATA IS A ONE-DIMENSION AL COMPLEX ARRAY
C     (I.E., THE REAL AND IMAGINARY PARTS OF DATA ARE
C     LOCATED IMMEDIATELY ADJACENT IN STORAGE, SUCH AS
C     FORTRAN IV PLACES THEM) WHOSE LENGTH NN IS A POWER OF
C     TWO. ISIGN IS +1 OR -1, GIVING THE SIGN OF THE
C     TRANSFORM.  TRANSFORM VALUES ARE RETURNED IN ARRAY
C     DATA, REPLACING THE INPUT DATA. THE TIME IS PROPOR-
C     TIONAL TO N*LOG2(N), RATHER THAN THE USUAL N**2
C     RMS RESOLUTION ERROR BEING BOUNDED BY 6*SQRT(I)*
C     LOG2(NN)*2**(-B), WHERE B IS THE NUMBER OF BITS IN THE
C     FLOATING POINT FRACTION. PROGRAM AUTOMATICALLY TAKES
C     INTO ACCOUNT DIMENSIONALITY
      DIMENSION DATA(1)
      N = 2 * NN
      IF(DT.EQ.0.0) DT = 1./(NN*DF)
      IF(DF.EQ.0.0) DF = 1./(NN*DT)
      IF(DT.NE.(NN*DF)) DF = 1./(NN*DT)
      J = 1
      DO 5 I=1,N,2
      IF(I-J)1,2,2
    1 TEMPR = DATA(J)
      TEMPI = DATA(J+1)
      DATA(J) = DATA(I)
      DATA(J+1)=DATA(I+1)
      DATA(I) = TEMPR
      DATA(I+1) = TEMPI
    2 M = N/2
    3 IF(J-M) 5,5,4
    4 J = J-M
      M = M/2
      IF(M-2)5,3,3
    5 J=J+M
      MMAX = 2
    6 IF(MMAX-N) 7,10,10
    7 ISTEP= 2 *MMAX
      THETA = 6.283185307/FLOAT(ISIGN*MMAX)
      SINTH=SIN(THETA/2.)
```

```
      WSTPR=-2.*SINTH*SINTH
      WSTPI=SIN(THETA)
      WR=1.0
      WI=0.0
      DO 9 M=1,MMAX,2
      DO 8 I=M,N,ISTEP
      J=I+MMAX
      TEMPR=WR*DATA(J)-WI*DATA(J+1)
      TEMPI=WR*DATA(J+1)+WI*DATA(J)
      DATA(J)=DATA(I)-TEMPR
      DATA(J+1)=DATA(I+1)-TEMPI
      DATA(I)=DATA(I)+TEMPR
    8 DATA(I+1) = DATA(I+1)+TEMPI
      TEMPR = WR
      WR = WR*WSTPR-WI*WSTPI + WR
    9 WI = WI*WSTPR+TEMPR*WSTPI + WI
      MMAX = ISTEP
      GO TO 6
   10 CONTINUE
      IF(ISIGN.LT.0) GO TO 1002
C     FREQUENCY TO TIME DOMAIN
      DO 1001 IIII = 1,N
 1001 DATA(IIII) = DATA(IIII) * DF
      RETURN
 1002 CONTINUE
C     TIME TO FREQUENCY DOMAIN
      DO 1003 IIII = 1,N
 1003 DATA(IIII) = DATA(IIII) * DT
      RETURN
      END

      SUBROUTINE SEISPLT(X,Y,N,DIST,ID,SYM)
      CHARACTER SYM
      DIMENSION X(1),Y(1)
      CALL PLOT(0,0,-11.0,-3)
      CALL PLOT(0,0,2.0,-3)
      YMIN = 1.0E+38
      YMAX = -1.0E+38
      DO 100 I = 1,N
      IF(Y(I).GT.YMAX) YMAX = Y(I)
      IF(Y(I).LT.YMIN) YMIN = Y(I)
  100 CONTINUE
      IF(ID.GT.0) PRINT 1,YMAX,YMIN,DIST
      IF(ID.EQ.0) PRINT 2,YMAX,YMIN
    1 FORMAT(1H ,6HYMAX =,E10.3,10H    YMIN = ,E10.3,3X,
```

```
     16HDIST = ,F6.1)
    2 FORMAT(1H ,6HYMAX =,E10.3,10H    YMIN = ,E10.3)
      IF(ABS(YMIN).GT.YMAX) YMAX = ABS(YMIN)
      X(N+1) = -5,0
      X(N+2) = 15.
      Y(N+1) = - YMAX
      Y(N+2) = 2. * YMAX
      CALL AXIS(0,25,0.0,10HT - X/4,67  ,-10,5,0,90.0,X(N+1)
     1,X(N+2))
      CALL AXIS(0,0,-0.25,1H    ,1,1.0,180.0,Y(N+1),Y(N+2))
      Y(N+2) = - Y(N+2)
      CALL LINE(Y,X,N,1,0,0)
      IF(ID,GT.0) CALL NUMBER(-0.75,4,5,0,14,DIST,90.0,-1)
      CALL SYMBOL(-1,0,-1,5,0.14,SYM,0.0,+6)
      CALL PLOT(3,0,0.0,-3)
      RETURN
      END

      SUBROUTINE SPPLT(DATA,X,Y,NP,DF,SYM)
C     THIS PLOTS AMPLITUDE SPECTRA ON 2 X 3 CYCLE LOG-LOG
C     SCALE
      DIMENSION DATA(1),Y(1),X(1)
      CHARACTER TTLX(2),TTLY(2)
      CHARACTER SYM
      CALL PLOT(0,0,-11.0,-3)
      CALL PLOT(0.0,2.0,-3)
      XMIN = 0.1
      XMAX = 10.
      YMAX = 1.0E-38
      J = 0
C     THE ZERO FREQUENCY POINT IS NOT PLOTTED
      DO 5700 I = 2,NP
      J = J + 1
      X(J) = (I-1) * DF
      IF(X(J).LT.XMIN) X(J) = XMIN
      IF(X(J).GT.XMAX) X(J) = XMAX
      K = 2 * I - 1
      L = 2 * I
      Y(J) = SQRT(ABS(DATA(K)*DATA(K) + DATA(L)*DATA(L)))
      IF(Y(J).GT.YMAX) YMAX = Y(J)
 5700 CONTINUE
      YY = ALOG10(YMAX)
      LY = YY
      YY=LY
      IF(YY.GT.LY) YY = LY + 1
```

```
      YMIN = 10.**(YY - 3.)
       YMAX = 10.**YY
      N = J
      DO 5701 I = 1,N
      IF(Y(I).LT.YMIN) Y(I) = YMIN
 5701 CONTINUE
      XAXLEN = 3.732
      YAXLEN = 5.598
      DELTAX = 2./XAXLEN
      DELTAY = 3./YAXLEN
      X1 = ALOG10(XMIN)
      NOCX = 2
      NOCY = 3
      Y1 = YY - NOCY
      TTLX(1)=6HFREQ (
      TTLX(2) = 6HHZ)
      TTLY(1) = 6HAMP (C
      TTLY(2) = 6HM-SEC)
      MTX = 12
      MTY = 12
      CALL ALOGAXES(XAXLEN,YAXLEN,NOCX,NOCY,TTLX,TTLY,MTX,
     1MTY,X1,Y1,DELTAX,DELTAY)
      DO 5703 I = 1,N
      Y(I) = ALOG10(Y(I))
 5703 X(I) = ALOG10(X(I))
      X(N+1) = X1
      X(N+2) = DELTAX
      Y(N+1) = Y1
      Y(N+2) = DELTAY
      CALL LINE(X,Y,N,1,0,0)
      CALL SYMBOL(0.0,-1.0,0.14,SYM,0.0,+6)
      CALL PLOT(10.0,0.0,-3)
      RETURN
      END

      SUBROUTINE ALOGAXES(XAXLEN,YAXLEN,NOCX,NOCY,TTLX,TTLY,
     1MTX,MTY,X1,Y1,DELTAX,DELTAY)
      CHARACTER TTLX(1),TTLY(1)
      SLT = 0.02*YAXLEN
      SST = 0.01 * YAXLEN
      SP = -0.06*YAXLEN
      SS = 0.035*YAXLEN
      SSP = SP + SS - 0.06
      TTLP = -0.11*YAXLEN - 0.1
      STTL = 0.035*YAXLEN
```

```
      XNUM = 1
      YL = Y1
      YU = Y1 + ANOCY
      IF(ABS(YL).GE.10. .OR. ABS(YU).GE.10. )XNUM = XNUM +1.
      IF(ABS(YL).GE.100..OR. ABS(YU).GE.100.)XNUM = XNUM +1.
      IF(Y1.LT.0) XNUM = XNUM + 1.0
      CALL PLOT(-SLT,0.0,2)
      CALL PLOT(0.0,-SLT,3)
      CALL PLOT(0.0,0.0,2)
      XPO = X1
      YPO = Y1
      IF(NOCX.EQ.0) GO TO 4
      ANOCX = NOCX
      FACTX = XAXLEN/ANOCX
      CALL SYMBOL(-.6*SS,SP,SS,2H10,0.0,2)
      CALL NUMBER(999.,SSP,0.6*SS,X1,0.0,-1)
      CALL PLOT(0.0,0.0,3)
      DO 3 J = 1,NOCX
      DO 2 I = 1,10
      X = I
      X = ALOG10(X) *FACTX + (J-1)*FACTX
      IF(I.EQ.1)GO TO 2
      CALL PLOT(X,0.0,2)
      CALL PLOT(X,-SST,2)
    2 CALL PLOT(X,0.0,3)
      CALL PLOT(X,-SLT,2)
      CALL SYMBOL(X-.6*SS,SP,SS,2H10,0.0,2)
      XPO = XPO + 1.0
      CALL NUMBER(999.,SSP,0.6*SS,XPO,0.0,-1)
    3 CALL PLOT(X,0.0,3)
      XTL = MTX
      XTL = (XAXLEN-XTL*STTL)/2.0
      CALL SYMBOL(XTL,TTLP,STTL,TTLX,0.0,MTX)
      GO TO 6
    4 CALL AXIS(0.0,0.0,TTLX,-MTX,XAXLEN,0.0,X1,DELTAX)
    6 CALL PLOT(0.0,0.0,3)
      IF(NOCY.EQ.0) GO TO 10
      ANOCY = NOCY
      SP = SP - (XNUM - 1.5) * 0.5 * SS
      TTLP = TTLP - (XNUM-1.)*0.5*SS
      FACTY = YAXLEN/ANOCY
      CALL SYMBOL(SP-0.4,-0.5*SS,SS,2H10,0.0,2)
      CALL NUMBER(999.,.5*SS-.06,.6*SS,Y1,0.0,-1)
      CALL PLOT(0.0,0.0,3)
      DO 9 J = 1,NOCY
```

```
      DO 8 I = 1,10
      Y = I
      Y = ALOG10(Y) * FACTY + (J-1)*FACTY
      IF(I.EQ.1)GO TO 8
      CALL PLOT(0.0,Y,2)
      CALL PLOT(-SST,Y,2)
    8 CALL PLOT(0.0,Y,3)
      CALL PLOT(-SLT,Y,2)
      CALL SYMBOL(SP-.4,Y-.5*SS,SS,2H10,0.0,2)
      YPO = YPO + 1
      CALL NUMBER(999.,Y+.5*SS-.06,.6*SS,YPO,0.0,-1)
    9 CALL PLOT(0.0,Y,3)
      YTL=MTY
      YTL = (YAXLEN-YTL*STTL)/2.0
      CALL SYMBOL(TTLP-.2,YTL,STTL,TTLY,90.,MTY)
      RETURN
   10 CALL AXIS(0.0,0.0,TTLY,MTY,YAXLEN,90.,Y1,DELTAY)
      RETURN
      END
```

APPENDIX C: COMPUTER PROGRAM DSVLAC

Function

This self-contained program takes the velocity time series computed by the program SHVEL, plots the displacement, velocity and acceleration time histories and also prepares an output file for use by the program SDSVSA. Input is from File 20, generated by SHVEL. CALCOMP output for off-line plotting is on File 10. File 21 contains data for use by the program SDSVSA. Printer output is through the PRINT statement and consists of the following for each source pulse:

Line 1	TL,NS,N,DT,DEPTH where the variables are as described for SHSPEC and SHVEL, except that NS indicates the number of focal mechanisms for each distance (NS=2 here since G1 and G2 traces are plotted)
Line 2	R, IOUT, TO
Line 3	SYM, YMAX, YMIN, R (tabulation of trace extrema. D1 is G1 displacement, D2 is G2 displacement, V1 is G1 velocity, A1 is G1 acceleration history, etc.)
	Line 3 repeats 3*NS times.

The subroutines are only three: SEISPLT plots the time traces; DISP calculates displacement time histories by trapezoidal rule; and ACCL calculates acceleration time histories by assuming linear velocity segments.

The program DSVLAC is given in Table C1.

Table C1


```
C       PROGRAM DSVLAC
C       THIS TAKES VELOCITIES GENERATED BY SHVEL AND COMPUTES
C        AND PLOTS ALL THREE
        DIMENSION IBUF(1000)
        DIMENSION V(1026),D(2050),T(2050)
        CHARACTER ID(2),IV(2),IA(2)
        ID(1) = 6H  D1
        ID(2) = 6H  D2
        IV(1) = 6H  V1
        IV(2) = 6H  V2
        IA(1) = 6H  A1
        IA(2) = 6H  A2
        REWIND 20
        REWIND 21
        CALL PLOTS(IBUF,1000,10)
      1 FORMAT(F10.5,2I5,2F10.5)
    600 FORMAT(8E11.4)
    601 FORMAT(E11.4,I5,E11.4)
   9998 CONTINUE
        READ(20,1)TL,NS,N,DT,DEPTH
        WRITE(21,1) TL,NS,N,DT,DEPTH
        IF(TL.LE.0.0) GO TO 9999
        PRINT 1,TL,NS,N,DT,DEPTH
   9997 CONTINUE
        READ(20,601) R,IOUT,TO
        WRITE(21,601)R,IOUT,TO
        IF(R.LT.0.0) GO TO 9998
        PRINT 601,   R,IOUT,TO
        DO 9996 L = 1,NS
        READ(20,600) (V(I),I=1,N)
        CALL DISP(V ,DT,N,T,D)
        CALL SEISPLT(T,D,N,R,1,ID(L),DMAX)
        CALL SEISPLT(T,V,N,R,1,IV(L),VMAX)
        CALL ACCL(V,DT,N,M,T,D)
        CALL SEISPLT(T,D,M,R,1,IA(L),AMAX)
        WRITE(21,604) AMAX,VMAX,DMAX
    604 FORMAT(3E11.4)
        WRITE(21,600)(V(I),I=1,N)
   9996 CONTINUE
        GO TO 9997
   9999 CONTINUE
        CALL PLOT(12.0,0.0,999)
        STOP
        END

        SUBROUTINE SEISPLT(X,Y,N,DIST,ID,SYM,YMAX)
```

```
      CHARACTER SYM
      DIMENSION X(1),Y(1)
      CALL PLOT(0,0,-11.0,-3)
      CALL PLOT(0,0,2.5,-3)
      YMIN = 1.0E+38
      YMAX = -1.0E+38
      DO 100 I = 1,N
      IF(Y(I).GT.YMAX) YMAX = Y(I)
      IF(Y(I).LT.YMIN) YMIN = Y(I)
  100 CONTINUE
      IF(ID.GT.0) PRINT 1,SYM,YMAX,YMIN,DIST
      IF(ID.EQ.0) PRINT 2,YMAX,YMIN
    1 FORMAT(1H ,A6,6HYMAX =,E10.3,10H    YMIN = ,E10.3,3X,
     16HDIST =,F6.1)
    2 FORMAT(1H ,6HYMAX =,E10.3,10H    YMIN = ,E10.3)
      IF(ABS(YMIN).GT.YMAX) YMAX = ABS(YMIN)
      X(N+1) = -5.0
      X(N+2) = 15.
      Y(N+1) = - YMAX
      Y(N+2) = 2. * YMAX
      CALL AXIS(0.25,0.0,10HT - X/4.67  ,-10,5.0,90.0,X(N+1)
     1,X(N+2))
      CALL AXIS(0.0,-0.25,1H    ,1,1.0,180.0,Y(N+1),Y(N+2))
      Y(N+2) = - Y(N+2)
      CALL LINE(Y,X,N,1,0,0)
      IF(ID.GT.0) CALL NUMBER(-0.75,4.5,0.14,DIST,90.0,-1)
      CALL SYMBOL(-1.0,-1.5,0.14,SYM,0.0,+6)
      CALL PLOT(3.0,0.0,-3)
      RETURN
      END

      SUBROUTINE DISP(V,DT,N,T,D)
      DIMENSION V(1),T(1),D(1)
      D(1) = 0.0
      SUM=0.0
      DO 100 I = 2,N
      T(I) = (I-1) * DT
      SUM = SUM + 0.5 * DT * (V(I)+V(I-1))
      D(I) = SUM
  100 CONTINUE
      RETURN
      END

      SUBROUTINE ACCL(V,DT,N,M,T,A)
      DIMENSION V(1),T(1),A(1)
```

```
      M = 2*N
      NM1 = N - 1
      DO 100 I = 1,NM1
      DIF = (V(I+1)-V(I))/DT
      J = 2*I - 1
      K = 2 * I
      T(J) = (I-1) * DT
      T(K) = I * DT
      A(J) = DIF
      A(K) = DIF
  100 CONTINUE
      DIF = (V(1) - V(N))/DT
      J = 2*N - 1
      K = 2*N
      T(J) = (N-1)*DT
      T(K) = N*DT
      A(J) = DIF
      A(K) = DIF
      RETURN
      END
```

APPENDIX D: COMPUTER PROGRAM SDSVSA

Function

This program used the output of DSVLAC to compute the response spectra of each trace using Equations 30 and 31. The input is on File 21 generated by the program DSVLAC. Off-line CALCOMP graphic output is on File 10. Printer output is through the use of the PRINT statement. The output consists of a plot of the response spectrum as well as a listing of the response spectrum values, including SD, SV, SA, PSV and the Fourier spectrum FS, for damping values of 0, 2, 5 and 10 percent critical and oscillator periods from DT to 100 sec (it is meaningless to compute the response for periods less than the sampling interval).

The subroutines are MOTION which performs the computations for each input time history, SVLOG which performs the logarithmic plot and AMATRIX which computes the matrix elements of Equation 30.

The program listing is given in Table D1.

Table D1


```
 C      PROGRAM SD,SV,SA,PSV,FS
        DIMENSION VEL(1024),TMAX(3)
        DIMENSION IBUF(1000)
        CHARACTER SYM(2)
        CALL PLOTS(IBUF,1000,10)
        REWIND 21
        SYM(1)= 6HG1
        SYM(2)= 6HG2
   100  READ(21,1000) TL,NS,N,DT,DEPTH
        IF( TL.LE.0.0 ) GO TO 300
        CALL AMATRIX(N,DT)
   105  CONTINUE
        READ(21,1100) R,IOUT,TO
        IF( R.LT.0.0 ) GO TO 100
        DO 200 I1=1,NS
        READ(21,1200) (TMAX(I),I=1,3)
        READ(21,1300) (VEL(I),I=1,N)
        CALL MOTION(VEL,TMAX,SYM(I1),R,DEPTH)
   200  CONTINUE
        GO TO 105
   300  CALL PLOT(10.0,0.0,999)
  1000  FORMAT(F10.5,2I5,2F10.5)
  1100  FORMAT(E11.4,I5,E11.4)
  1200  FORMAT(3E11,4)
  1300  FORMAT(8E11,4)
        STOP
        END

        SUBROUTINE MOTION(VEL,TMAX,SYM,R,DEPTH)
 C
 C   THIS PROGRAM TAKES THE VELOCITY GENERATED AND FINDS
 C   SD,SV,SA,PSV,FS BY THE MODIFIED NIGAM-JENNINGS METHOD
 C   THE INPUT VELOCITY GRID POINTS ARE CONNECTED BY LINEAR
 C      SEGMENT
 C
 C       VEL = VELOCITY GENERATED, USED AS INPUT
 C       SYM = NAME OF THE INPUT VELOCITY
 C         R = EPICENTER DISTANT
 C     DEPTH = SOURCE DEPTH
 C
        DIMENSION VEL(1),TMAX(1)
        DIMENSION SD(49,4),SV(49,4),SA(49,4),PSV(49,4),FS(49)
        COMMON/ABCOEF/A11(49,4),A12(49,4),A21(49,4),A22(49,4)
      *                 ,B1(49,4),B2(49,4),PERIOD(49),KNDT(49)
      *                 ,KN1(49),DAMP(4),L
```

```
      CHARACTER SYM,E*153,F(102),G(3)
      DO 200 I1=L,49
      NDT   = KNDT(I1)
      N1    = KN1(I1)
      FREQ = 6.283185/PERIOD(I1)
      T4    = FREQ*FREQ
      DO 200 I2=1,4
      T5    = 2.*FREQ*DAMP(I2)
      DMAX = 0.
      VMAX = 0.
      AMAX = 0.
      X1    = 0.
      V1    = 0.
C  THE MAIN DO LOOP
      DO 100 I=1,N1
      J = (I+NDT-1)/NDT
      DVEL = (VEL(J+1)-VEL(J))/NDT
      X = A11(I1,I2)*X1+A12(I1,I2)*V1+B1(I1,I2)*DVEL
      V = A21(I1,I2)*X1+A22(I1,I2)*V1+B2(I1,I2)*DVEL
      X1 = X
      V1 = V
      A   = T4*X+T5*V
      XABS = ABS(X)
      VABS = ABS(V)
      AABS = ABS(A)
      IF( DMAX.LT.XABS )  DMAX = XABS
      IF( VMAX.LT.VABS )  VMAX = VABS
      IF( AMAX.LT.AABS )  AMAX = AABS
  100 CONTINUE
      IF( I2.EQ.1 )  FS(I1) = SQRT(T4*X*X+V*V)
       SD(I1,I2) = DMAX
       SV(I1,I2) = VMAX
       SA(I1,I2) = AMAX
      PSV(I1,I2) = FREQ*DMAX
  200 CONTINUE
      CALL SVLOG(PSV,SYM,R)
      G(1) = 6H AMAX=
      G(2) = 6H VMAX=
      G(3) = 6H DMAX=
      PRINT 1000, SYM,R,DEPTH,((G(I),TMAX(I)),I=1,3)
      PRINT 1080,(DAMP(I),I=1,4)
      DO 300 I=L,49
      ENCODE(E,1100) FS(I),SD(I,1),SV(I,1),SA(I,1),PSV(I,1)
     *                    ,SD(I,2),SV(I,2),SA(I,2),PSV(I,2)
     *                    ,SD(I,3),SV(I,3),SA(I,3),PSV(I,3)
```

```
     *                         ,SD(I,4),SV(I,4),SA(I,4),PSV(I,4)
      DECODE( E,1200 ) F
      PRINT 1300,(PERIOD(I),F)
  300 CONTINUE
 1000 FORMAT(1H1,////51X,A6,2X,3H(R=,F7.2,3H KM,8H  DEPTH=
     1       ,F6.2,4H KM)//49X,3(A6,E9.2,1X))
 1080 FORMAT(/34X,4(5HDAMP=,F4.2,15X)/14X,6HPERIOD,3X,2HFS,
     *       4(4X,2HSD,4X,2HSV,4X,2HSA,3X,3HPSV))
 1100 FORMAT(17E9.2)
 1200 FORMAT(17(A1,1X,3A1,1X,A1,1X,A1))
 1300 FORMAT(13X,F6.2,1X,102A1)
      RETURN
      END

      SUBROUTINE SVLOG(SVP,SYM,R)
C
C  PLOT PSV-PERIOD ON LOG-LOG SCALE
C
      DIMENSION SVP(49,4)
      DIMENSION PSV(49,4),FS(51),FP(51)
      CHARACTER SYM
      COMMON/ PERLOG / PERIOD1(51),L
      CYCLE = 1.84
      NOCX  = 3
      NOCY  = 4
      CALL PLOT(0.,-11.,-3)
      CALL PLOT(0.,2.,-3)
      YMIN = 1.E+38
      DO 400 I1=L,49
      DO 400 I2=1,4
      T = SVP(I1,I2)
      PSV(I1,I2) = ALOG10(T)
      T = PSV(I1,I2)
      IF( T.LT.YMIN )  YMIN = T
  400 CONTINUE
      DO 450 I=2,9
      T = I
  450 FS(I) = ALOG10(T)*CYCLE
      XLEN  = NOCX*CYCLE
      YLEN  = NOCY*CYCLE
      SEG   = 0.01*XLEN
      SIZE  = 0.027*XLEN
      SIZE1 = 0.6*SIZE
      LYMIN = YMIN-1.
      IF( YMIN.GT.0. )  LYMIN = LYMIN+1
```

```
      DO 800 I1=1,2
      IF( I1.EQ.2 )  GO TO 490
      T1     = 1.
      T2     = 0.
      T3     = 0.09
      T4     = 0.015
      NOC    = NOCY
      POWER = LYMIN-1
      GO TO 500
  490 T1     = 0.
      T2     = 1.
      T3     = 0.022
      T4     = 0.04
      NOC    = NOCX
      POWER = -2.
  500 X0     = -T3*XLEN
      Y0     = -T4*XLEN
      Y01    = Y0+0.62*SIZE
      NOC1 = NOC+1
      DO 600 I=1,NOC1
      X1 = T2*(I-1)*CYCLE
      Y1 = T1*(I-1)*CYCLE
      CALL PLOT(X1,Y1,3)
      X2 = X1+X0
      Y2 = Y1+Y0
      CALL NUMBER(X2,Y2,SIZE,10.,0.,-1)
      POWER = POWER+1.
      Y2 = Y1+Y01
      CALL NUMBER(999.,Y2,SIZE1,POWER,0.,-1)
      CALL PLOT(X1,Y1,3)
      X2 = T2*X1+T1*XLEN
      Y2 = T1*Y1+T2*YLEN
      CALL PLOT(X2,Y2,2)
  600 CONTINUE
      CALL PLOT(0.,0.,3)
      DO 700 I2=1,2
      S1 = (I2-1)*(T1*XLEN+T2*YLEN)
      S2 = (3.-2.*I2)*SEG
      DO 700 I=1,NOC
      S3 = (I-1)*CYCLE
      DO 700 J=2,9
      X1 = T1*S1+T2*(FS(J)+S3)
      Y1 = T2*S1+T1*(FS(J)+S3)
      CALL PLOT(X1,Y1,3)
      X2 = X1+T1*S2
```

```
      Y2 = Y1+T2*S2
      CALL PLOT(X2,Y2,2)
  700 CONTINUE
      CALL PLOT(0.,0.,3)
  800 CONTINUE
      SIZE = 0.035*XLEN
      CALL SYMBOL(0.30*XLEN,-0.11*XLEN,SIZE,12HPERIOD (SEC),
     10.0,12)
      CALL PLOT(0,0,0.0,3)
      CALL SYMBOL(-0.13*XLEN,0.45*XLEN,SIZE,12HPSV (CM/SEC),
     190.0,12)
      CALL PLOT(0,0,0.0,3)
      X1 = 0.30*XLEN
      Y1 = -0.23*XLEN
      CALL SYMBOL(X1,Y1,SIZE,SYM,0.,6)
      CALL SYMBOL(999.,Y1,SIZE,2HR=,0.,2)
      CALL NUMBER(999.,Y1,SIZE,R,0.,-1)
      CALL SYMBOL(999.,Y1,SIZE,2HKM,0.,2)
      CALL PLOT(0.,0.,3)
      K1 = 50-L
      FP(K1+1) = -1.
      FP(K1+2) = 1./CYCLE
      FS(K1+1) = LYMIN
      FS(K1+2) = 1./CYCLE
      DO 900 J=1,4
      DO 890 I=L,49
      K = I+1-L
      FP(K) = PERIOD1(I)
      FS(K) = PSV(I,J)
  890 CONTINUE
  900 CALL LINE(FP,FS,K1,1,0,0)
      CALL PLOT(10.,0.,-3)
      RETURN
      END

      SUBROUTINE AMATRIX(NO,DTO)
C
C       NO = NUMBER OF GRID POINTS
C      DTO = TIME INTERNAL USED IN SAMPLING THE INPUT VEL
C
      COMMON/ABCOEF/A11(49,4),A12(49,4),A21(49,4),A22(49,4)
     *                ,B1(49,4),B2(49,4),PERIOD(49),KNDT(49)
     *                ,KN1(49),DAMP(4),L
      COMMON/ PERLOG / PERIOD1(51),L1
      DAMP(1) = 0.
```

```
      DAMP(2) = 0.02
      DAMP(3) = 0.05
      DAMP(4) = 0.1
      J=0
      PERIOD(1) = 0.1
      DO 90 I1=1,3
      ADD = 0.02*10.**(I1-1.)
      DO 80 I2=1,5
      J = J+1
   80 PERIOD(J+1) = PERIOD(J)+ADD
      ADD = 2.5*ADD
      DO 85 I2=6,11
      J = J+1
   85 PERIOD(J+1) = PERIOD(J)+ADD
      ADD = 2.*ADD
      DO 90 I2=12,16
      J = J+1
   90 PERIOD(J+1) = PERIOD(J)+ADD
      TNYG = 2.*DT0
      DO 92 I=1,49
      T = PERIOD(I)
      IF(T.GE.TNYG) GO TO 94
   92 CONTINUE
   94 L  = I
      L1 = L
      DO 95 I=L,49
      T = PERIOD(I)
   95 PERIOD1(I) = ALOG10(T)
      DO 100 I1=L,49
C  FIND THE PROPER TIME INTERVEL
      DT1 = PERIOD(I1)/10.
      NDT = DT0/DT1+1.
      DT  = DT0/NDT
      N   = (N0-1)*NDT+1
      N1  = N-1
      FREQ = 6.283185/PERIOD(I1)
      KN1(I1)  = N1
      KNDT(I1) = NDT
      DO 100 I2=1,4
C  FIND THE MATRIX A,B USED IN CALCULATING X,V
      SQRT1= SQRT(1.-DAMP(I2)*DAMP(I2))
      WD   = FREQ*SQRT1
      WDT  = WD*DT
      T1   = -FREQ*DAMP(I2)*DT
      T2   = DAMP(I2)/SQRT1
```

```
      EXP1 = EXP(T1)
      SIN1 = SIN(WDT)
      COS1 = COS(WDT)
      T3   = -1.+EXP1*(COS1+T2*SIN1)
      T4   = FREQ*FREQ
      A11(I1,I2) = EXP1*(T2*SIN1+COS1)
      A12(I1,I2) = EXP1*SIN1/WD
      A21(I1,I2) = -FREQ*EXP1*SIN1/SQRT1
      A22(I1,I2) = EXP1*(COS1-T2*SIN1)
      B1(I1,I2)  = T3/(T4*DT)
      B2(I1,I2)  = -EXP1*SIN1/WDT
  100 CONTINUE
      RETURN
      END
```

SAINT LOUIS UNIVERSITY PUBLICATIONS IN

EARTHQUAKE HAZARDS MITIGATION

Sponsored by the National Science Foundation

1. "Analysis of Strong Motion Data from the New Madrid Seismic Zone: 1975-1976," by Robert B. Herrmann, August 1977. (NTIS PB 280 148/AS).

2. "A Time Domain Study of the Attenuation of 10-Hz Waves in the New Madrid Seismic Zone," by Otto W. Nuttli, Bulletin, Seismological Society of America, Vol. 68, April 1978, pp. 343-356.

3. "SH Wave Generation by Dislocation Sources - A Numerical Study," by Robert B. Herrmann (submitted to Bulletin, Seismological Society of America), 1978.

4. "On the Relation Between MM Intensity and Body-Wave Magnitude," by Otto W. Nuttli, G.A. Bollinger, and Donald W. Griffiths (submitted to Bulletin, Seismological Society of America), 1978.

5. "Computer Programs in Earthquake Seismology, Volume 1: General Programs," edited by Robert B. Herrmann, Department of Earth and Atmospheric Sciences, Saint Louis University, October 1978.

6. "Computer Programs in Earthquake Seismology, Volume 2: Surface Wave Programs," edited by Robert B. Herrmann, Department of Earth and Atmospheric Sciences, Saint Louis University, October 1978.

7. "Seismicity of the Central United States," by O.W. Nuttli, Monograph in Engineering Geology Series of Geological Society of America, 1979.

8. "SH-A Computer Program for Generating Far-field Tangential Time Histories for Point Earthquake Sources," by Robert B. Herrmann and Chien Y. Wang, Department of Earth and Atmospheric Sciences, Saint Louis University, January 1979.